Overview of Relativistic Heavy Ion Collisions

Che-Ming Ko
Texas A&M University

- QCD phase diagram
- Signatures of QGP
- Experimental observations at RHIC and theoretical interpretations
- RHIC low energy run and FAIR
- HIC at LHC

Supported by National Science Foundation and The Welch Foundation

Phases of nuclear matter

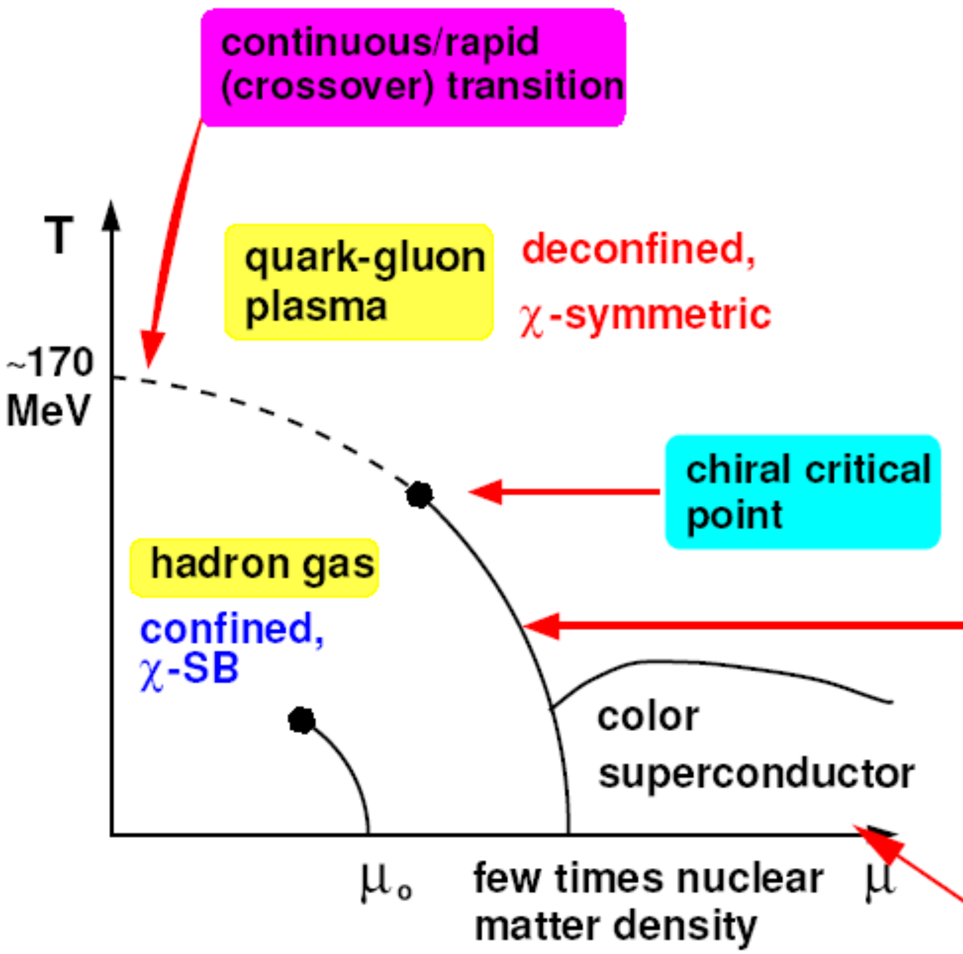

continuous transition for
small chemical potential
and small quark masses at

$T_c \simeq 170\ MeV$

$\epsilon_c \simeq 0.7\ GeV/fm^3$

2nd order phase transition;
Ising universality class

$T_c(\mu)$ under investigation
(cut-off and m_q-dependence!!)

1st order phase transition ???

expected - however, so far no
direct evidence from lattice QCD

attractive 1–gluon exchange
=> qq–condensates

F. Karsch, Quark Matter 2004 – p.20/25

Phase transition in lattice GCD

Karsch et al., NPA 698, 199 (02)

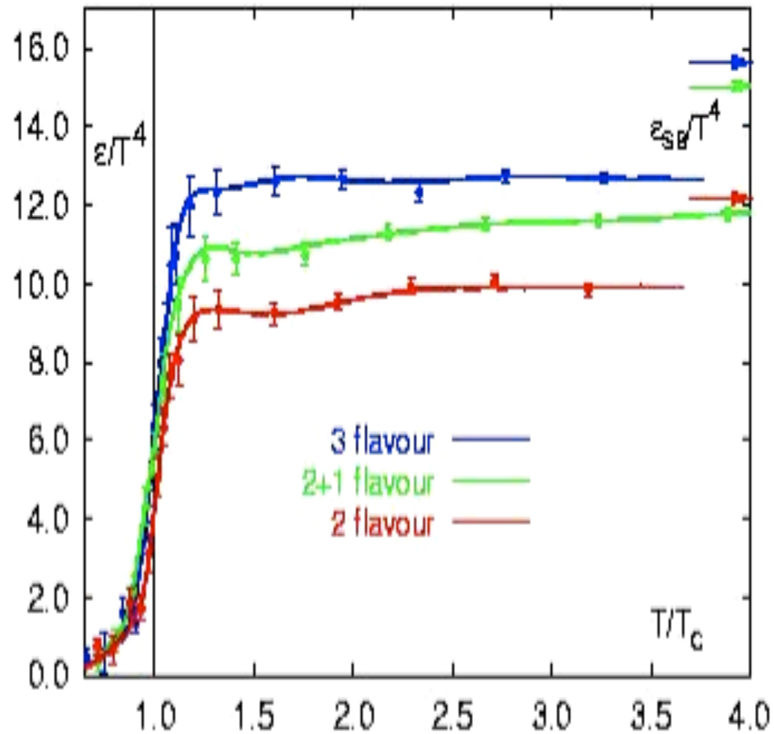

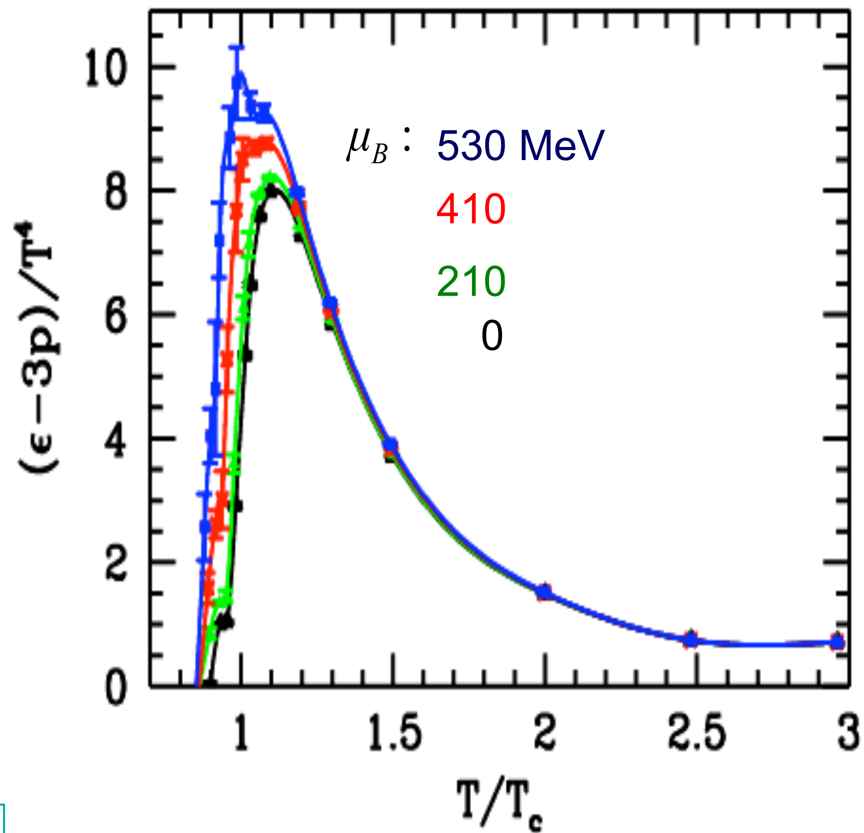

- Soft equation of state (p< e/3)
- $e_c \sim 6T_c^4 \sim 0.66$ GeV/fm^3
- Appreciate interaction energy
- $T_c \sim 170$ MeV

$$\frac{\varepsilon_{SB}}{T^4} = \left(16 + \frac{21}{2} n_f\right) \frac{\pi^2}{30}, \quad \frac{\varepsilon_\pi}{T^4} = 3\frac{\pi^2}{30}$$

QCD phase diagram probed by HIC

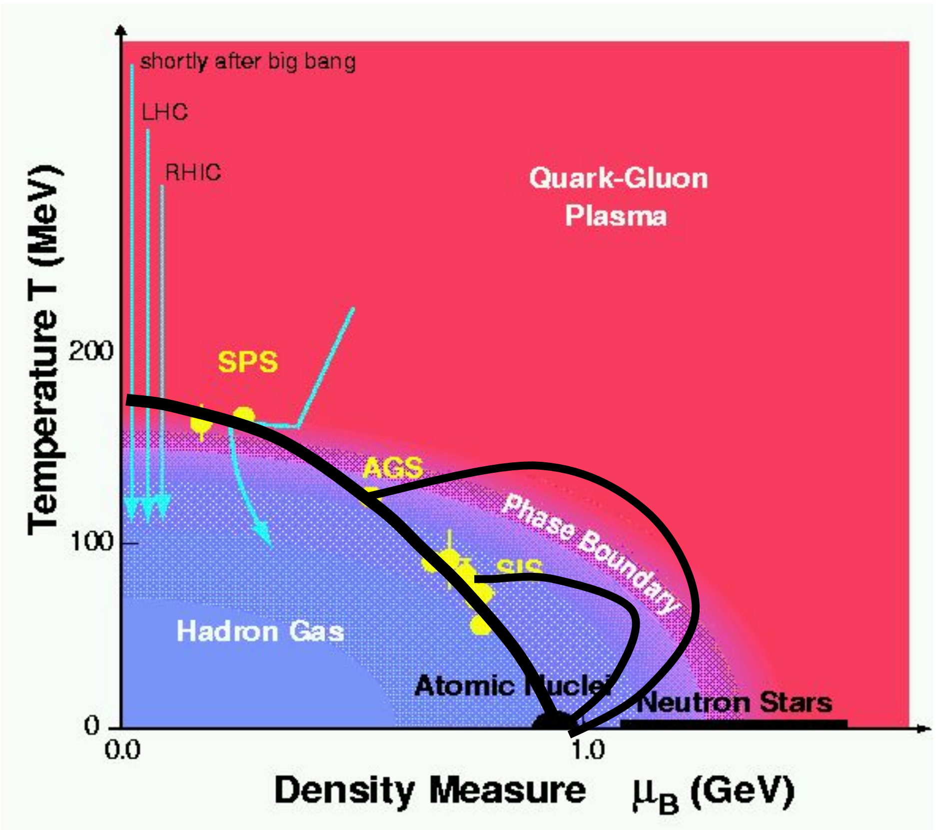

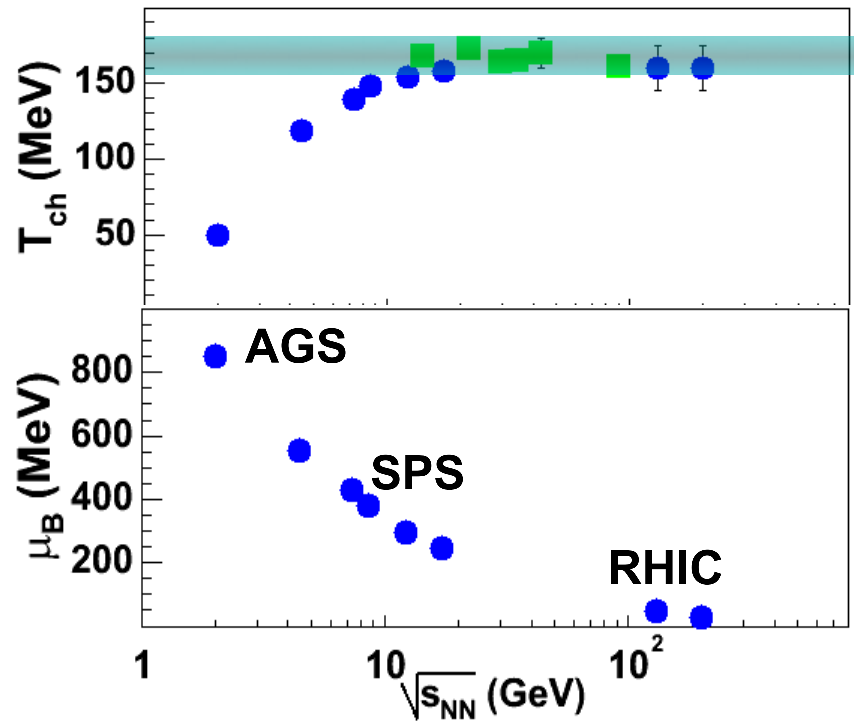

$$s_{NN} = (p_A + p_B)^2 = E^2_{CMS}$$

We do not observe hadronic systems with T > 170 MeV (Hagedon prediction)

Statistical model

Assume thermally and chemically equilibrated system of non-interacting hadrons and resonances with density

$$n_i = \frac{g}{2\pi^2}\int_0^\infty \frac{p^2 dp}{e^{(E_i(p)-\mu_i)/T} \pm 1}, \quad E_i = \sqrt{p^2 + m_i^2}$$

Determine chemical freeze out temperature T_{ch} and baryon chemical potential μ_B by fitting experimental data after inclusion of feed down from short lived particles and resonances decay.

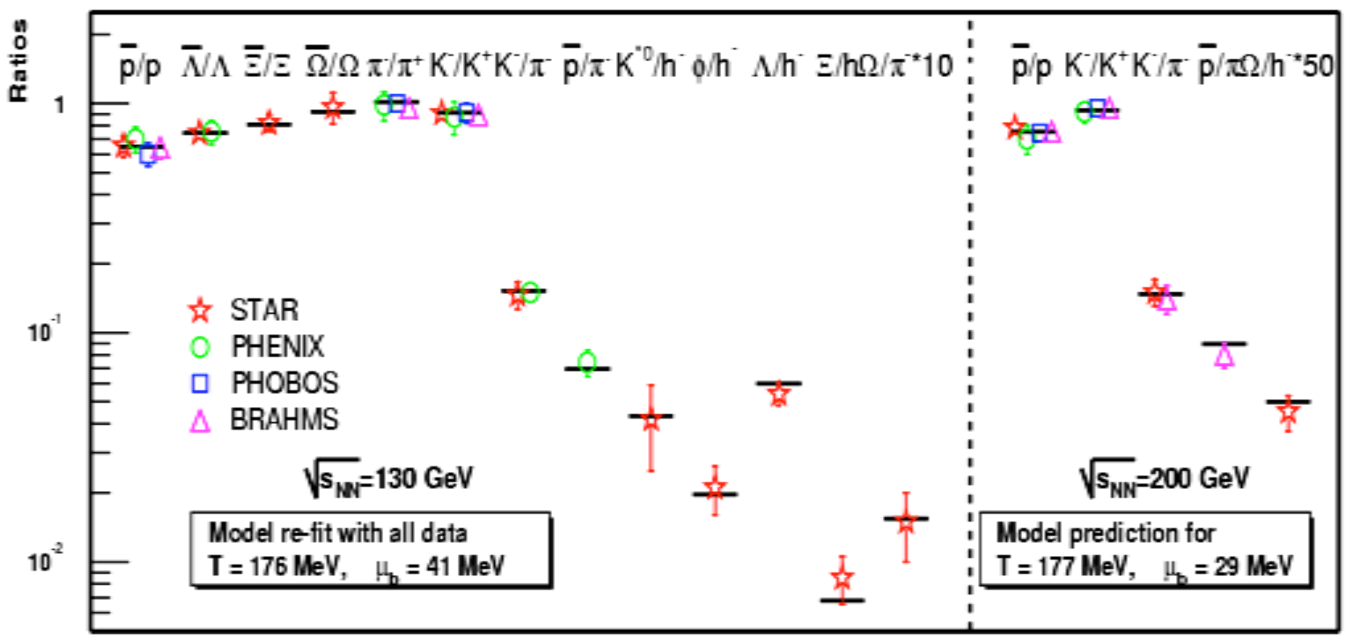

$T_{ch} \sim T_c$

Hydrodynamic model

Kolb & Heinz; Teany & Shuryak; Hirano, ……..

Hydrodynamic Equations

$$\partial_\mu T^{\mu\nu}(x) = 0$$ Energy-momentum conservation

$$\partial_\mu n_j u^\mu(x) = 0$$ Charge conservations (baryon, strangeness,…)

For perfect fluids without viscosity

$$T^{\mu\nu}(x) = \left[e(x) + p(x)\right] u^\mu(x) u^\nu(x) - p(x) g^{\mu\nu}$$

e: energy density
p: pressure
u^μ: four velocity

Equation is closed by the equation of state p(e)

Cooper-Frye instantaneous freeze out

$$\boxed{E\frac{dN_i}{d^3q} = \frac{g_i}{(2\pi)^3}\int q\cdot d\sigma \frac{1}{\exp(q\cdot u)\pm 1}}$$

dσ is an element of space-like hypersurface

Transverse momentum spectra from hydrodynamic model

Kolb & Heinz, nucl-th/0305084

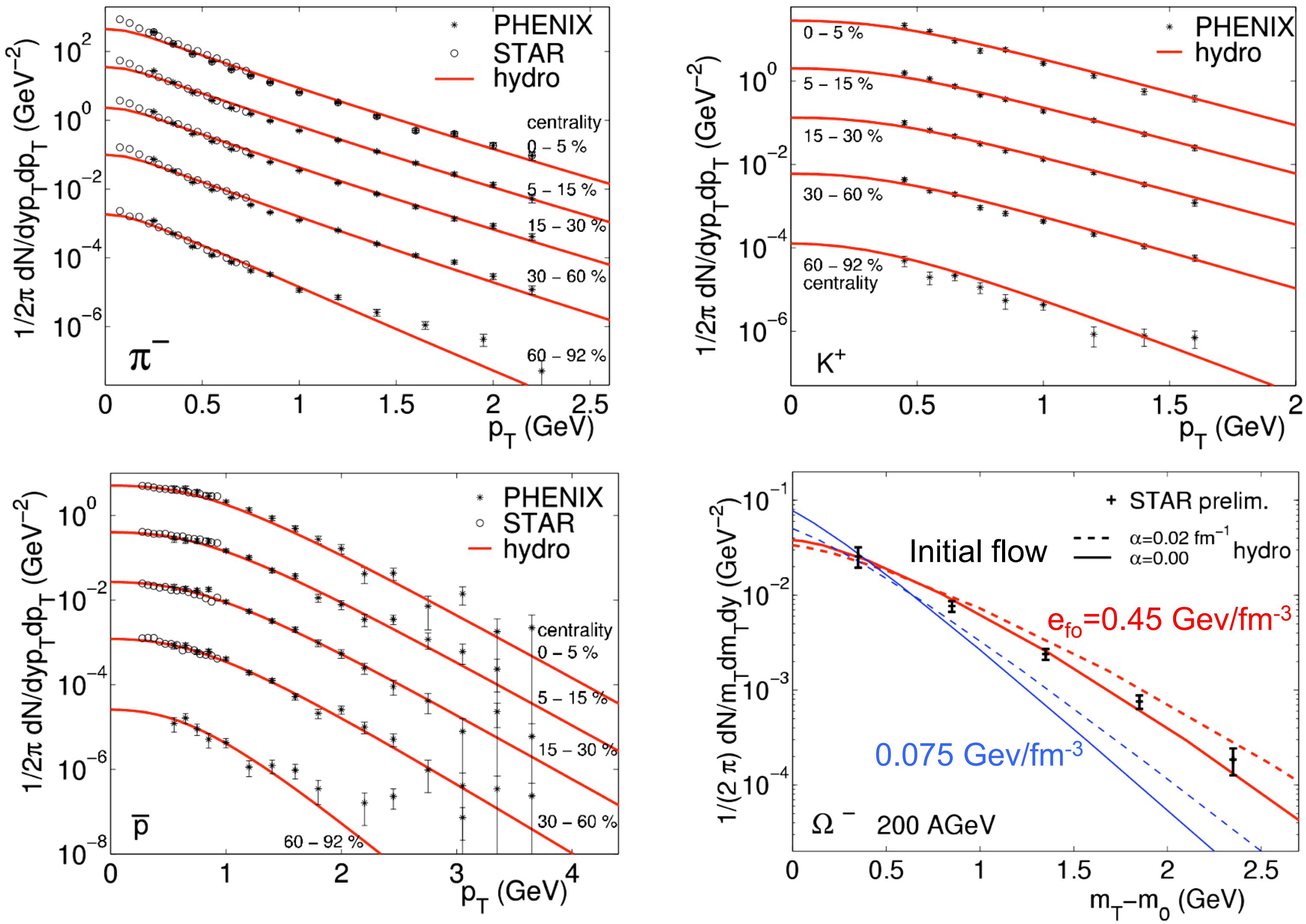

Initial T_i=340 MeV, e_i=25 GeV/fm^3

Freezeout T_f=128 MeV

Parton cascade

Bin Zhang, Comp. Phys. Comm. 109, 193 (1998)
D. Molnar, B.H. Sa, Z. Xu & C. Greiner

$$p^\mu \partial_\mu f_1(x,p,t) \propto \int dp_2 d\Omega |\vec{v}_1 - \vec{v}_2| \frac{d\sigma}{d\Omega}\left(f_1^{'} f_2^{'} - f_1 f_2\right)$$

$$\frac{d\sigma}{dt} \approx \frac{9\pi\alpha_s^2}{2(t-\mu^2)^2}, \quad \sigma = \frac{9\pi\alpha_s^2}{2\mu^2}\frac{1}{1+\mu^2/s}$$

- Using α_s=0.5 and screening mass μ=gT≈0.6 GeV at T≈0.25 GeV, then $\langle s\rangle^{1/2}$≈4.2T≈1 GeV, and pQCD gives σ≈2.5 mb and a transport cross section

$$\sigma_t = \int d\Omega \frac{d\sigma}{d\Omega}\left(1-\cos\theta\right) \approx 1.5\text{mb}$$

- σ=6 mb → μ≈0.44 GeV, σ_t≈2.7 mb
- σ=10 mb → μ≈0.35 GeV, σ_t≈3.6 mb

A multiphase transport (AMPT) model

Default: Lin, Pal, Zhang, Li & Ko, PRC 61, 067901 (00); 64, 041901 (01)

- Initial conditions: HIJING (soft strings and hard minijets)
- Parton evolution: ZPC
- Hadronization: Lund string model for default AMPT
- Hadronic scattering: ART

String melting: PRC 65, 034904 (02); PRL 89, 152301 (02)

- Convert hadrons from string fragmentation into quarks and antiquarks
- Evolve quarks and antiquarks in ZPC
- When partons stop interacting, combine nearest quark and antiquark to meson, and nearest three quarks to baryon (coordinate-space coalescence)
- Hadron flavors are determined by quarks' invariant mass

PRC 72, 064901 (05); http://www. cunuke.phys.columbia.edu/OSCAR

Transverse momentum and rapidity distribution from AMPT

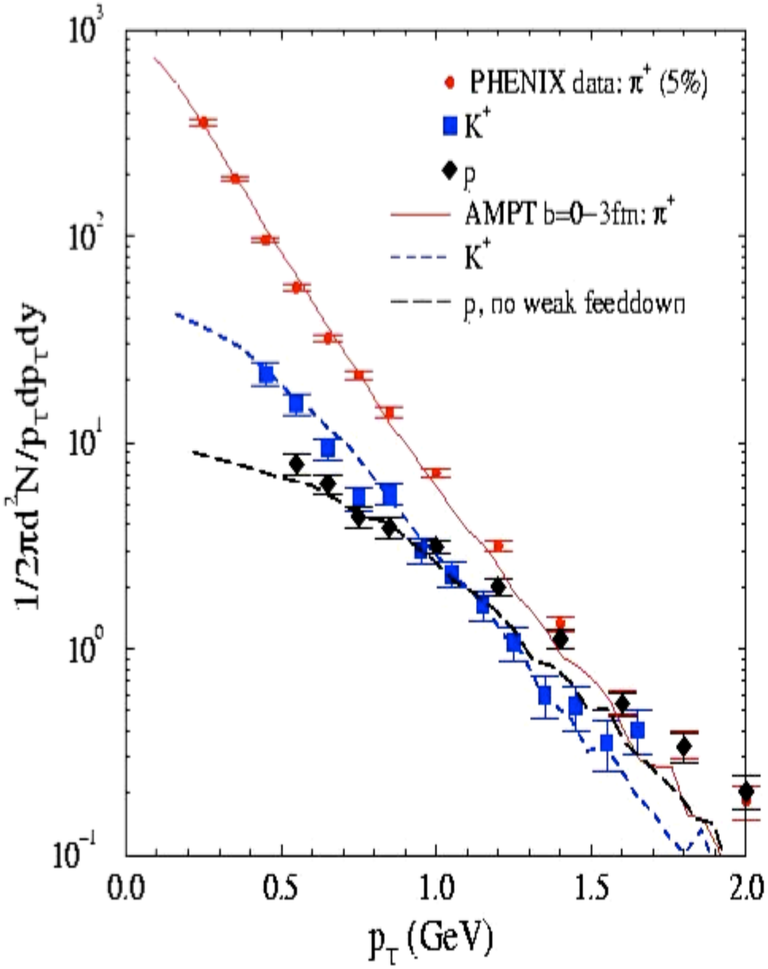

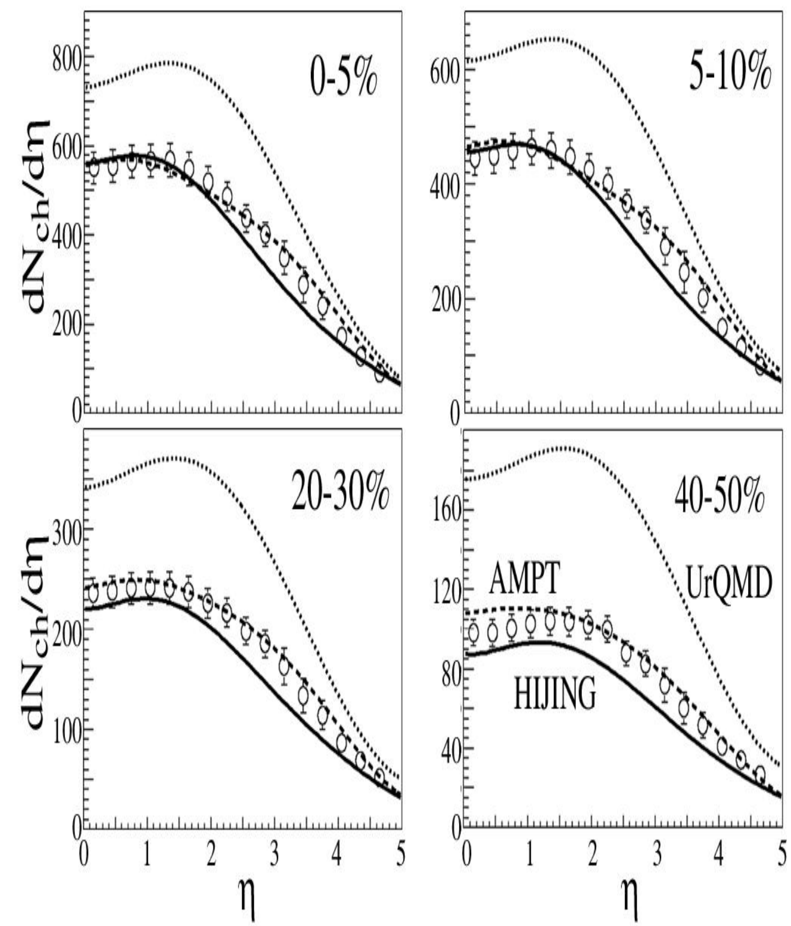

BRAHMS Au+Au @ 200 GeV

What have we learnt?

Matter formed in relativistic heavy ion collisions reaches

- thermalization early in time $\tau < 1$ fm/c
- high initial energy density $\varepsilon \sim 10$ GeV/fm^3
- chemical equilibrium with limiting temperature $T_c \sim 170$ MeV
- final thermal equilibrium at $T_{th} \sim 120$ MeV with large radial collective flow velocity $\langle\beta_T\rangle \sim 0.5$

Is the matter a quark-gluon plasma?

Signatures of quark-gluon plasma

- Dilepton enhancement (Shuryak, 1978)
- Strangeness enhancement (Meuller & Rafelski, 1982)
- J/ψ suppression (Matsui & Satz, 1986)
- Pion interferometry (Pratt; Bertsch, 1986)
- Elliptic flow (Ollitrault, 1992)
- Jet quenching (Gyulassy & Wang, 1992)
- Net baryon and charge fluctuations (Jeon & Koch; Asakawa, Heinz & Muller, 2000)
- Quark number scaling of hadron elliptic flows (Voloshin 2002)
- ……………

Dilepton spectrum at RHIC

PHENIX, Hemmick

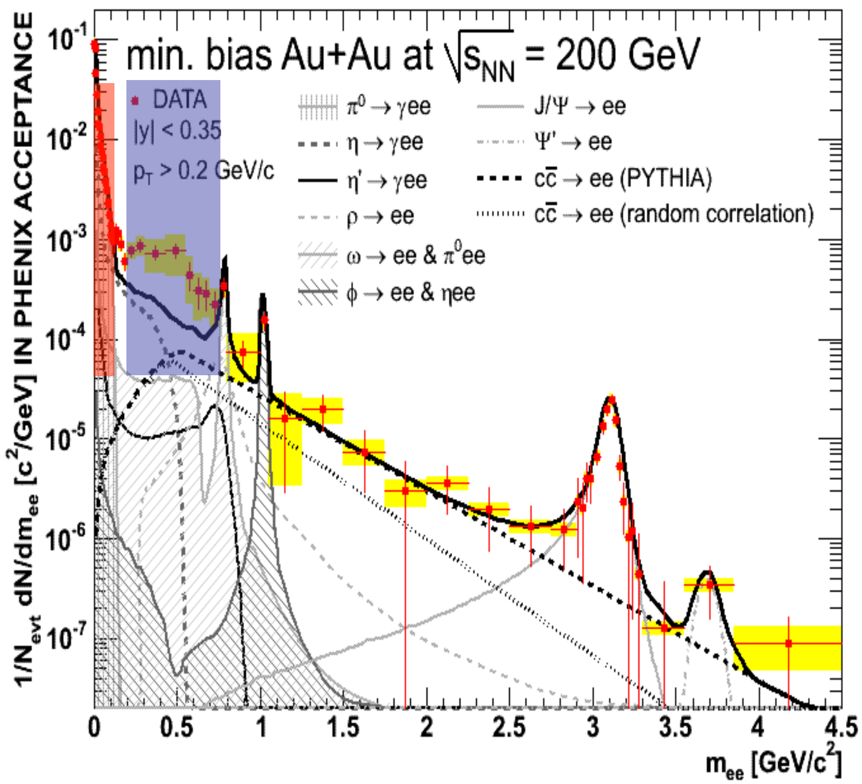

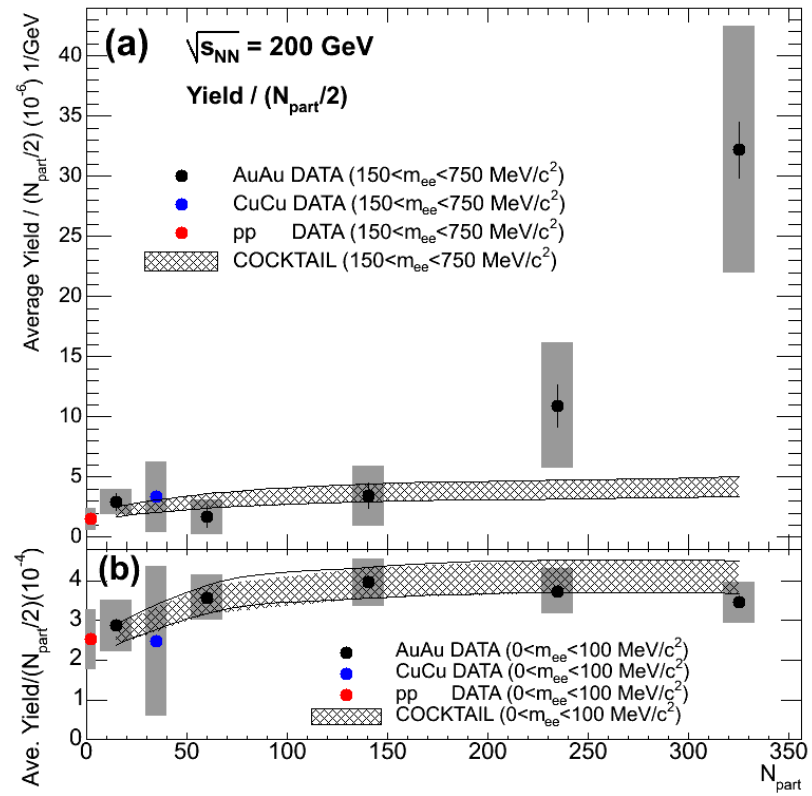

- Excess 150 <m_{ee}<750 MeV: 3.4 ± 0.2(stat.) ± 1.3(syst.) ± 0.7(model)

- π^0 region: production scales approximately with N_{part}
- Excess region: expect contribution from hot matter

Strangeness enhancement

- In QGP

$$q+\bar{q}\rightarrow s+\bar{s}$$
$$g+g\rightarrow s+\bar{s}$$
$$Q=2m_s\approx 250-300\,\mathrm{MeV}$$

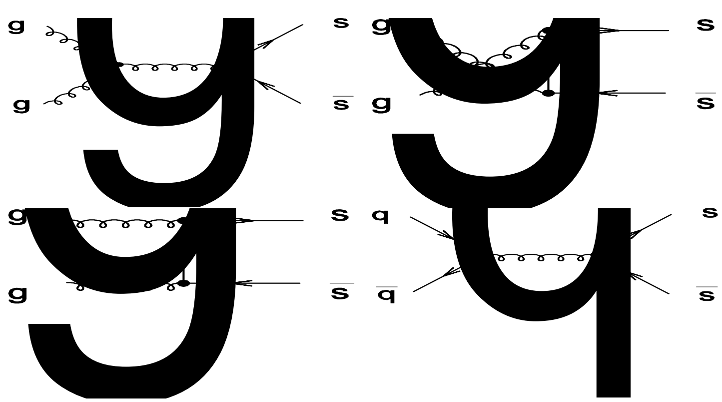

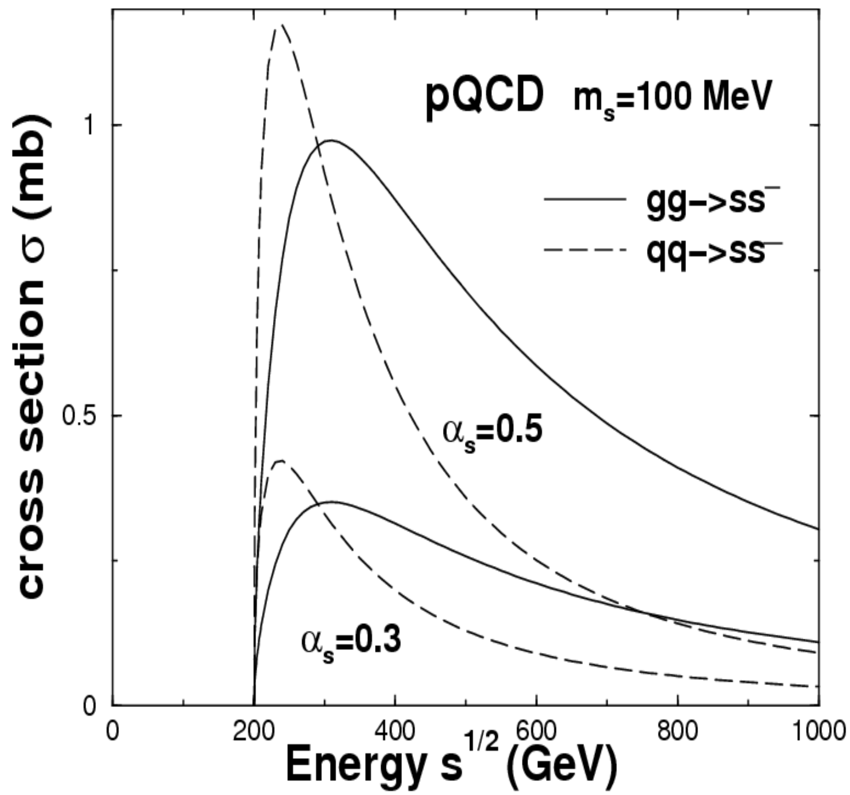

Strangeness equilibration Time

Kinetic equation

$$\frac{d\rho_s}{dt} \propto \langle \sigma v \rangle_{12 \to s\bar{s}} \rho_1 \rho_2 - \langle \sigma v \rangle_{s\bar{s} \to 12} \rho_s^2$$

Equilibrium density

$$\rho_{eq} = g \int \frac{d^3p}{(2\pi)^3} f(p) = \frac{Tm^2}{2\pi} \sum_{n=1}^{\infty} \frac{1}{n} K_2\left(\frac{nm}{T}\right)$$

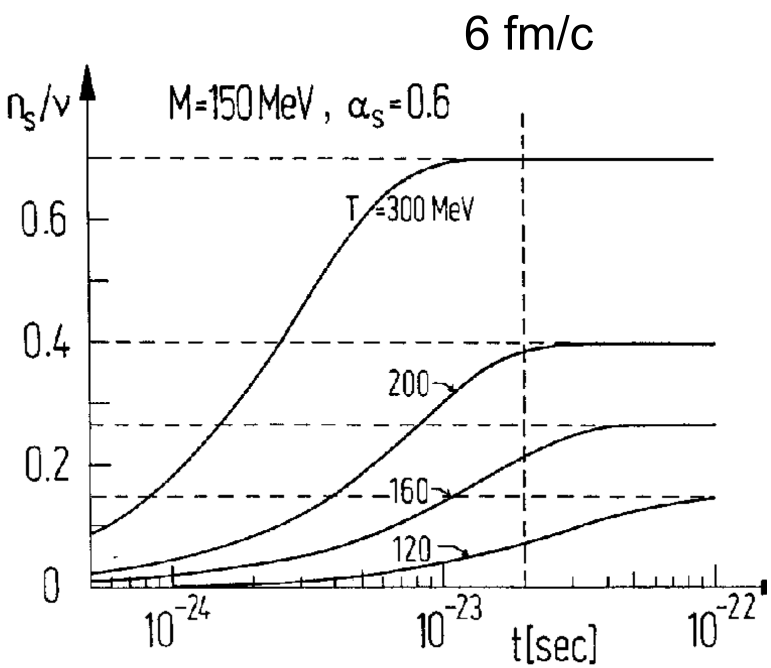

Strangeness equilibration time in QGP from lowest-order QCD $t_{eq} \sim 6$ fm/c is comparable to lifetime t_{QGP} of QGP in HIC

Strangeness production in hadronic matter

- In hadronic matter

$$\pi\pi \rightarrow K + \overline{K} \quad (Q = 2m_K - 2m_\pi \approx 710\,\mathrm{MeV})$$
$$NN \rightarrow N\Lambda K \quad (Q = m_\Lambda + m_K - m_N \approx 670\,\mathrm{MeV})$$
$$\pi N \rightarrow K\Lambda \quad (Q = m_\Lambda + m_K - m_N - m_\pi \approx 530\,\mathrm{MeV})$$

$\rightarrow$ cross sections ~ a few mb

$$N\Delta \rightarrow N\Lambda\Lambda \quad (Q \approx 380\mathrm{MeV})$$
$$\pi\Delta \rightarrow K\Lambda \quad (Q \approx 240\,\mathrm{MeV})$$
$$\Delta\Delta \rightarrow N\Lambda\Lambda \quad (Q \approx 90\mathrm{MeV})$$
$$\pi\rho \rightarrow K\Lambda \quad (Q \approx 80\mathrm{MeV})$$

Cross sections are unknow but expected to be a few mb as well

Strangeness equilibration time in hadronic matter t_{eq} ~ 30 fm/c is longer than hadronic life time t_{had} ~ 15 fm/c

Experimental results

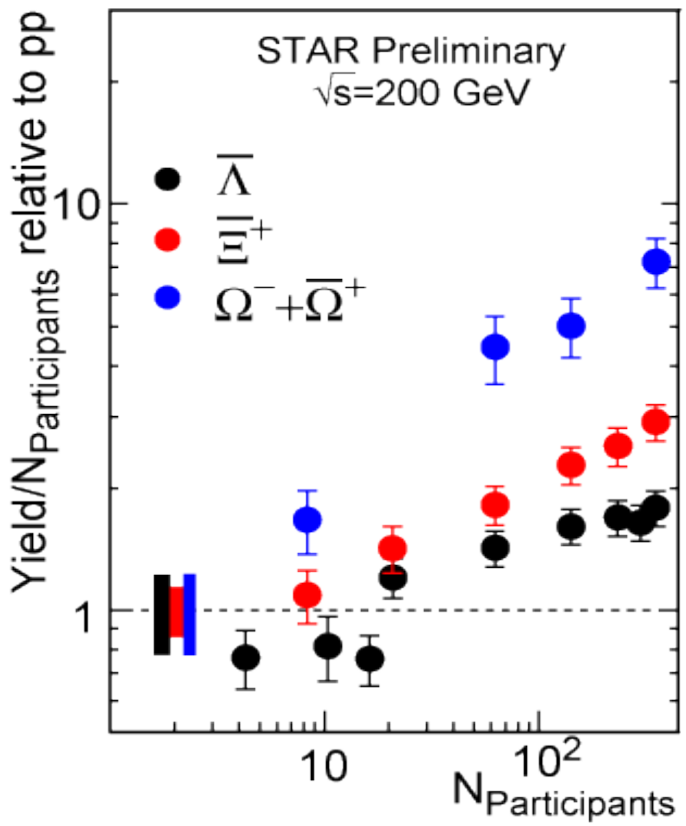

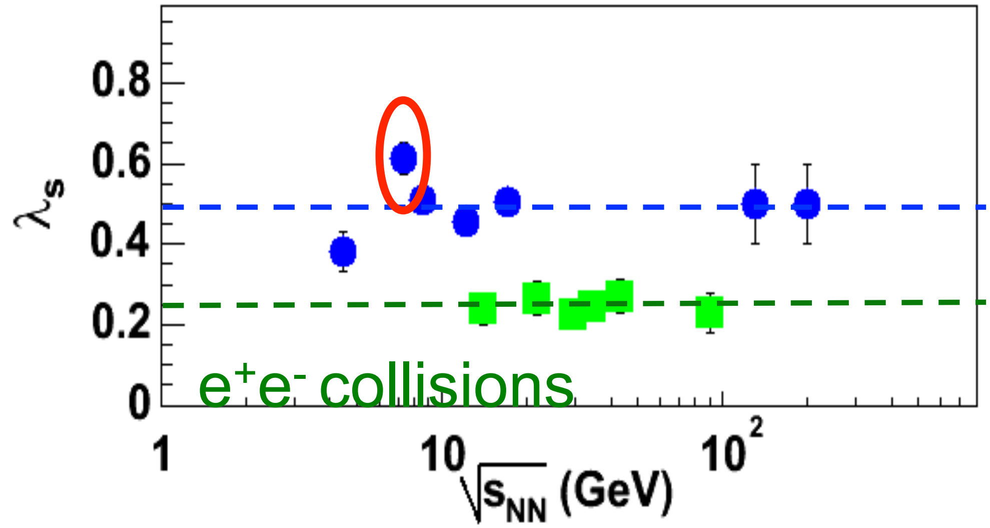

$$\lambda_s = \frac{2s\bar{s}}{u\bar{u} + d\bar{d}}$$

Multistrange baryons are significantly enhanced and can be accounted for by the statistical model → Strangeness equilibration

J/ψ suppression

- Color charge is subject to screening in QGP

$$V = -\frac{\alpha_s}{r} \longrightarrow V = -\frac{\alpha_s}{r} e^{-r/\lambda_D}$$

One loop pQCD

$$\lambda_D = \left(\frac{N_c}{3} + \frac{N_f}{6}\right)^{-\frac{1}{2}} (gT)^{-1} \approx \sqrt{2/3}\,(gT)^{-1}$$

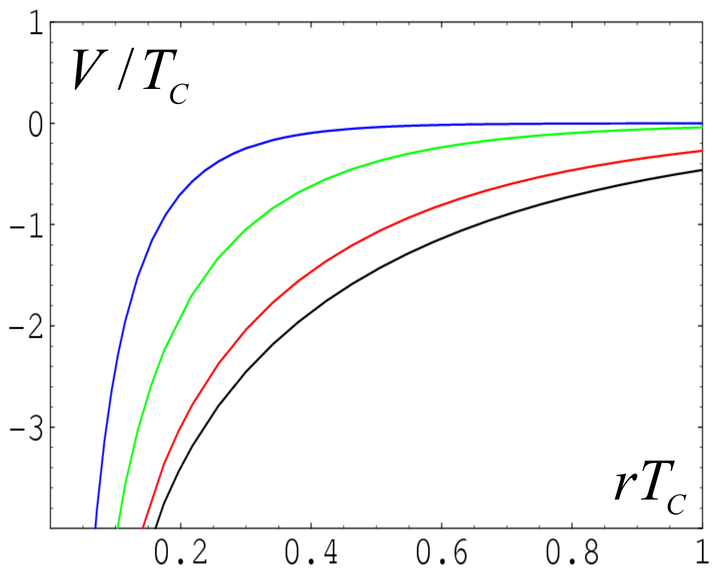

Lattice result for J/ψ spectral function

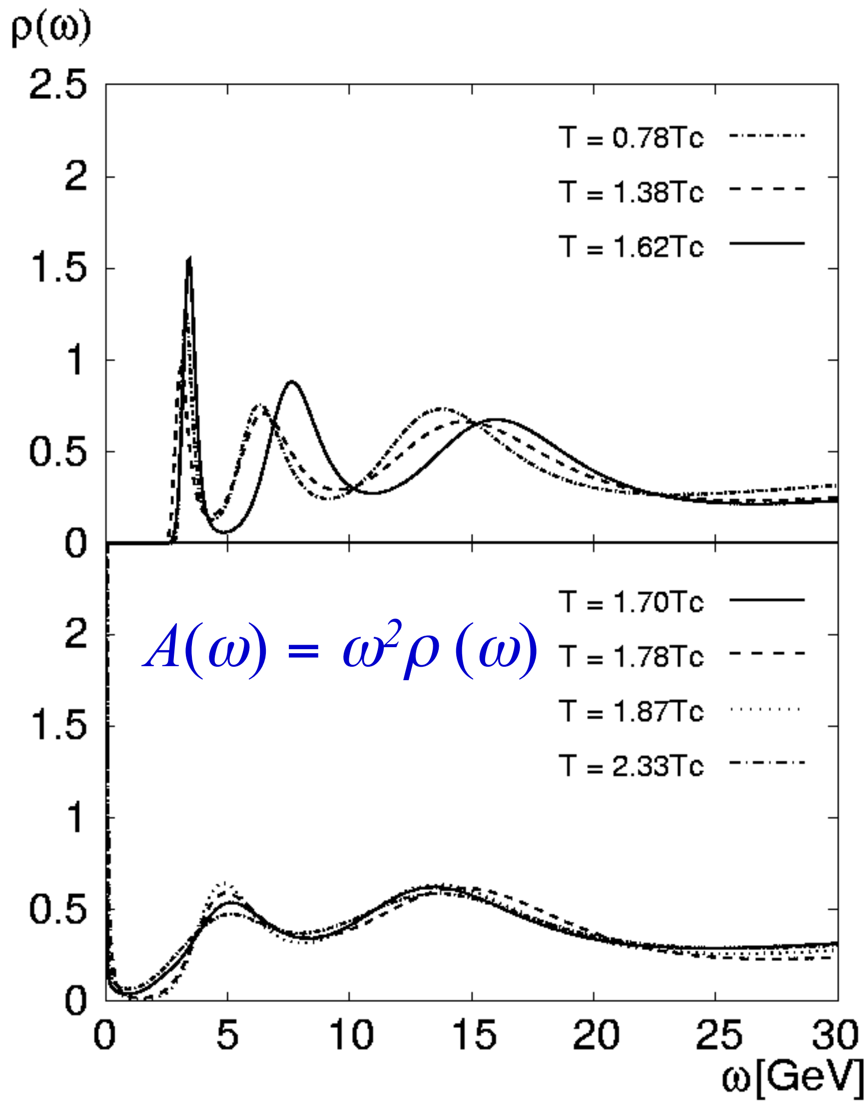

J/ψ disappears between $1.62T_c$ and $1.70T_c$

J/ψ absoprtion and production in HIC

- Nuclear absorption: $J/\psi+N\rightarrow D+\Lambda_c$; p+A data → $\sigma\sim$ 6 mb
- Absorption and regeneration in QGP: $J/\Psi + g \leftrightarrow c\bar{c}$
- Absorption and regeneration in hadronic matter: $J/\Psi + \pi \leftrightarrow D\bar{D}$

RHIC Zhao & Rapp, arXiv:0810.4566 [nucl-th] SPS

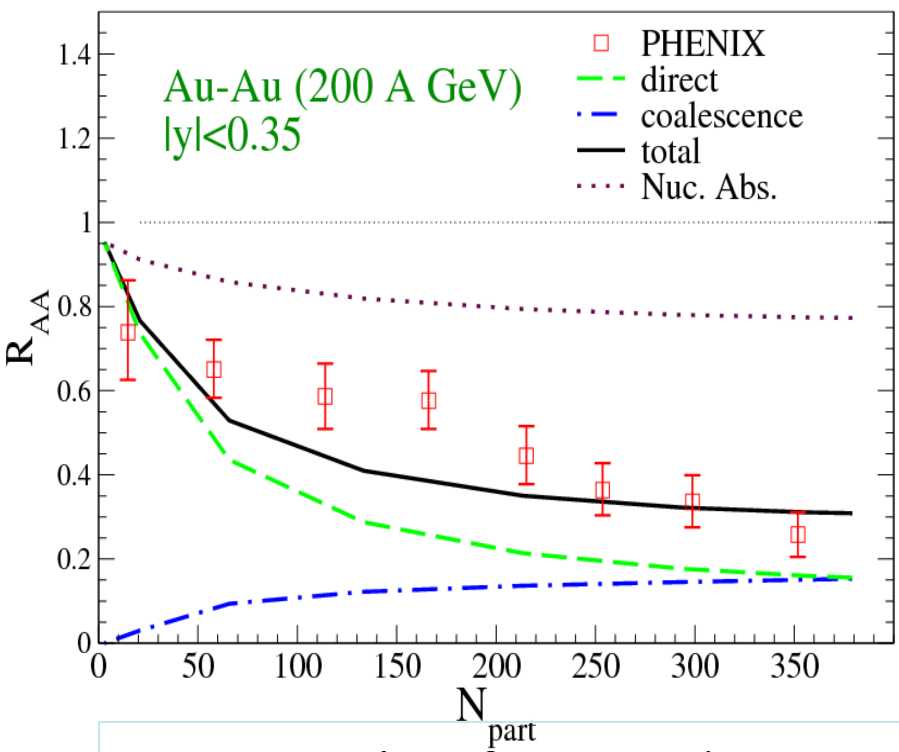

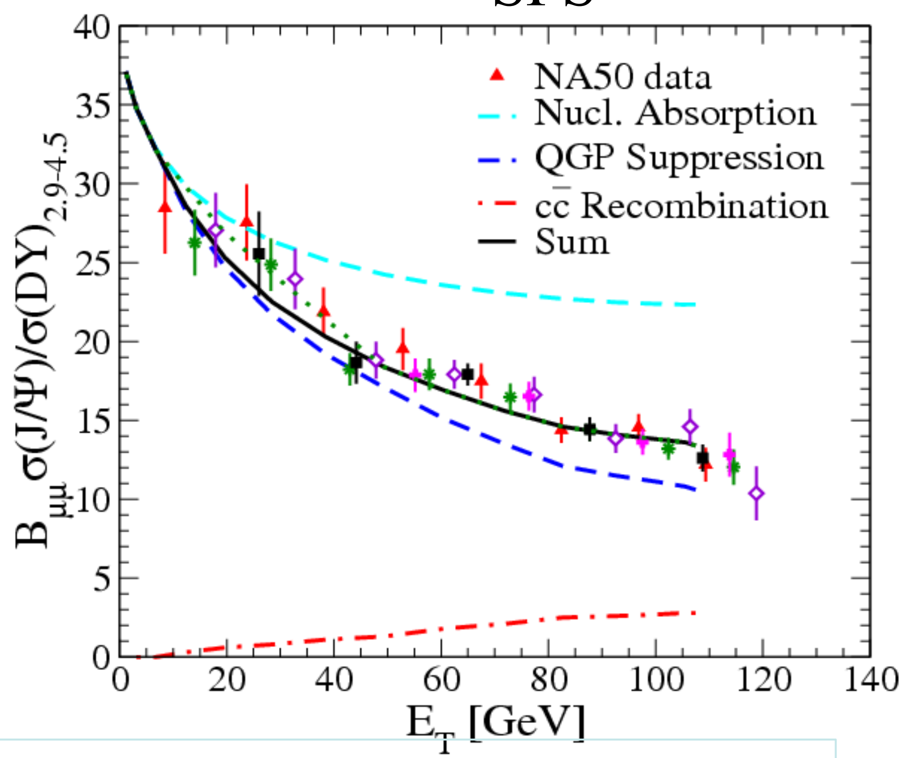

Regeneration from coalescence of charm and anticharm quark is non-negligible at RHIC as first pointed out by Thews

Hanbury-Brown-Twiss interferometry

Two-particle correlation function

$$C(\vec{K},\vec{q})=1+\frac{\int d^4x_1 d^4x_2 S(x_1,p_1)S(x_2,p_2)\cos[q\cdot(x_1-x_2)]}{\int d^4x_1 S(x_1,p_1)\int d^4x_2 S(x_2,p_2)}$$

with $\vec{K}=\left(\vec{p}_1+\vec{p}_2\right)/2,\ q=(\vec{p}_1-\vec{p}_2,\ E_1-E_2)$

- S(x,p) is the emission source function given by the particle phase-space distribution at freeze out in the AMPT model
- C(K,q) can be evaluated using the Correlation After Burner (Pratt, NPA 566, 103c (94))

Pion interferometry

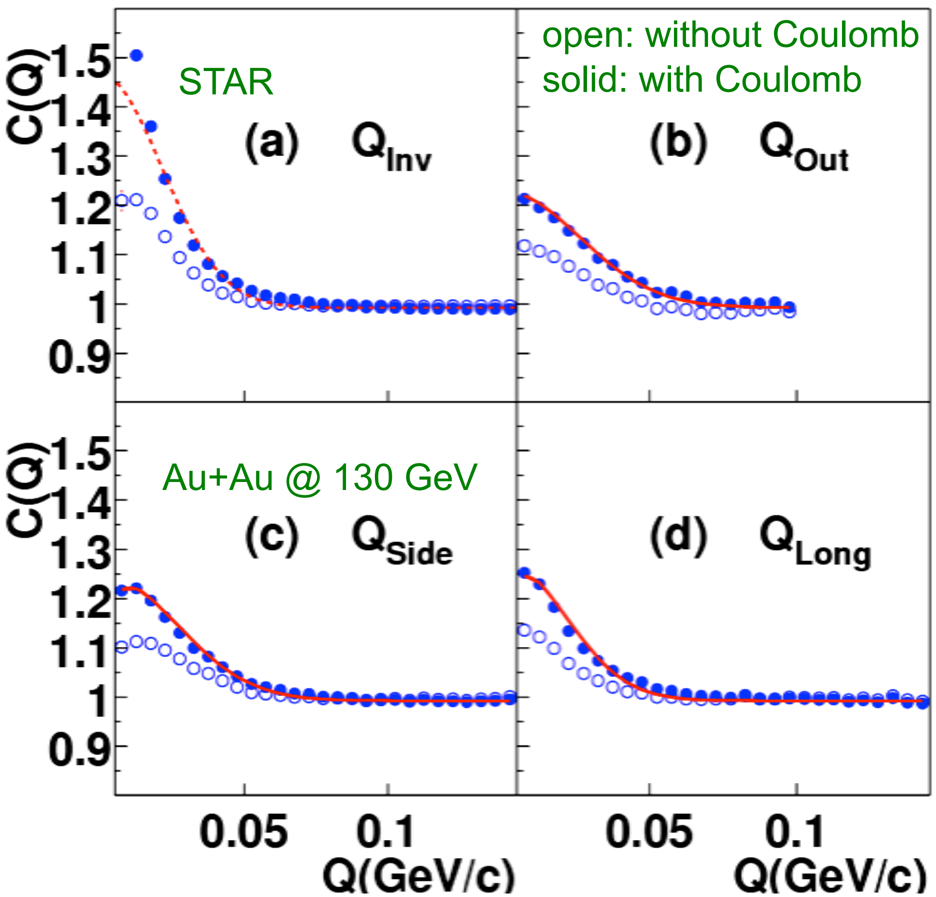

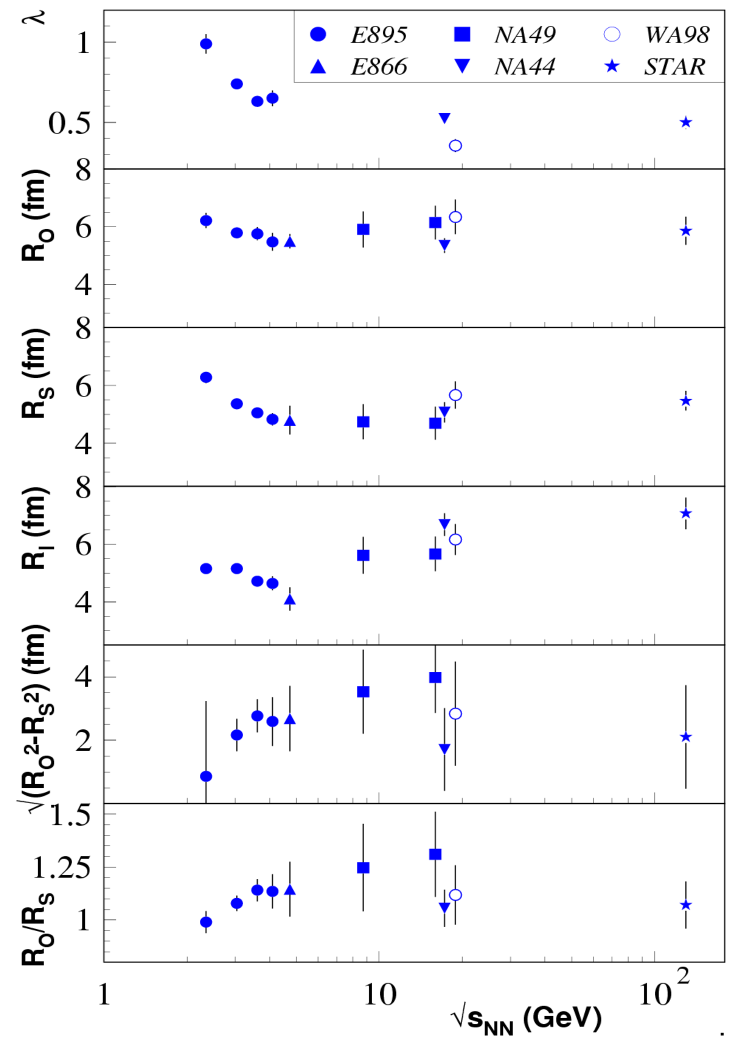

$$C(q) = 1 + \lambda \exp(-q_o^2 R_o^2 - q_s^2 R_s^2 - q_l^2 R_l^2) = 1 + \lambda \exp(-q_{inv}^2 R_{inv}^2)$$

$R_o/R_s \sim 1$ smaller than expected ~1.5

Source radii from hydrodynamic model

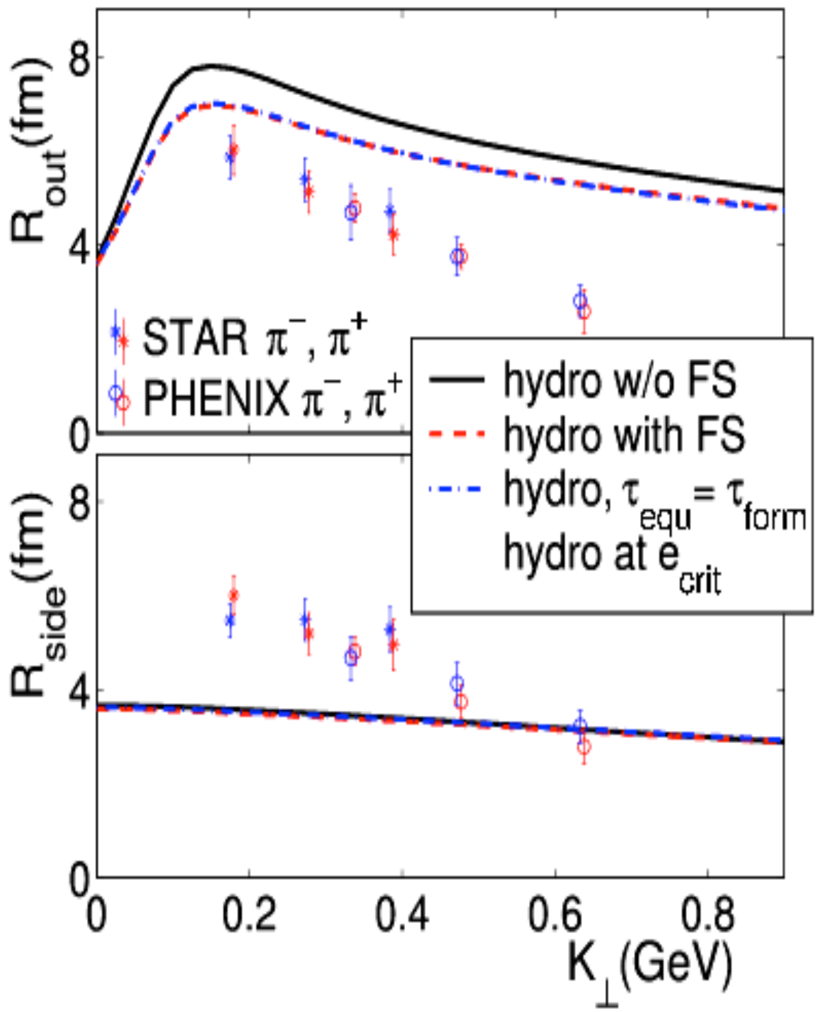

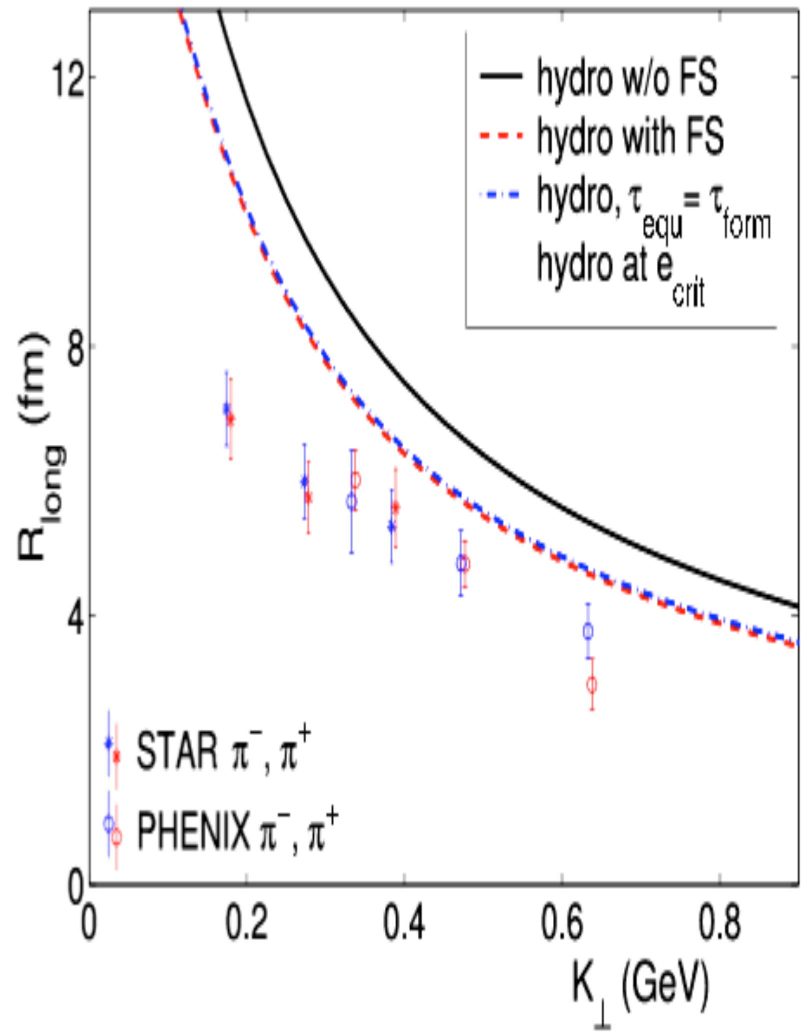

Fails to explain the extracted source sizes

Two-Pion Correlation Functions and source radii from AMPT

Lin, Ko & Pal, PRL 89, 152301 (2002)

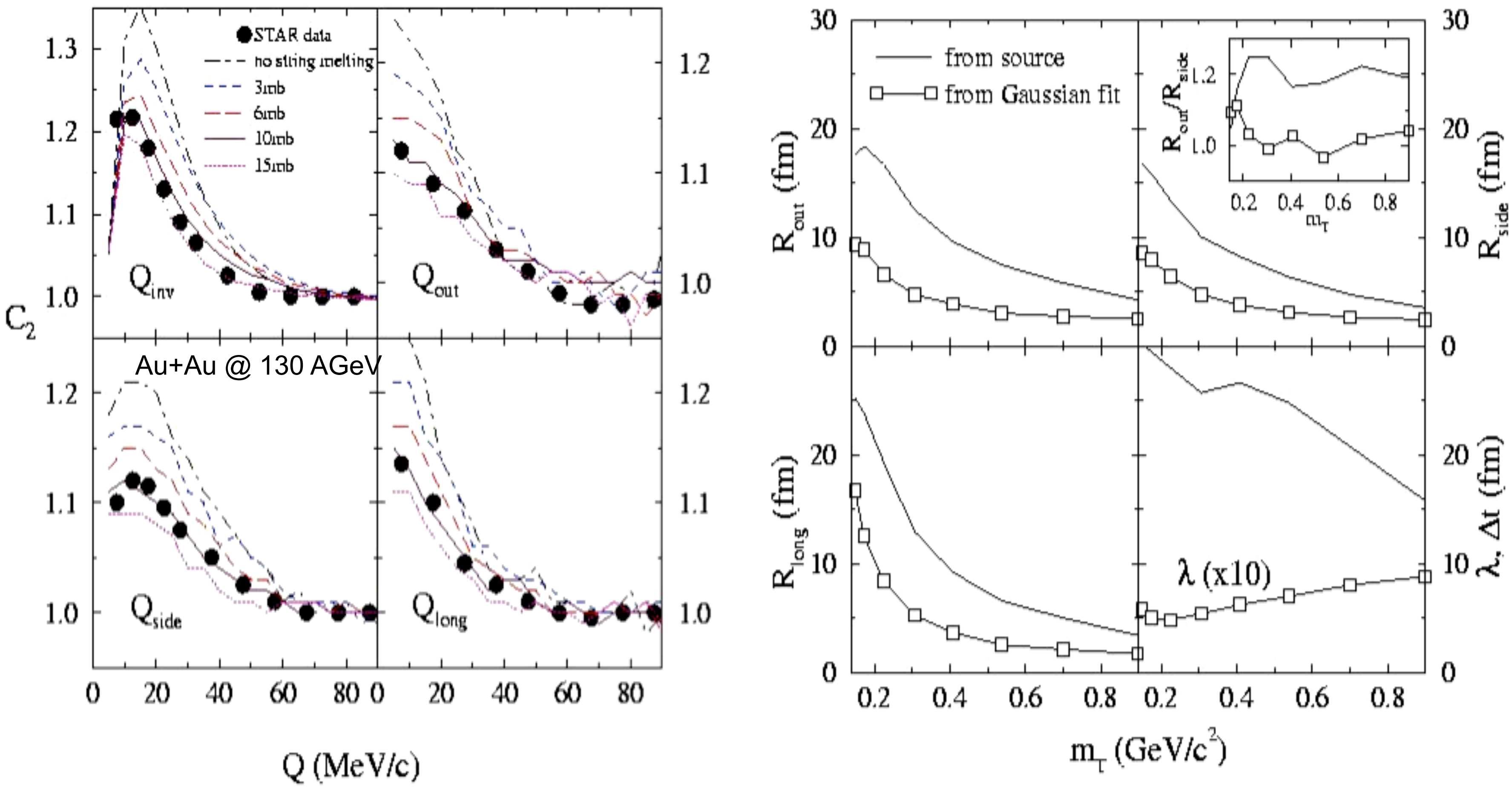

Need string melting and large parton scattering cross sections

Emission Function from AMPT

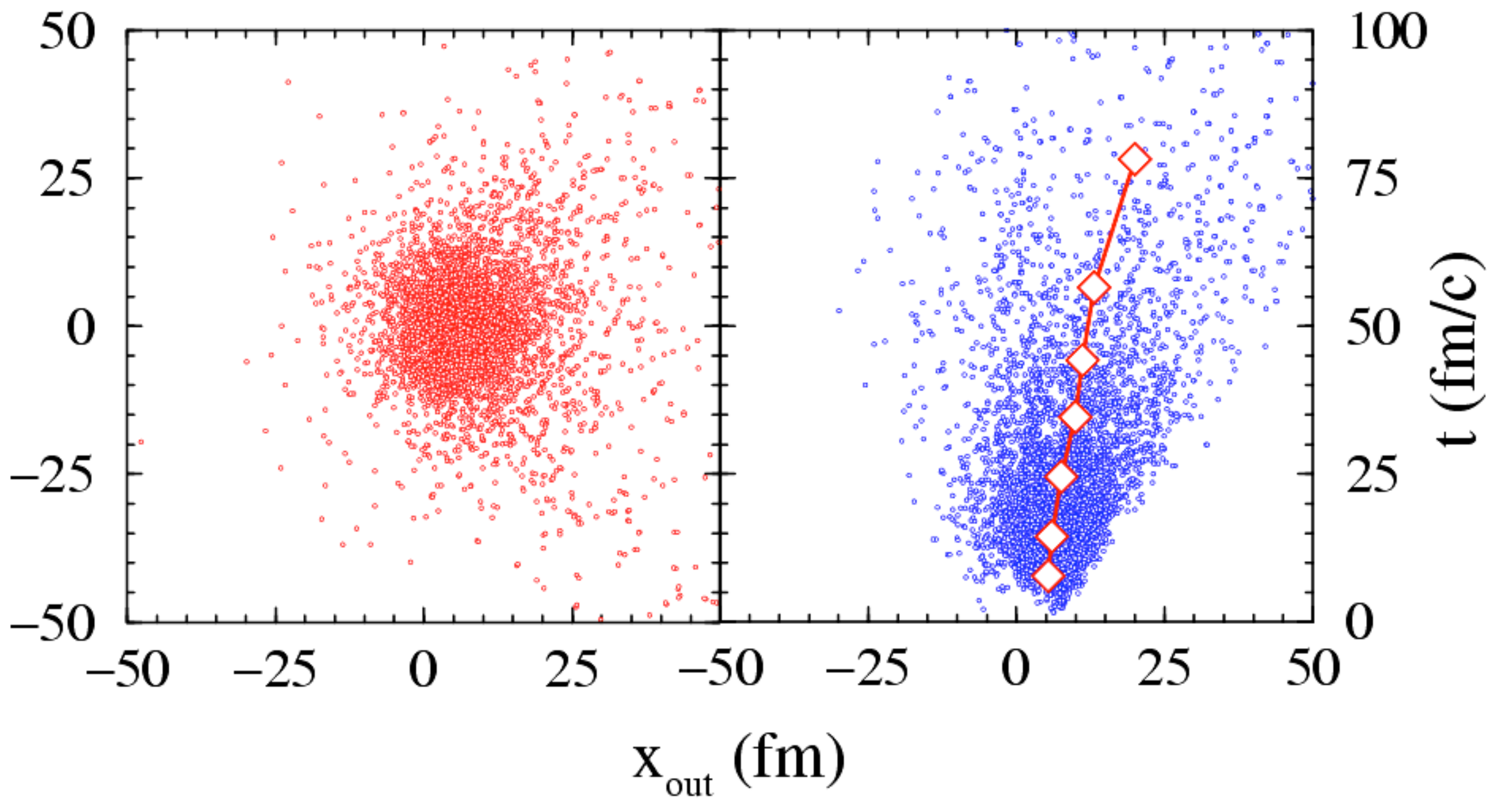

- Shift in out direction ($\langle x_{out} \rangle > 0$)
- Strong positive correlation between out position and emission time
- Large halo due to resonance (ω) decay and explosion
  → non-Gaussian source

High P_T hadron suppression

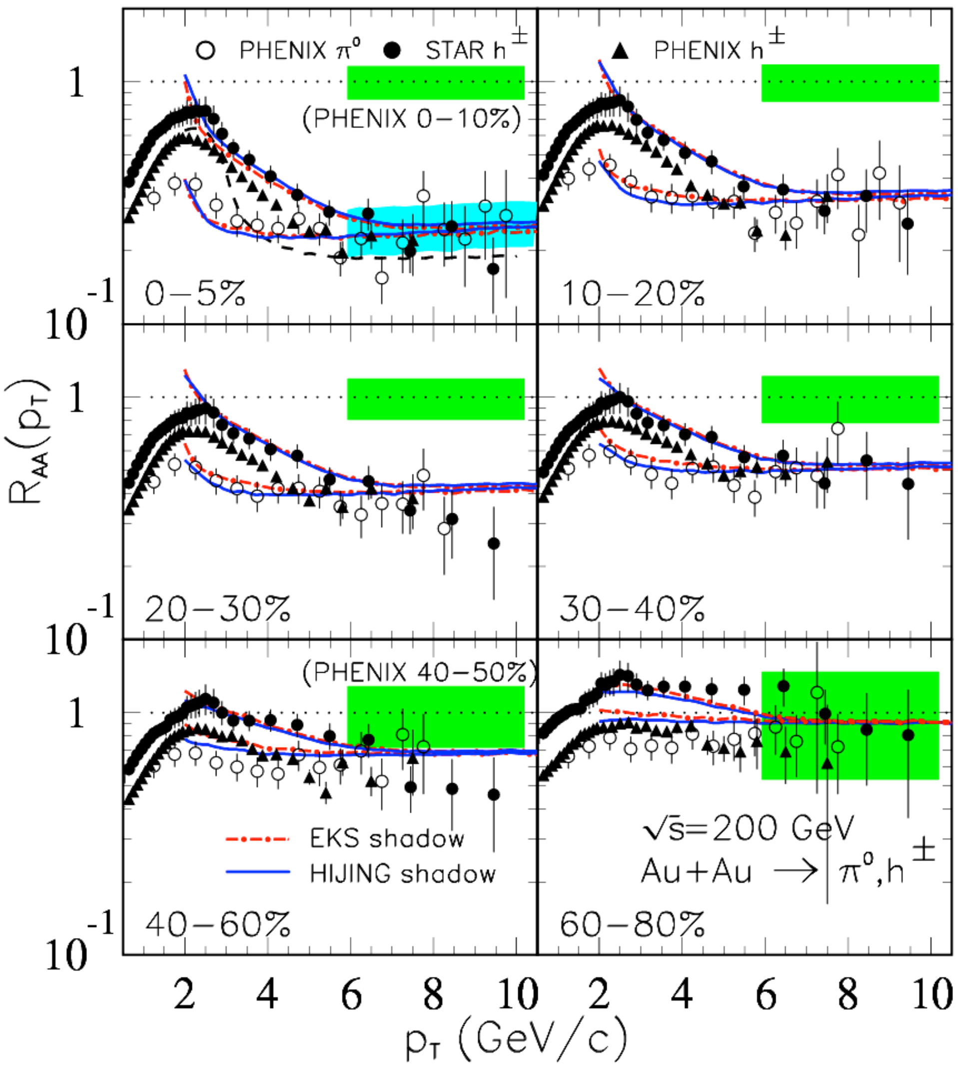

$$R_{AA} = \frac{dN_{Au+Au}}{\langle T_{AA} \rangle d\sigma_{p+p}}$$

Gyulassy, Levai & Vitev, PRL 85, 5535 (00)

Wang & Wang, PRL 87, 142301 (01)

Parton energy loss due to radiation

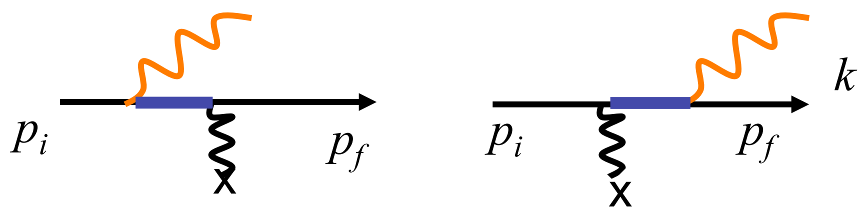

Jet quenching → initial energy density → 5-10 GeV/fm^3

p/π⁺ and pbar/π⁻ ratios at high transverse momentum

STAR Collaboration, PRL 97, 152301 (07)

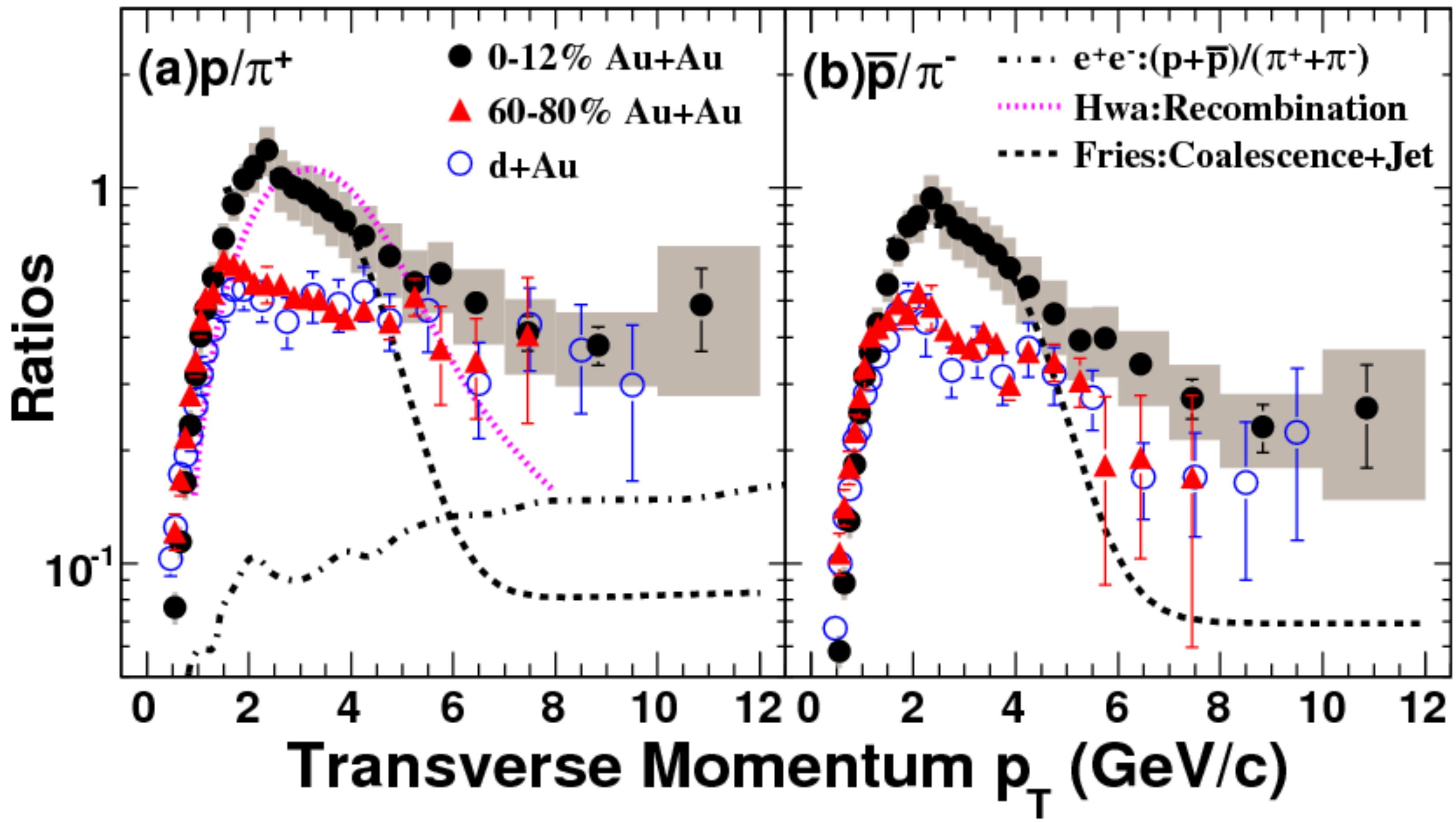

Same p/π⁺ and $\overline{p}$/π⁻ ratios in central and peripheral collisions → Same R_{AA} for gluon and quark jets, which is not expected from radiative energy loss as gluon jets lose more energy than quark jets.

Jet conversions in QGP

Liu, Zhang & Ko, PRC 75, 05190 (R) (2007); Few Body Sys. 41, 63 (2007).

- Quark jet conversion

Elastic process: qg→gq

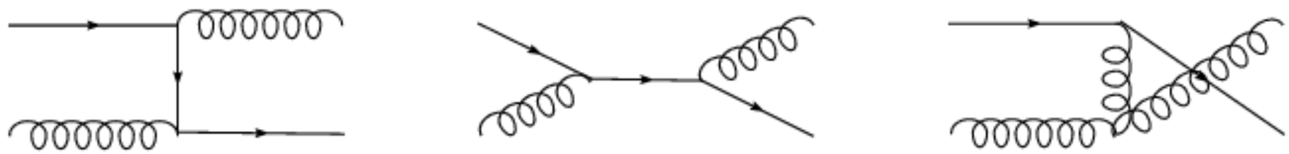

Gluon is taken to have a larger momentum in the final state

Inelastic process: $q\overline{q} \rightarrow gg$

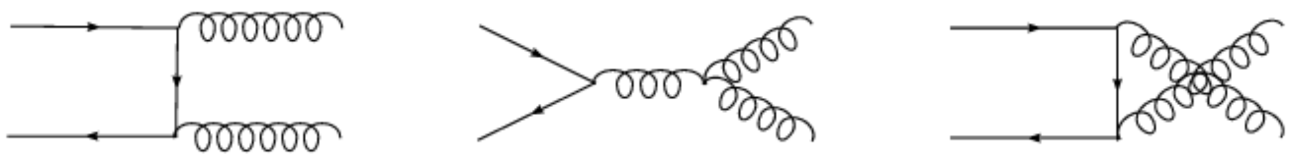

- Gluon jet conversion: similar to above via inverse reactions

- Radiative conversion: 2→3

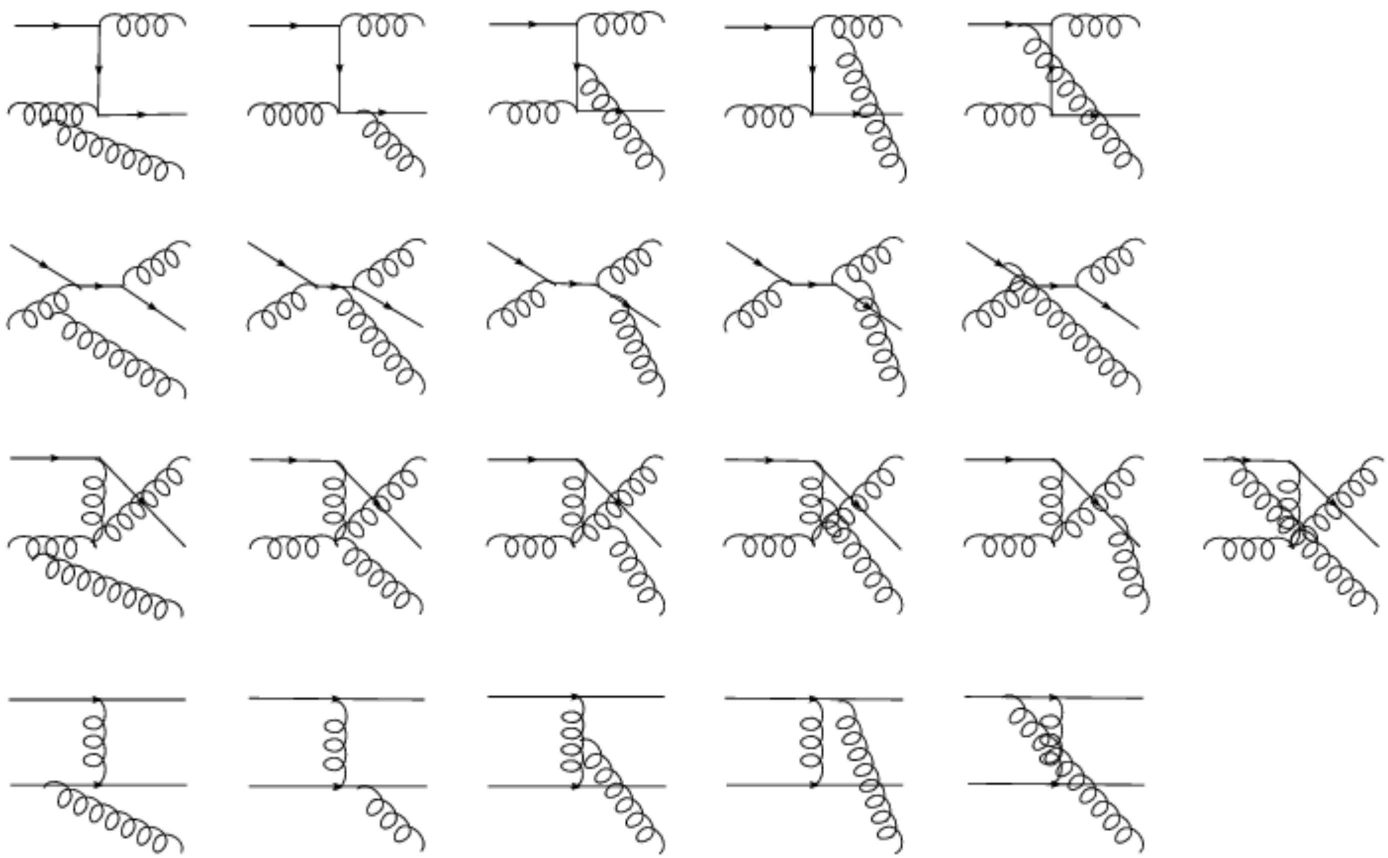

+ ………

<u>Coalescence + jet quenching + jet conversion</u>

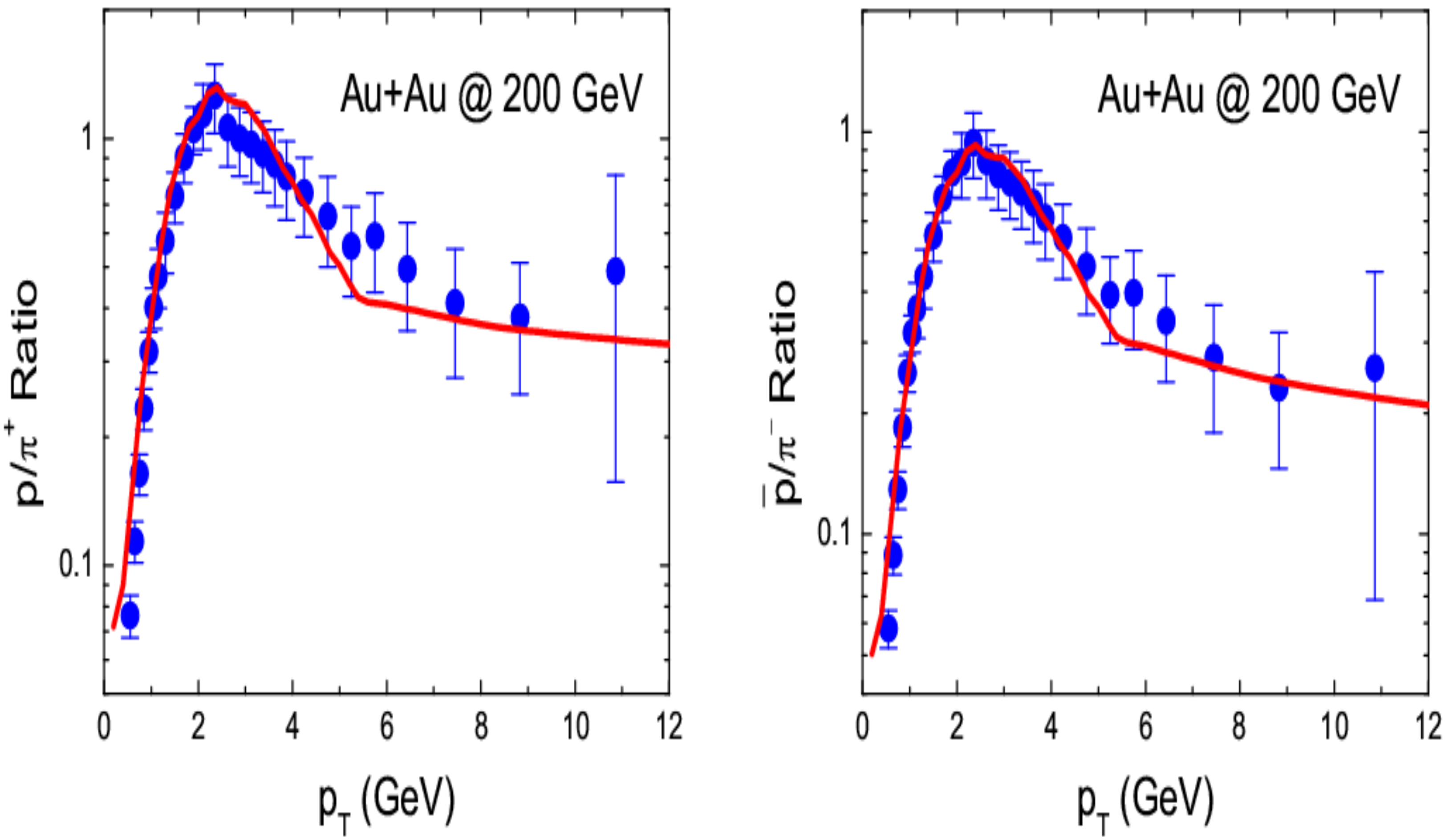

Jet conversion leads to good description of data

Anisotropic flow

Anisotropic flow v_n

$$E\frac{d^3N}{d^3\vec{p}} = \frac{dN}{p_T dp_T d\varphi dy} = \frac{1}{2\pi}\frac{dN}{p_T dp_T dy}\left[1 + \sum_{n=1}^{\infty} 2v_n(p_T, y)\cos(n\varphi)\right]$$

Sine terms vanish because of the symmetry Φ ➔ -Φ in A+A collisions

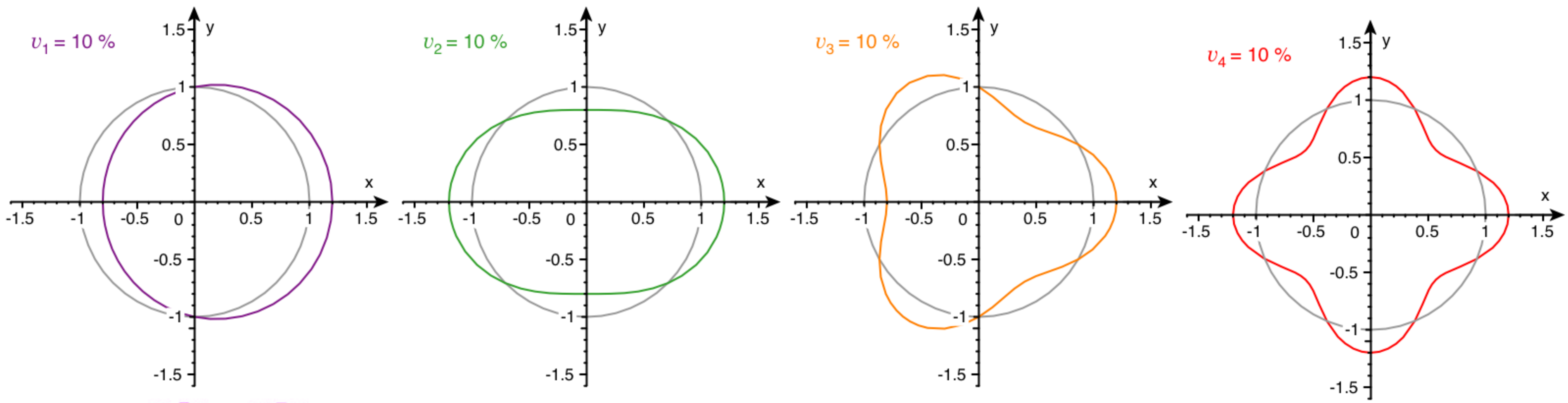

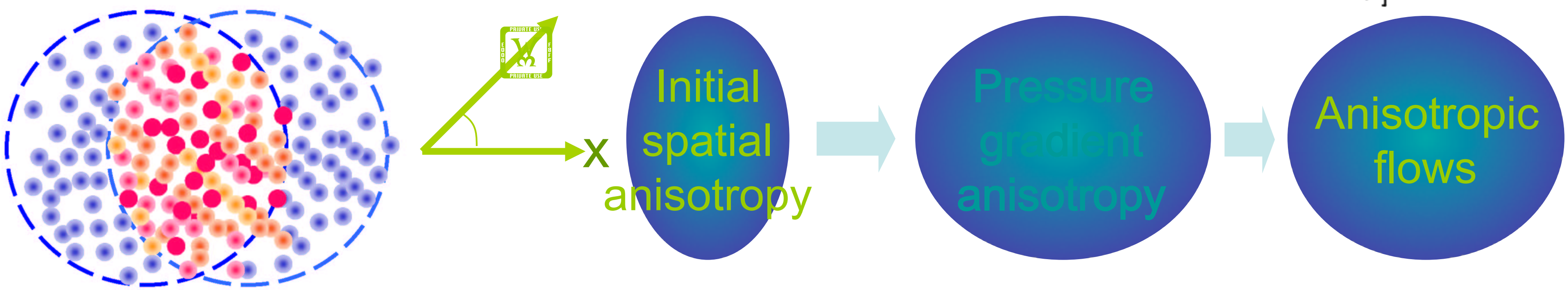

Elliptic flow from hydrodynamic model

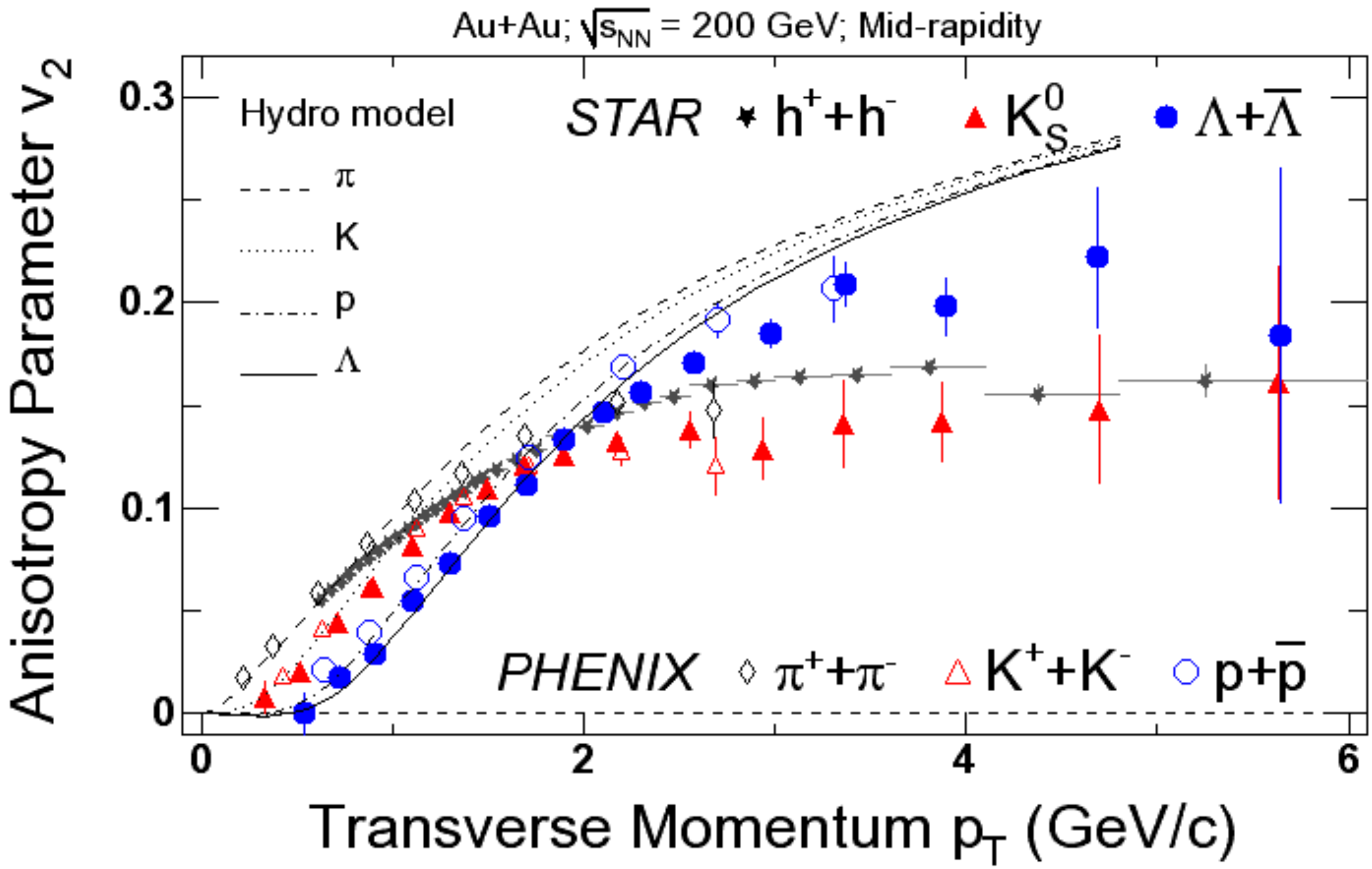

Ideal hydro describes very well data at low p_T (mass effect) but fails at intermediate $p_T \rightarrow$ viscous effect.

Elliptic flow from AMPT

Lin & Ko, PRC 65, 034904 (2002)

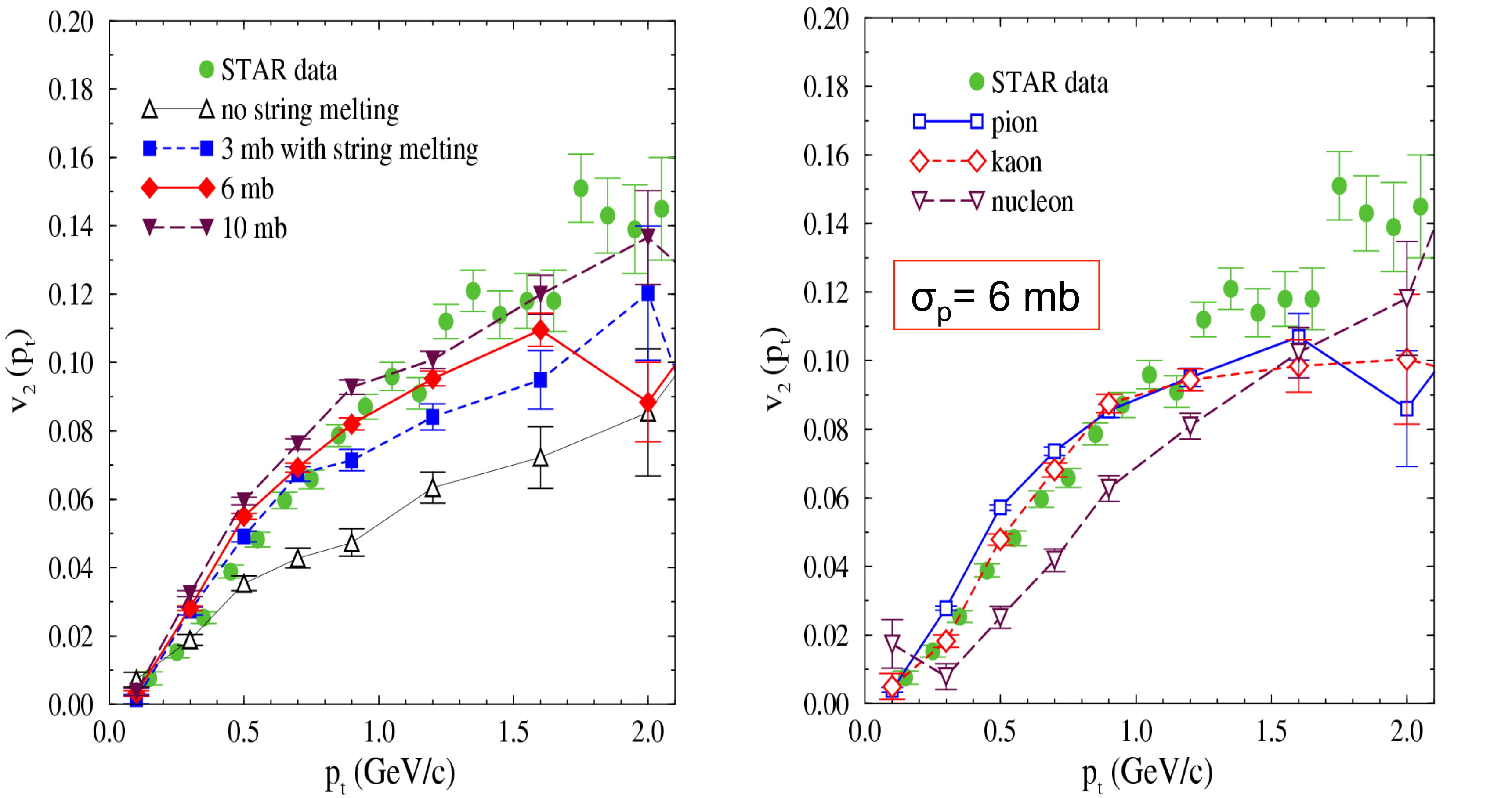

- Need string melting and large parton scattering cross section
- Mass ordering of v_2 at low p_T as in hydrodynamic model

Surprise: quark number scaling of hadron elliptic flow

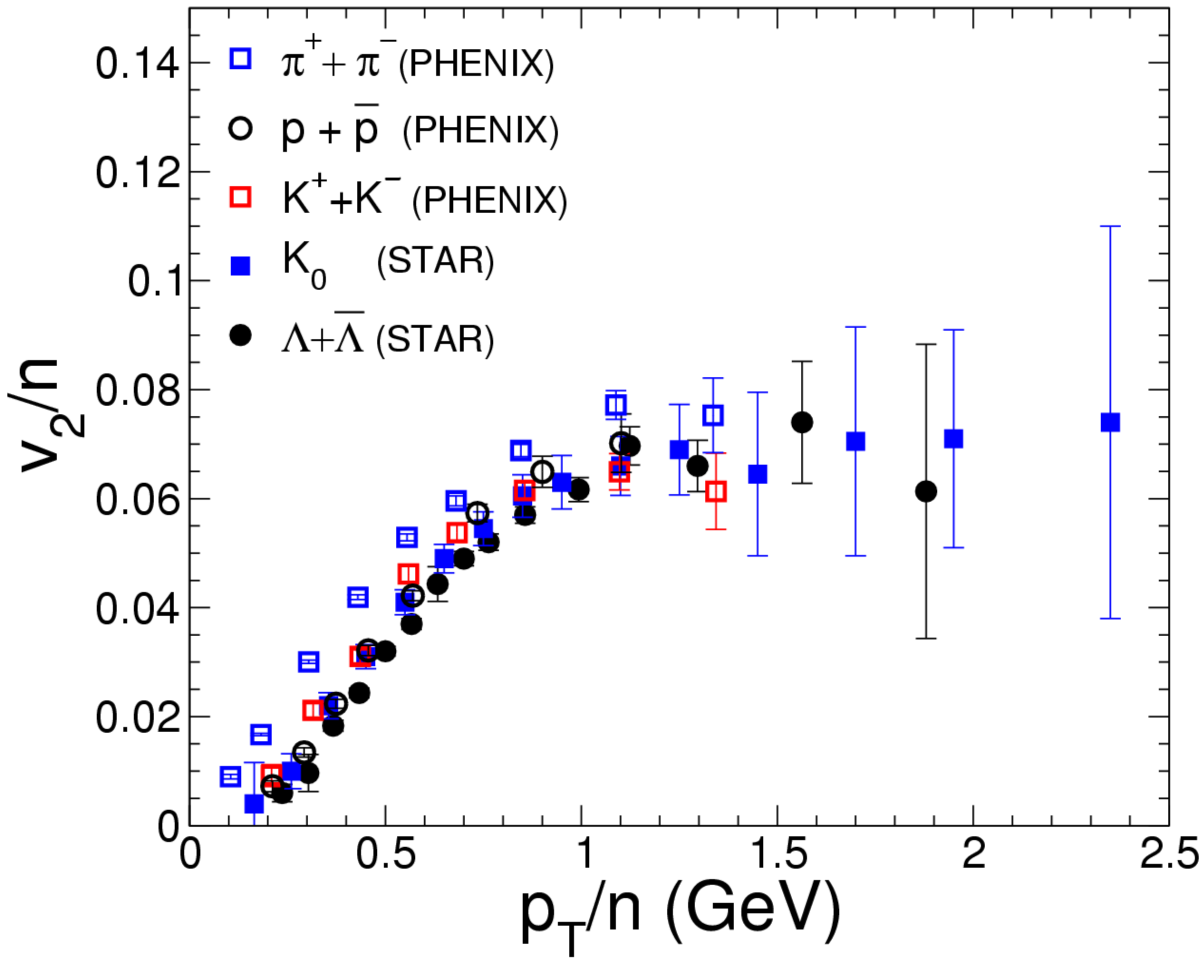

Except pions, $v_{2,M}(p_T) \sim 2\, v_{2,q}(p_T/2)$ and $v_{2,B}(p_T) \sim 3\, v_{2,q}(p_T/3)$ consistent with hadronization via quark recombination

Momentum-space quark coalescence model

Only quarks of same momentum can coalescence, i.e., $\Delta p=0$

Quark transverse momentum distribution

$$f_q(p_T) \propto 1 + 2v_{2,q}(p_T)\cos(2\phi)$$

Meson elliptic flow

$$v_{2,M}(p_T) = \frac{2v_{2,q}(p_T/2)}{1+2v_{2,q}^2(p_T/2)} \approx 2v_{2,q}(p_T/2)$$

Baryon elliptic flow

$$v_{2,B}(p_T) = \frac{3v_{2,q}(p_T/3)}{1+6v_{2,q}^2(p_T/3)} \approx 3v_{2,q}(p_T/3)$$

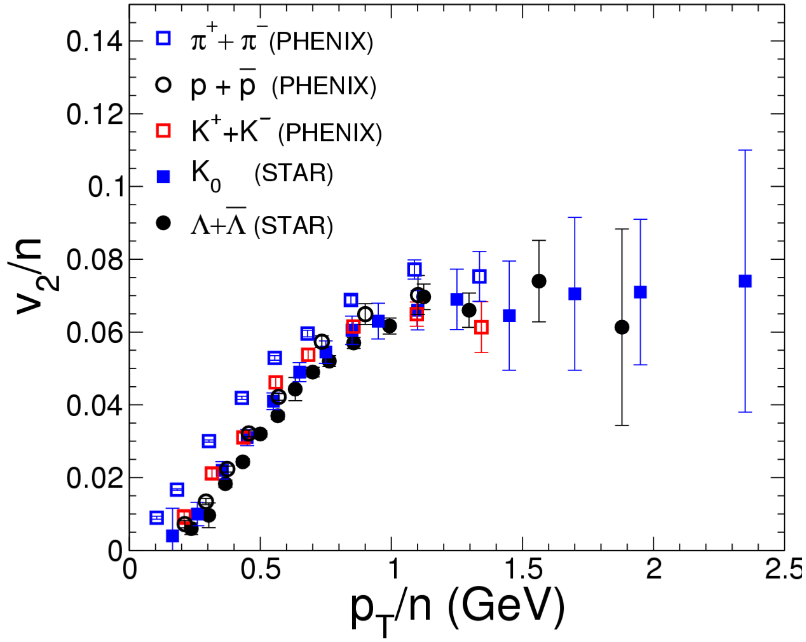

Quark number scaling of hadron v_2 (except pions):

$$\frac{1}{n} v_2(p_T/n)$$

same for mesons and baryons

Coalescence model

PRL 90, 202102 (2003); PRC 68, 034904 (2003)

Number of hadrons with n quarks and/or antiquarks

$$N_n = g \int \prod_{i=1}^{n} p_i d\sigma_i \frac{dp_i}{(2\pi)^3 E_i} f_{q,i}(x_i, p_i) f_n(x_1, \ldots, x_n; p_1, \ldots, p_n)$$

Spin-color statistical factor g_M e.g. $g_\pi = g_K = 1/36 \quad g_\rho = g_{K^*} = 1/12$

$$g_p = g_{\bar{p}} = 1/108, \quad g_\Delta = g_{\bar{\Delta}} = 1/54$$

Quark distribution function $f_q(x, p)$

$$\int p \cdot d\sigma \frac{d^3 p}{(2\pi)^3 E} f_q(x, p) = N_q$$

Coalescence probability function

$$\begin{aligned} f_M(x_1, x_2; p_1, p_2) &= f_2(x_1 - x_2; p_1 - p_2) \\ &= \exp[(x_1 - x_2)^2 / 2\Delta_x^2] \\ &\times \exp\{[(p_1 - p_2)^2 - (m_1 - m_2)^2]/2\Delta_p^2\} \end{aligned}$$

$$\Delta_x \cdot \Delta_p \geq \hbar$$

For baryons, Jacobi coordinates for three-body system are used.

Effects of hadron wave function and resonance decays

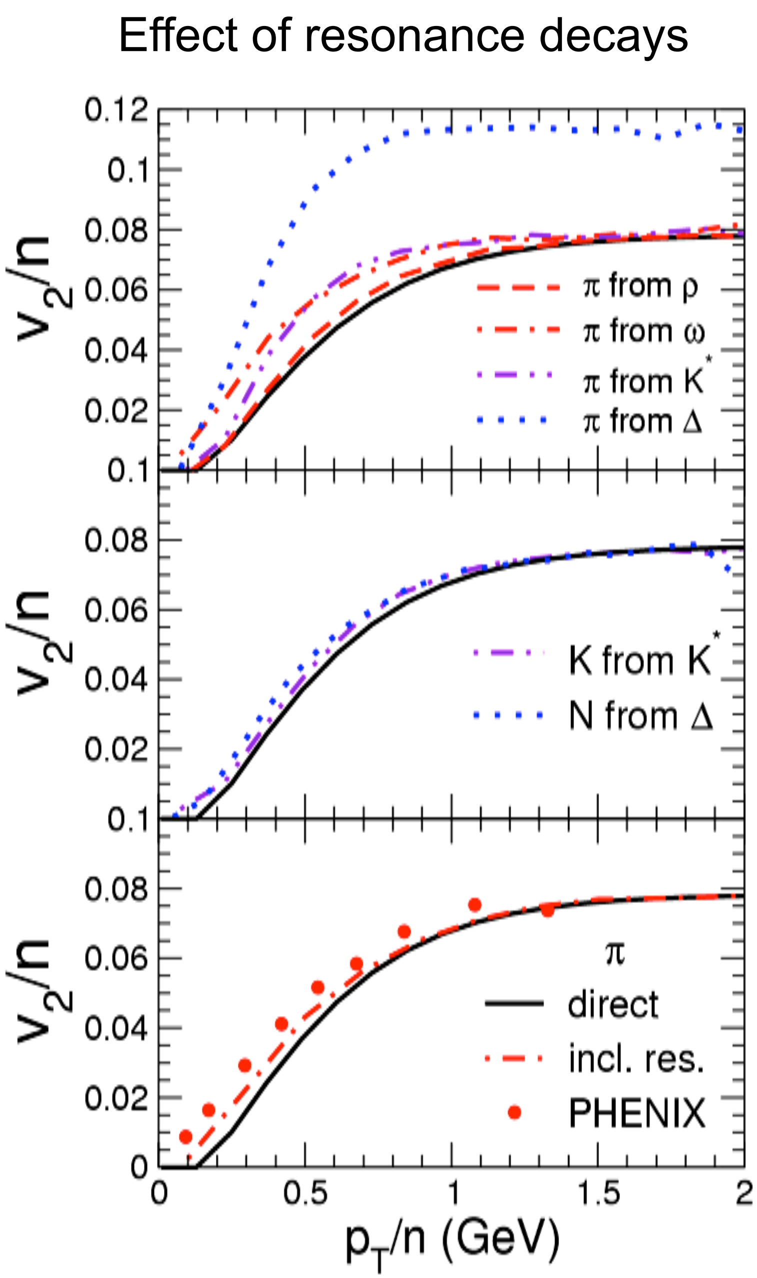

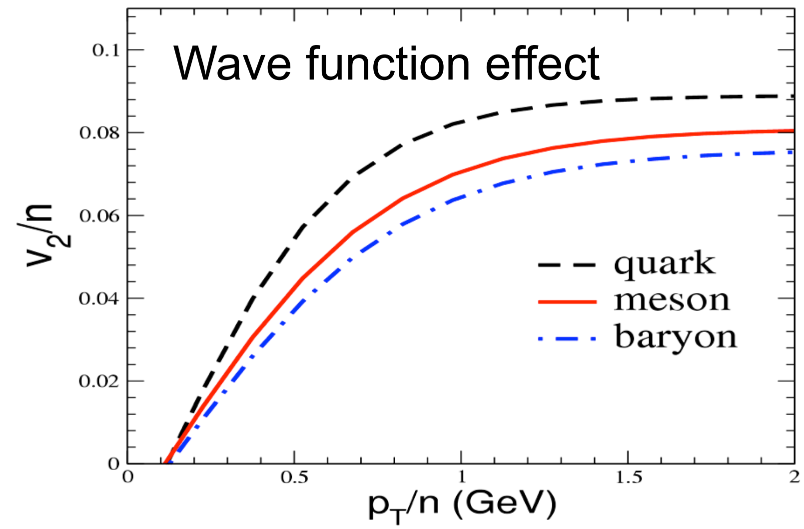

Higher fock states → similar effect (Duke)

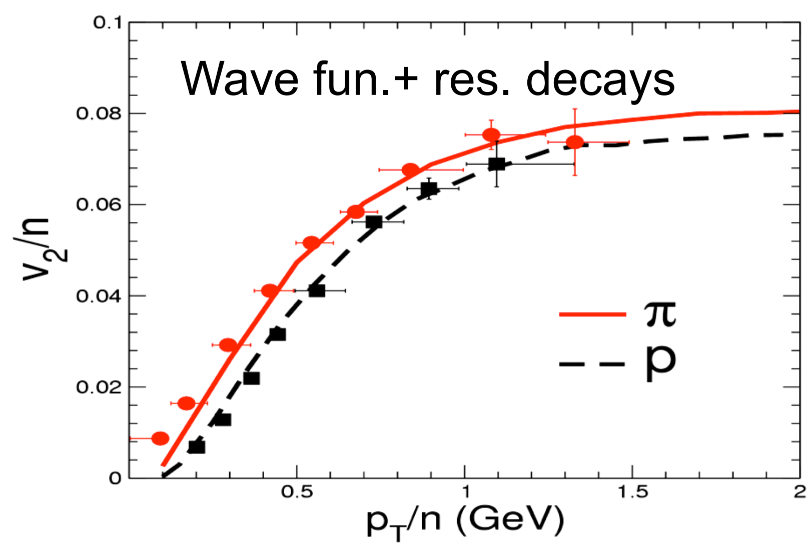

Puzzle: Large proton/meson ratio

PHENIX, nucl-ex/0304022

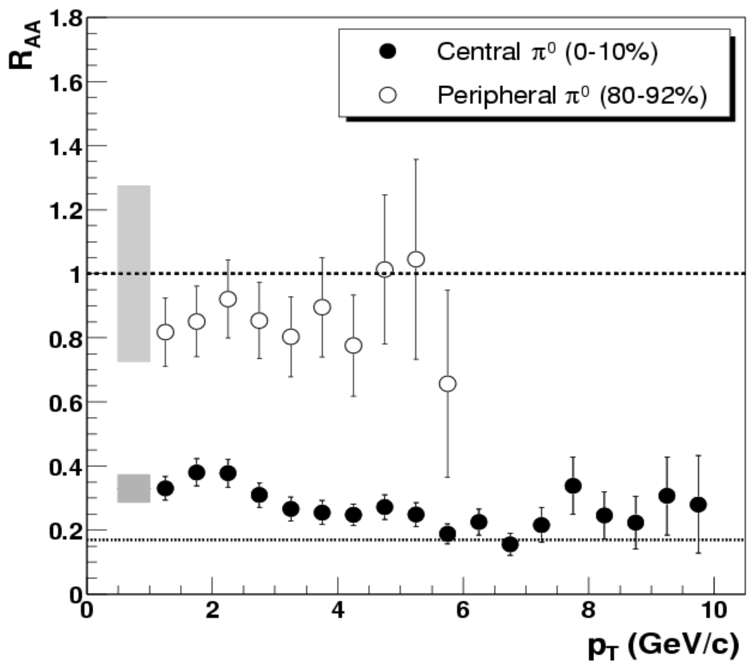

$$R_{AA} = \frac{dN_{Au+Au}}{\langle N_{bin} \rangle dN_{p+p}}$$

π^0 suppression: evidence of jet quenching before fragmentation

PHENIX, nucl-ex/0212014

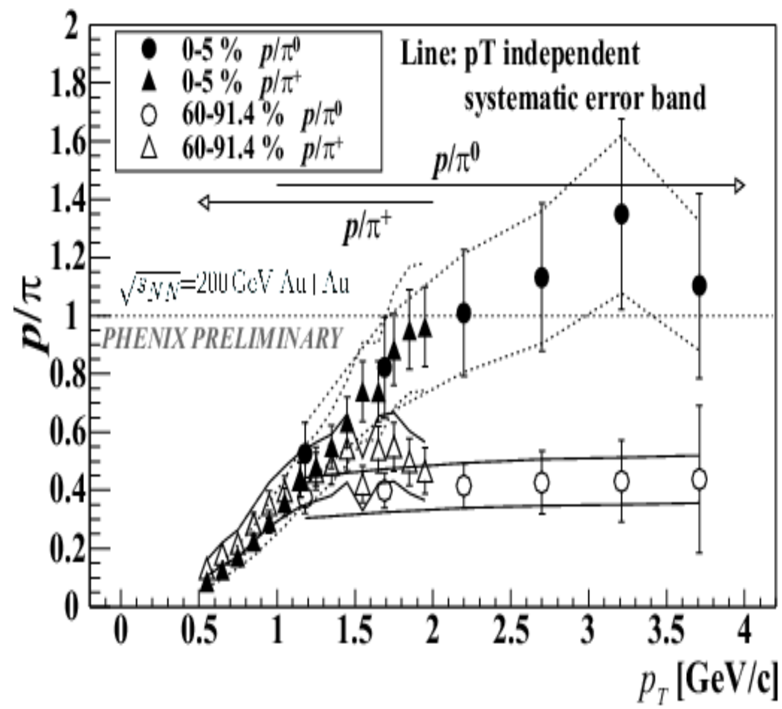

- Fragmentation leads to p/π ~ 0.2
- Jet quenching affects both
- Fragmentation is not the dominant mechanism of hadronization at p_T < 4-6 GeV

Large proton to pion ratio

Quark coalescence or recombination can also explain observed large p/pi ratio at intermediate transverse momentum in central Au+Au collisions.

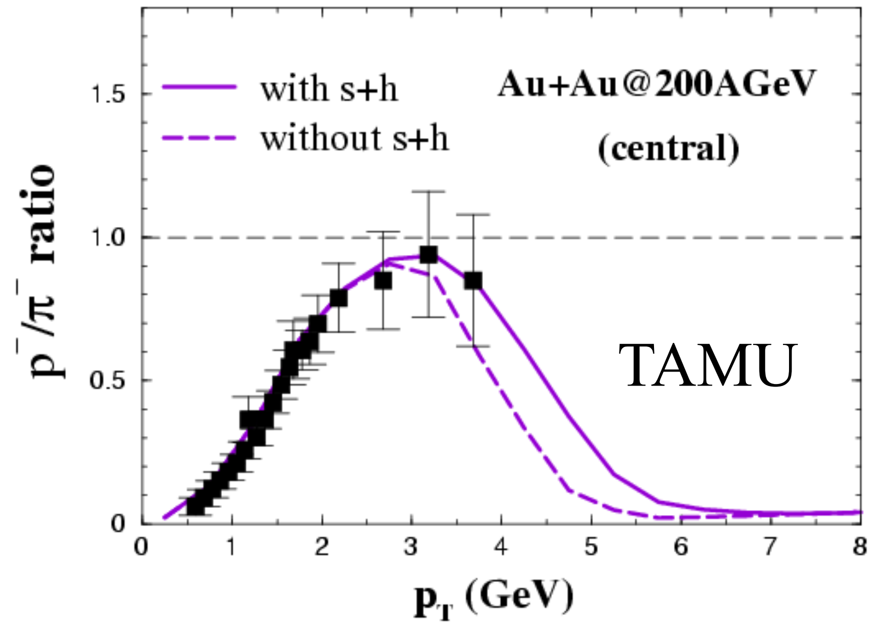

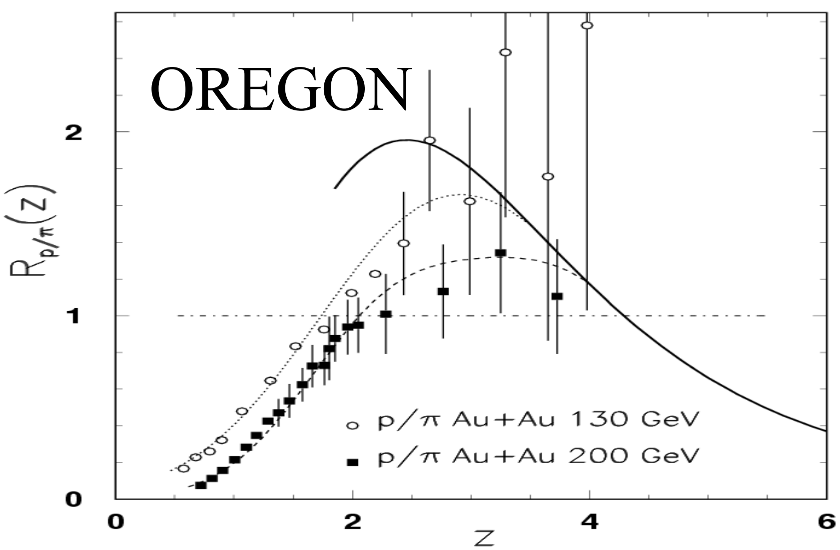

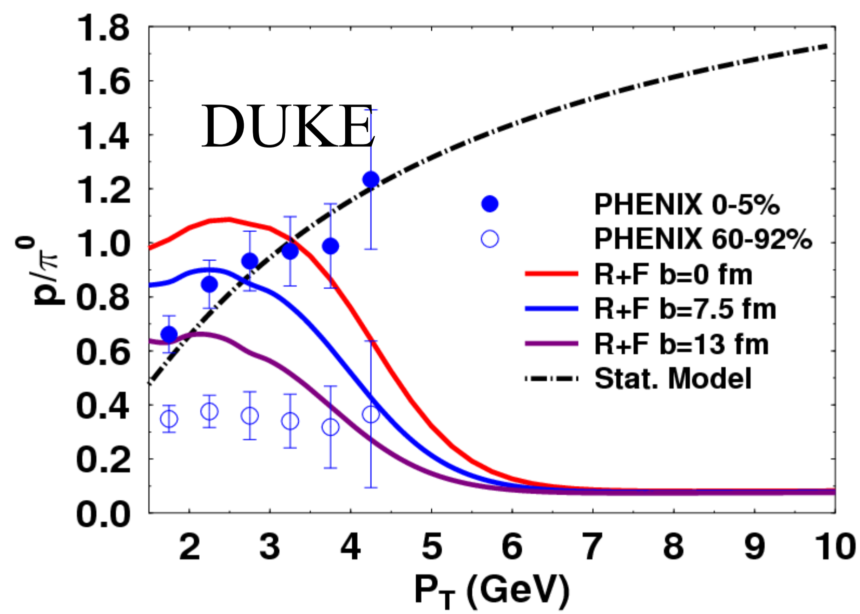

Higher-order parton anisotropic flows

Including 4th order quark flow   Kolb, Chen, Greco, Ko, PRC 69 (2004) 051901

$$f_q(p_T) \propto 1 + 2v_{2,q}(p_T)\cos(2\phi) + 2v_{4,q}(p_T)\cos(4\phi)$$

Meson elliptic flow

$$v_{2,M} = \frac{2v_{2,q} + 2v_{2,q}v_{4,q}}{1+2(v_{2,q}^2 + v_{4,q}^2)}, \quad v_{4,M} = \frac{2v_{4,q} + v_{2,q}^2}{1+2(v_{2,q}^2 + v_{4,q}^2)}$$

Baryon elliptic flow

$$v_{2,B} = \frac{3v_{2,q} + 6v_{2,q}v_{4,q} + 3v_{2,q}^3 + 6v_{2,q}v_{4,q}^2}{1+6(v_{2,q}^2 + v_{4,q}^2 + v_{2,q}^2 v_{4,q})}, \quad v_{4,B} = \frac{3v_{4,q} + 3v_{2,q}^2 + 6v_{2,q}^2 v_{4,q} + 3v_{4,q}^3}{1+6(v_{2,q}^2 + v_{4,q}^2 + v_{2,q}^2 v_{4,q})}$$

$$\Rightarrow \frac{v_{4,M}}{v_{2,M}^2} = \frac{1}{4} + \frac{1}{2}\frac{v_{4,q}}{v_{2,q}^2}, \quad \frac{v_{4,B}}{v_{2,B}^2} = \frac{1}{3} + \frac{1}{3}\frac{v_{4,q}}{v_{2,q}^2}$$

Higher-order anisotropic flows

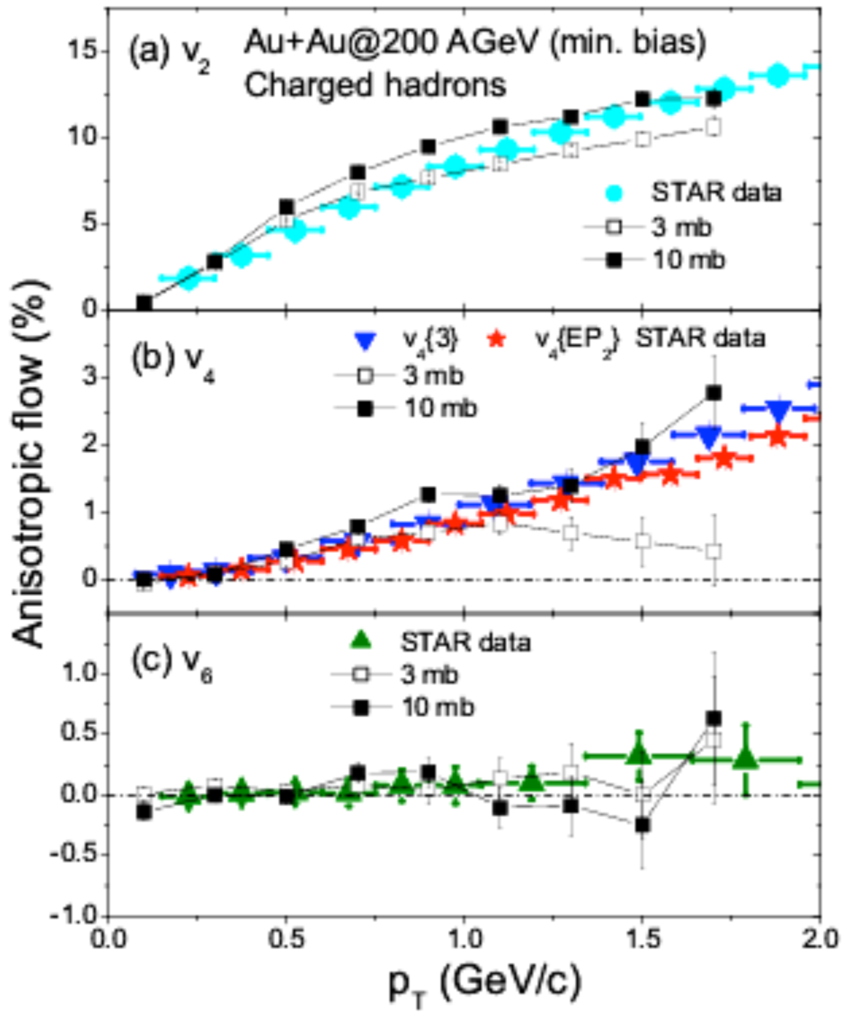

Data can be described by a multiphase transport (AMPT) model with large parton cross sections.

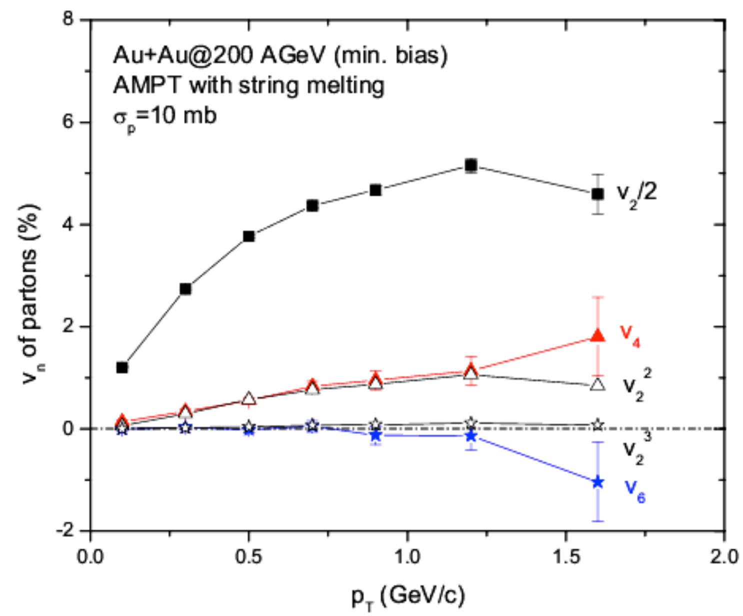

Data $$\frac{v_4}{v_2^2} \approx 1.2 \Rightarrow v_{4,q} \approx 2v_{2,q}^2$$

Parton cascade gives $v_{4,q} \sim v_{2,q}^2$

Charmed meson elliptic flow

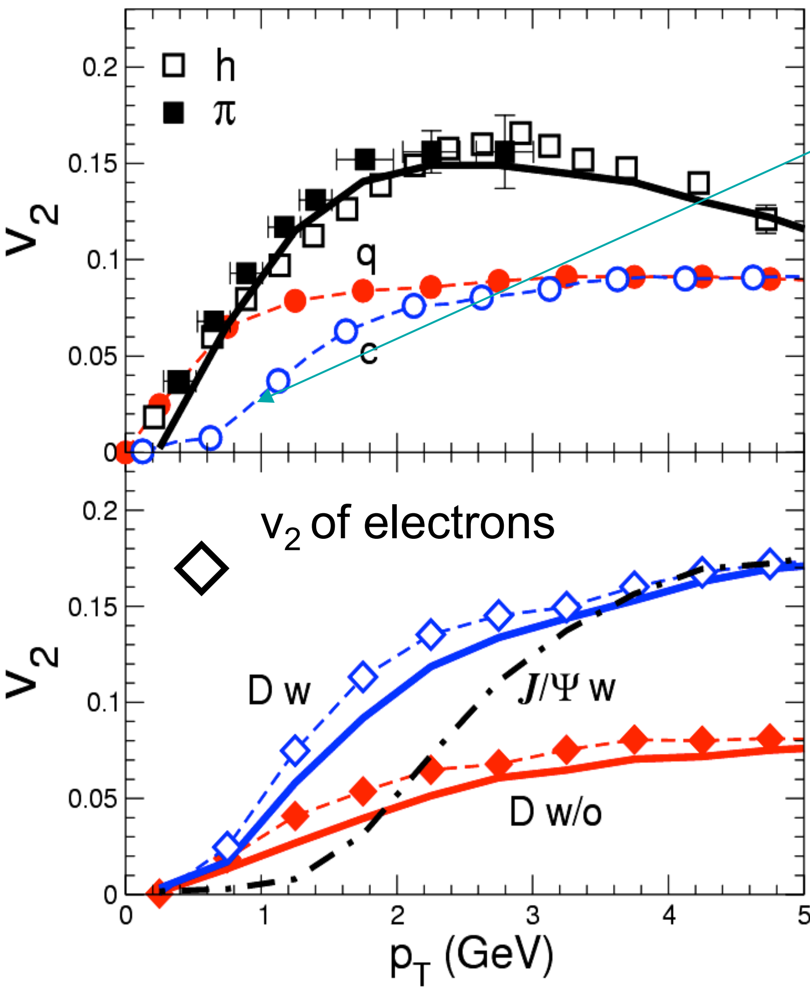

Greco, Rapp, Ko, PLB595 (04) 202

Smaller charm v_2 than light quark v_2 at low p_T due to mass effect

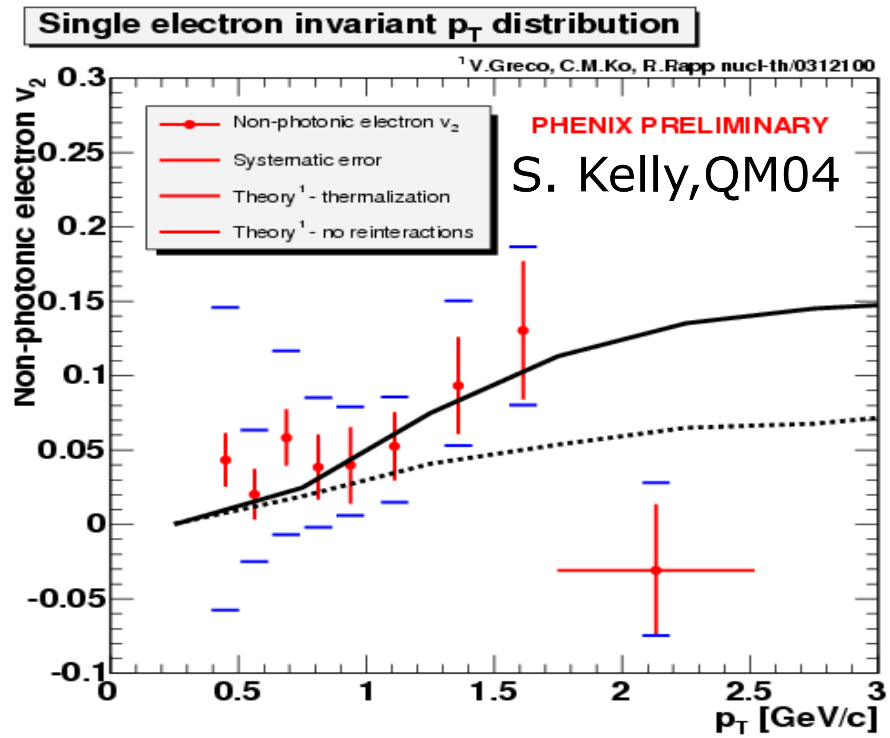

Data consistent with thermalized charm quark with same v_2 as light quarks before boosted by radial flow

Charm R_{AA} and elliptic flow from AMPT

Zhang, Chen & Ko, PRC 72, 024906 (05)

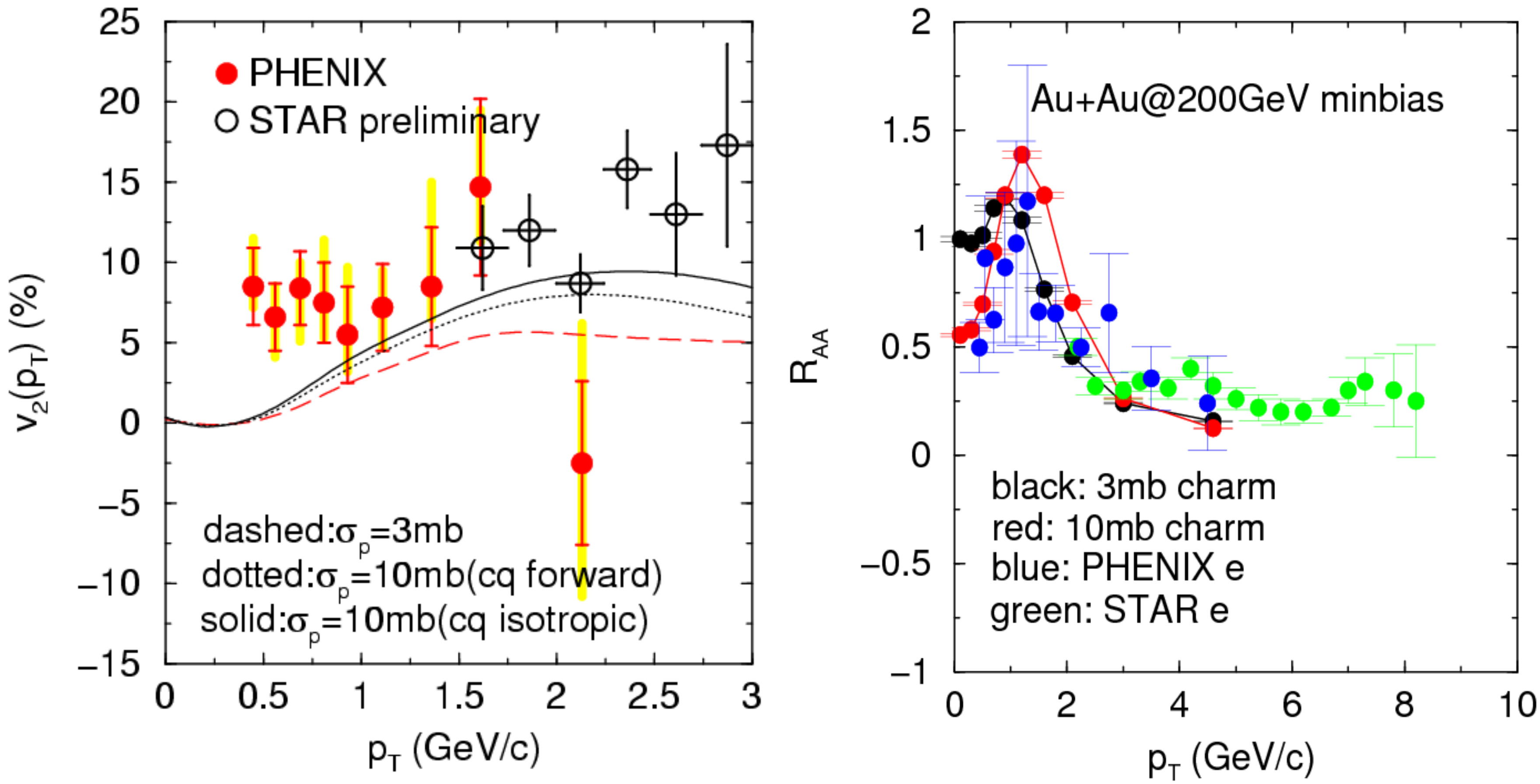

- Need large charm scattering cross section to explain data
- Smaller charmed meson elliptic flow is due to use of current light quark masses

Resonance effect on charm scattering in QGP

Van Hees & Rapp, PRC 71, 034907 (2005)

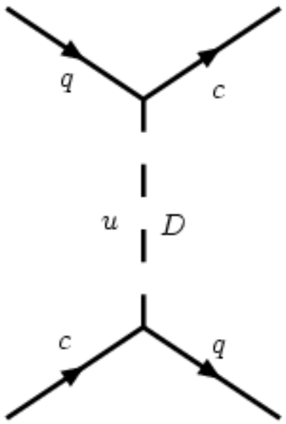

$$\boxed{\sigma_{c\bar{q}?c\bar{q}} = \frac{1}{9}\,\frac{2J+1}{4}\,\frac{\pi}{k^2}\,\frac{\Gamma_D^2}{\left(s^{1/2}-m_D\right)^2+\Gamma_D^2/4}}$$

With $m_c \approx 1.5$ GeV, $m_q \approx 5$-10 MeV, $m_D \approx 2$ GeV, $\Gamma_D \approx 0.3$-0.5 GeV, and including scalar, pseudoscalar, vector, and axial vector D mesons gives

$$\boxed{\sigma_{cq\to cq}(s^{1/2}=m_D)\approx 6\text{ mb}}$$

Since the cross section is isotropic, the transport cross section is 6 mb, which is about 4 times larger than that due to pQCD t-channel diagrams, leading to a charm quark drag coefficient $\gamma \sim 0.16$ c/fm in QGP at T=225 MeV.

Heavy quark energy loss in pQCD

a) Radiative energy loss (Amesto *et al.,* hep-ph/0511257)

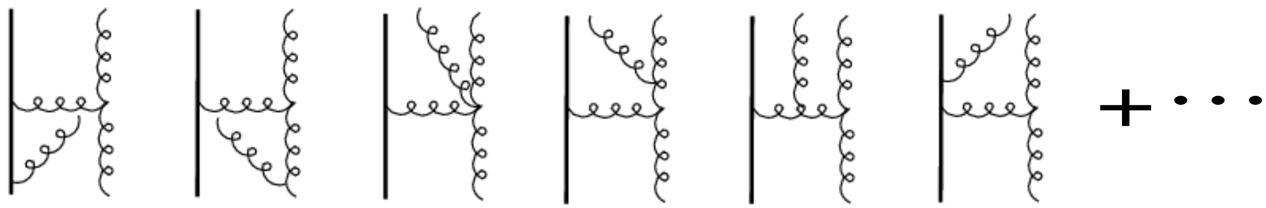

b) Radiative and elastic energy loss (Wicks *et al.,* nucl-th/0512076)

a) +

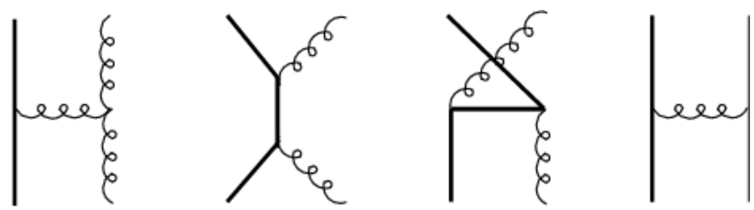

c) Three-body elastic scattering (Liu & Ko, nucl-th/0603004: NPA 783,233c (2007))

a) +b) +

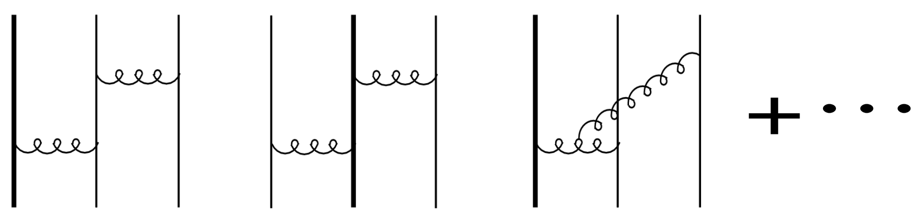

- May be important as interparton distance ~ range of parton interaction
- At T=300 MeV, N_g~(N_q+N_{qbar})~ 5/fm^3, so interparton distance ~ 0.3 fm
- Screening mass m_D=gT~600 MeV, so range of parton interaction ~ 0.3 fm

Spectrum and nuclear modification factor of electrons from heavy meson decay

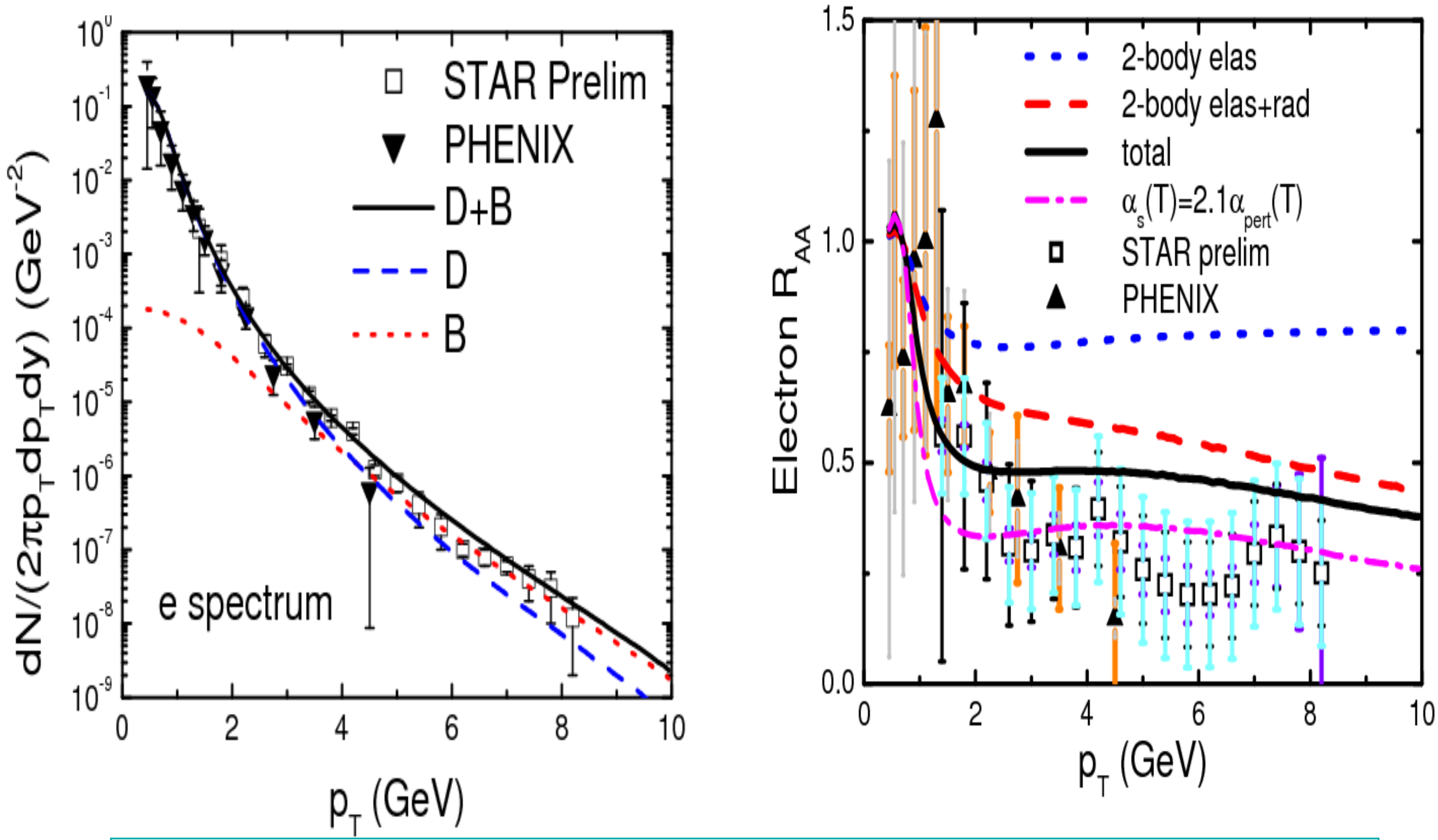

Reasonable agreement with data from Au+Au @ 200A GeV after including heavy quark three-body scattering.

Enhancement of charmed baryon to meson ratio on non-photonic electrons in HIC

- Sorenson, EJPC 49, 379 (2007)

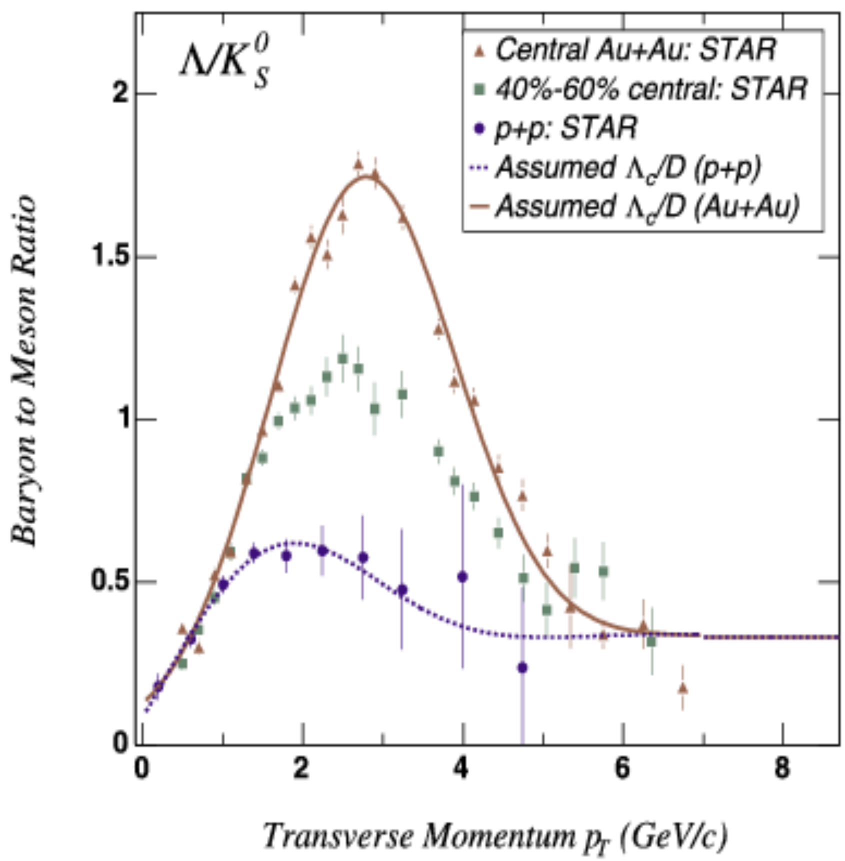

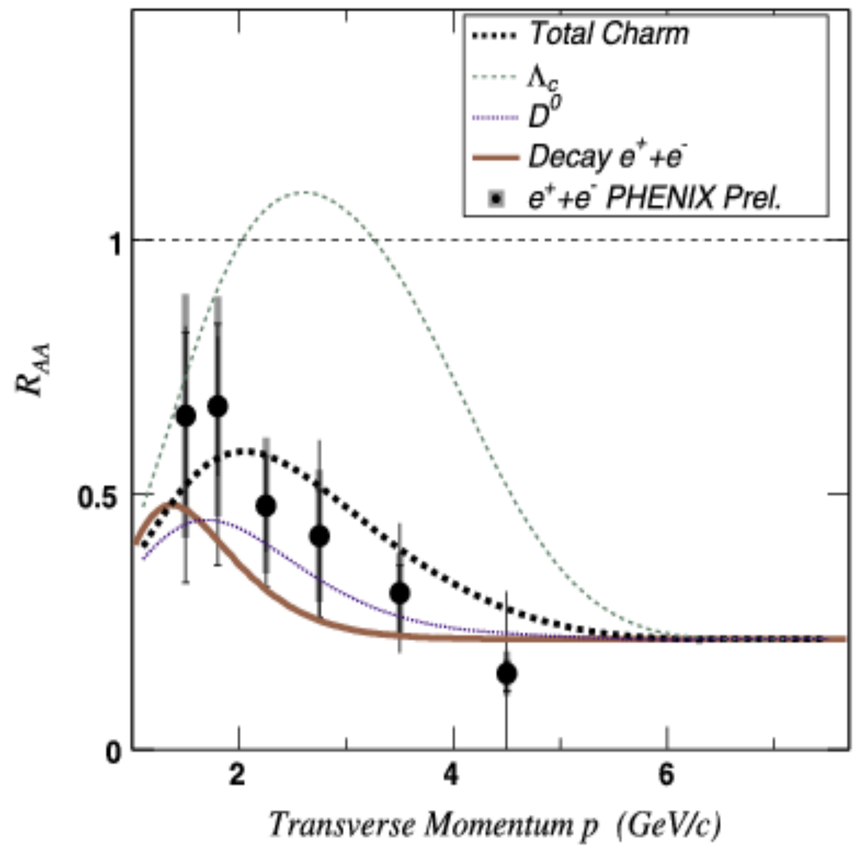

Assuming that same Λ_c/D^0 and Λ/K^0 ratios could also explain observed nuclear modification factor for charmed mesons

Diquark in sQGP and Λ_c enhancement

Lee, Yasui, Ohnishi, Yoo & Ko, PRL 100, 222301 (08)

Diquark mass due to color-spin interaction:

$$m_{[ud]} \approx m_u + m_d - C\,\vec{s}_u \cdot \vec{s}_d \frac{1}{m_u m_d} \approx 450\,\mathrm{MeV}$$

for $m_u=m_d= 300$ MeV and $C/m_u^2 \sim 195$ Me V from $m_\Delta - m_N$

Coalescence model

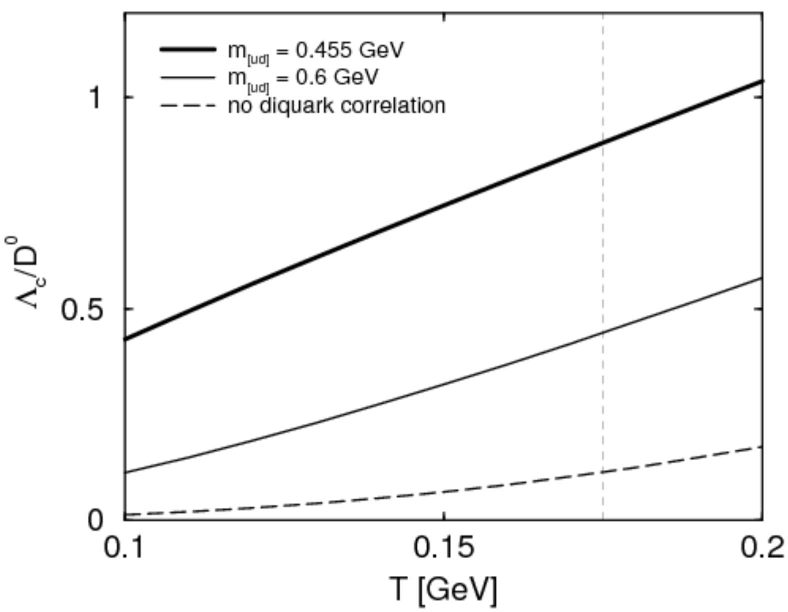

Statistical model

$$\frac{\Lambda_c}{D_0} \approx 2\left(\frac{m_{\Lambda_c}}{m_{D_0}}\right)^{3/2} e^{-(m_{\Lambda_c}-m_{D_0})/T_c} \approx 0.24$$

- Enhanced by a factor of 4-8
- Similar for Λ_B/B_0

Inclusion of resonances and fragmentation

Oh et al., PRC 79, 044905 (09)

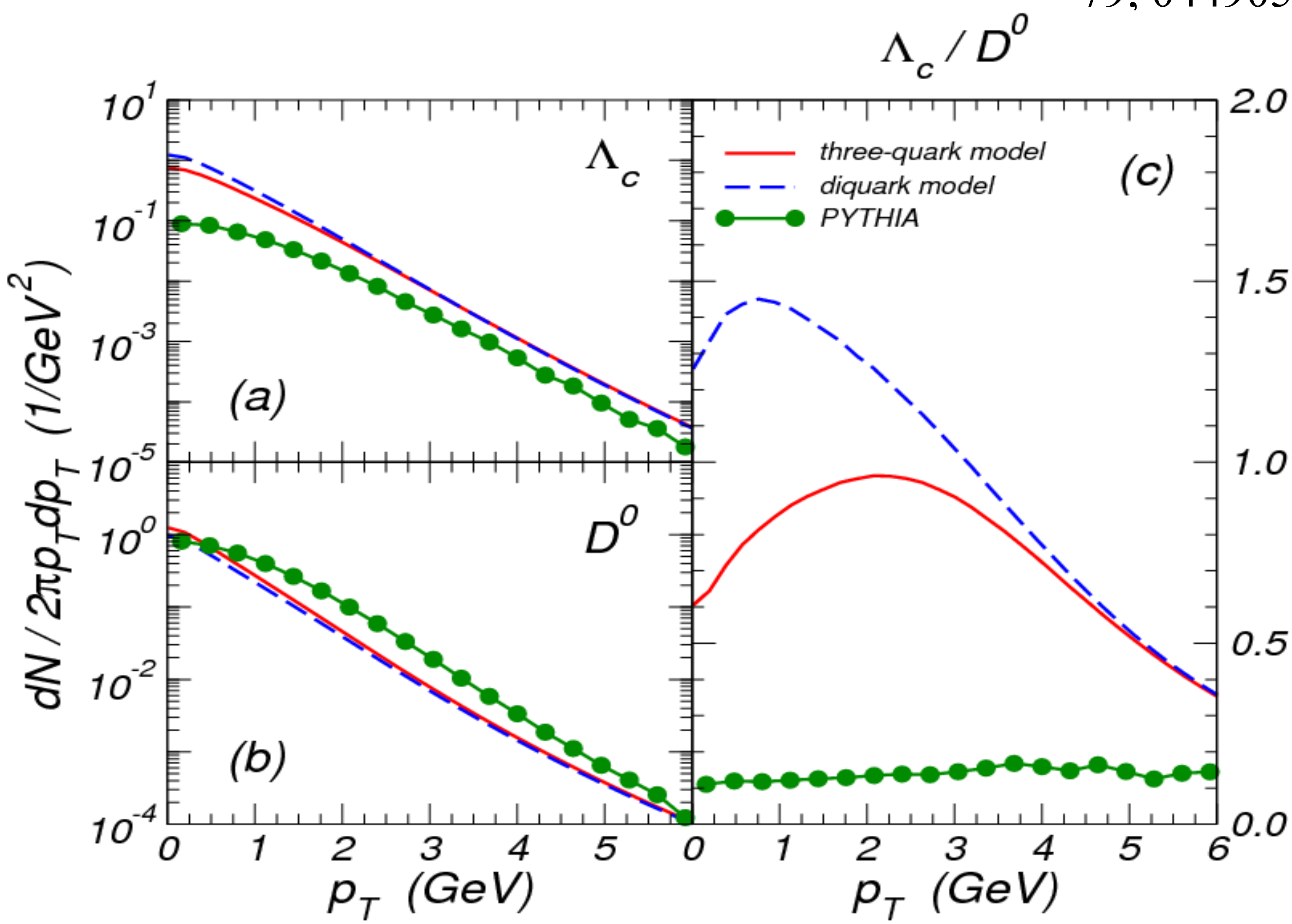

Including coalescence contribution enhances Λ_c/D^0 ratio, which is further enhanced by the presence of diquarks in QGP

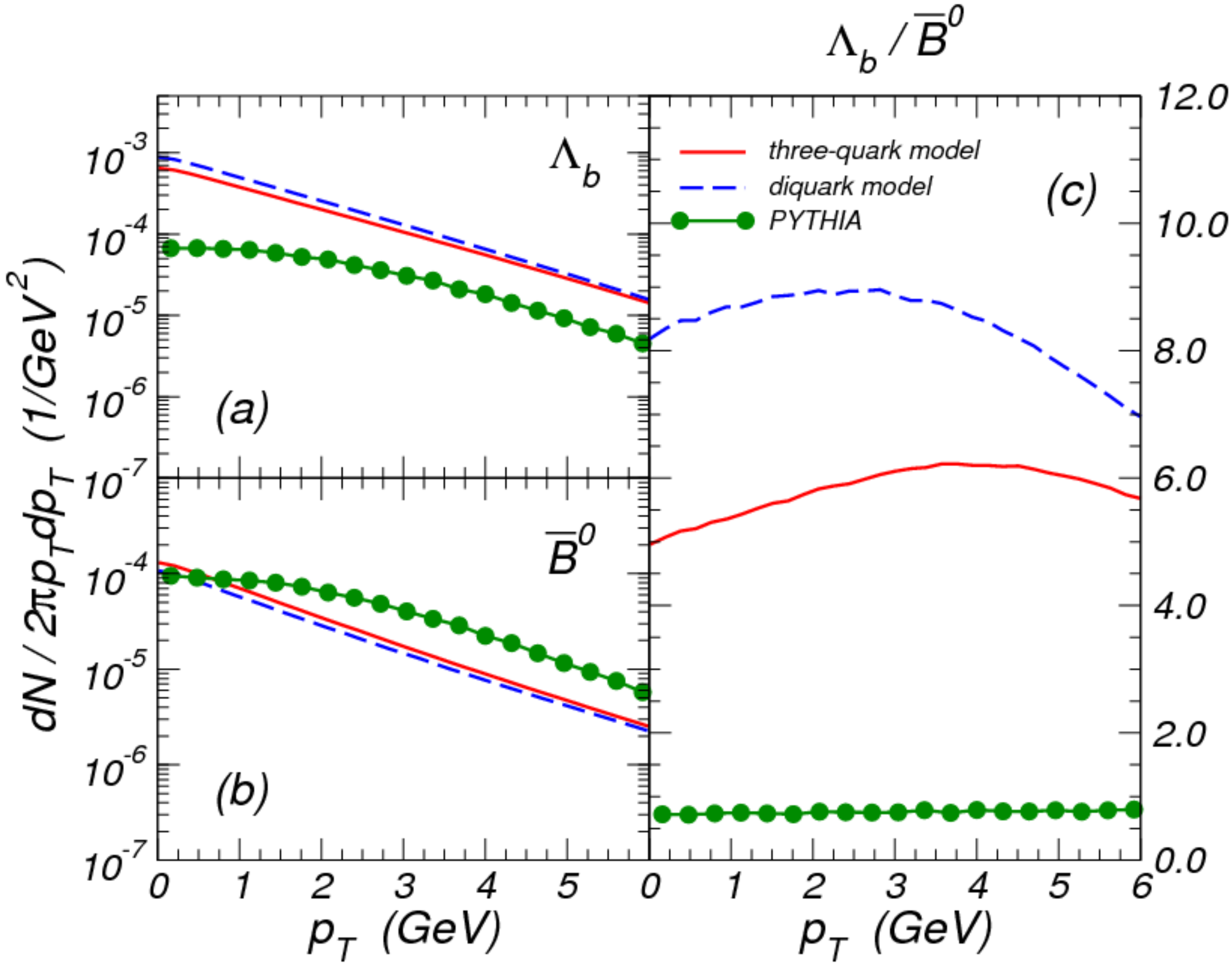

As for Λ_c/D^0, including coalescence contribution enhances Λ_b/B^0 ratio, and it is further enhanced by the presence of diquarks in QGP

Effect of Λ_c enhancement on non-photonic electron R_{AA}

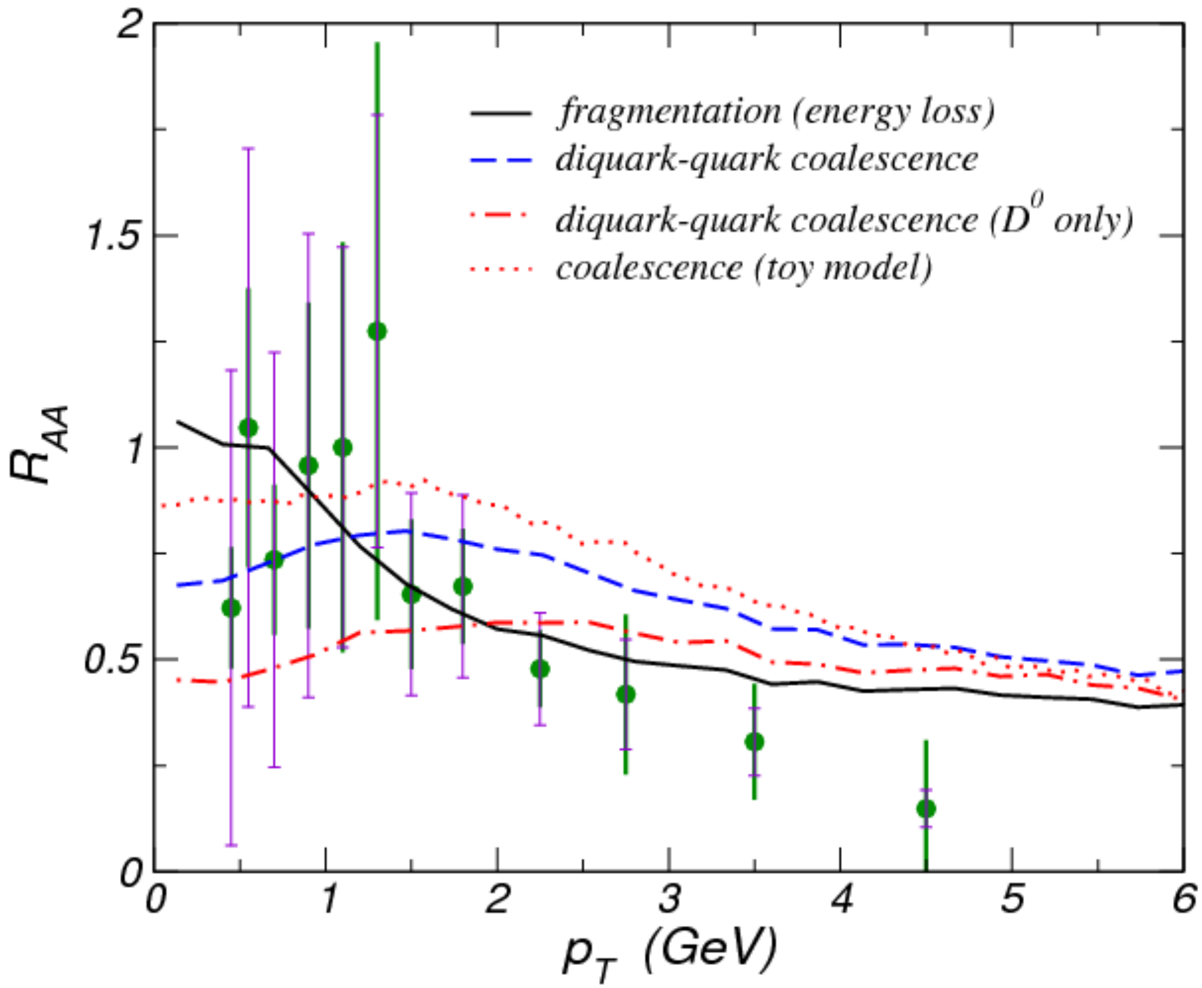

Oh & Ko, PRC 79, 067902 (2009)

R_{AA} at large p_T increases as Λ_c enhancement is at low p_t

Net charge fluctuations

Adams et al., STAR Collaboration, PRC 68, 044905 (2003)

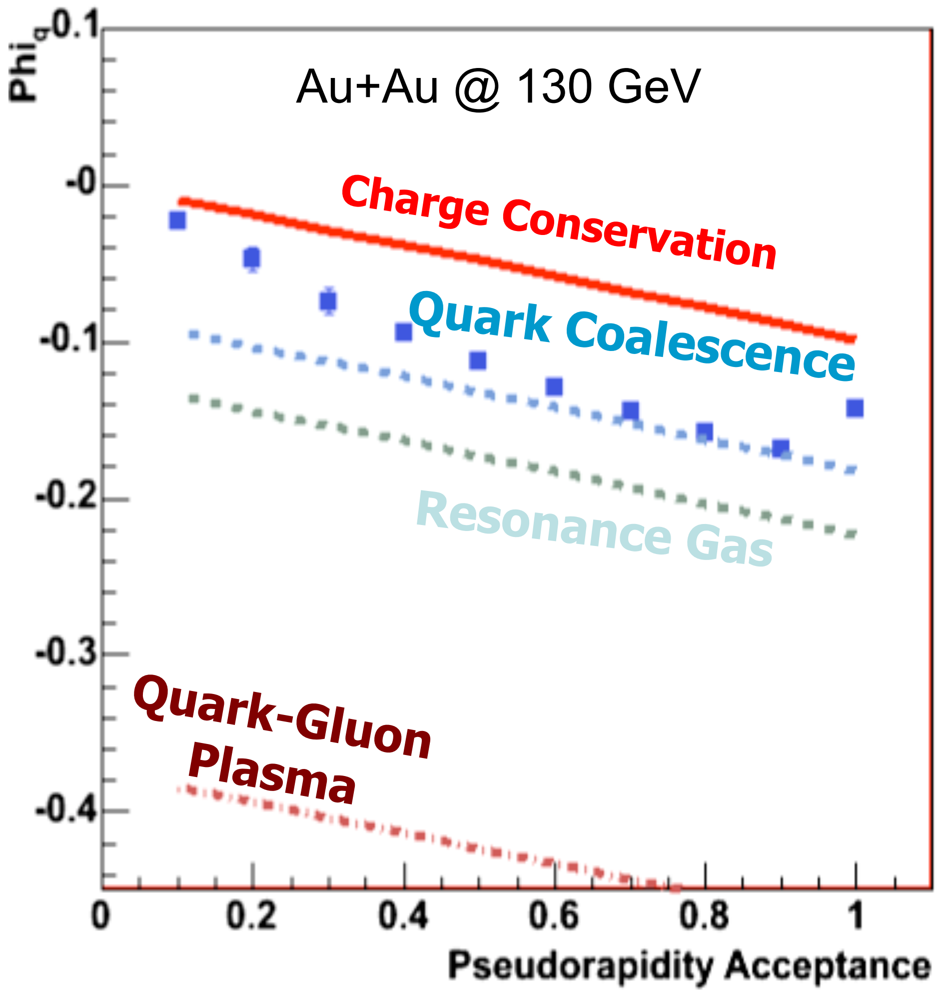

$$Z = Q - \frac{\langle Q \rangle}{\langle N_{CH} \rangle} N_{CH}$$

$$\overline{Z^2} = 4 \frac{\langle N_+ \rangle \langle N_- \rangle}{\langle N_{CH}^2 \rangle}$$

$$\Phi_q = \sqrt{\frac{Z^2}{\langle N_{CH} \rangle}} - \sqrt{\overline{Z^2}}$$

Favor quark coalescence picture for hadronization

RHIC low energy run and FAIR

Chen, Ko, Liu & Zhang, Proc. Of Science 034 (2009)

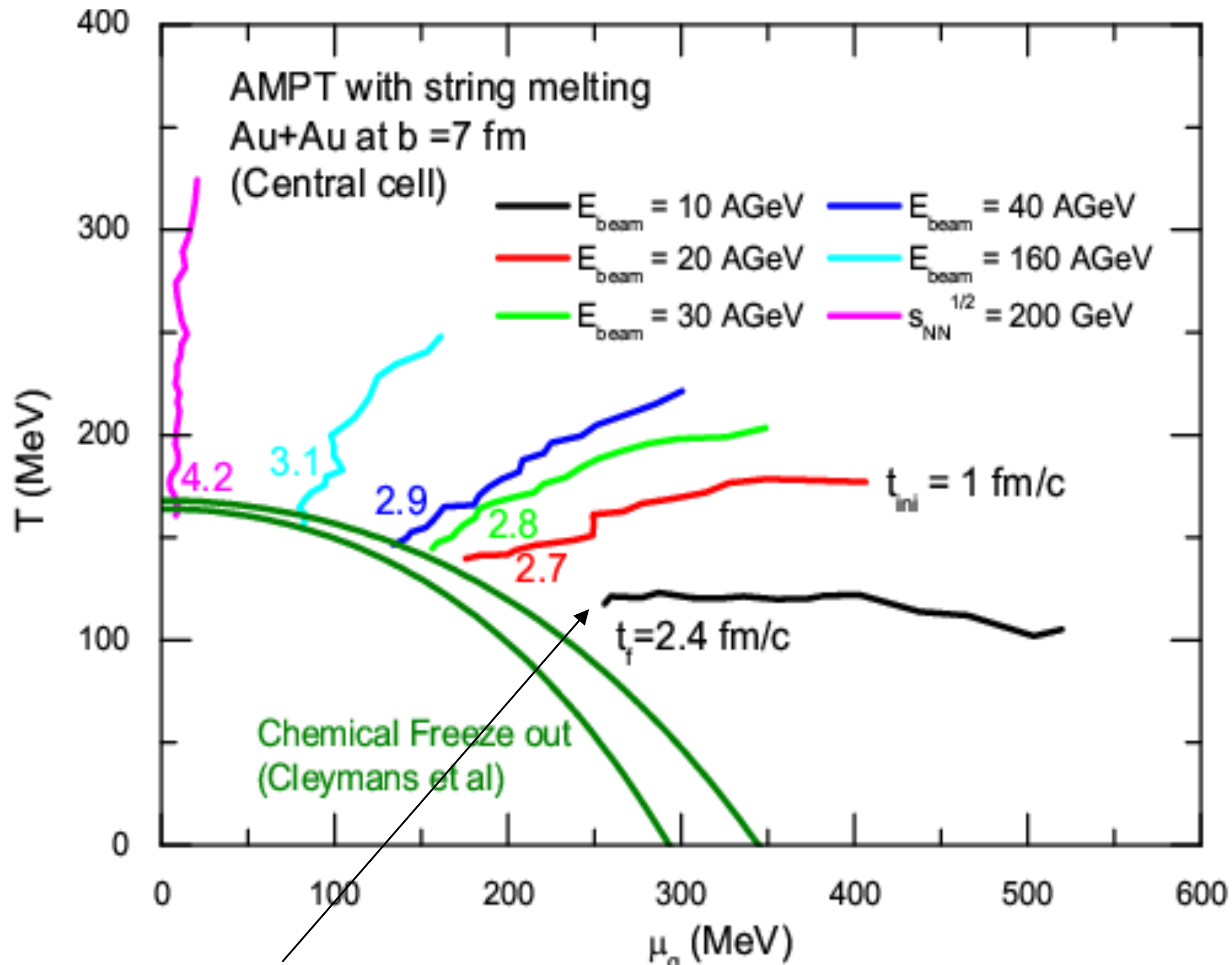

Require first-order phase transition ?

Rapidity distributions

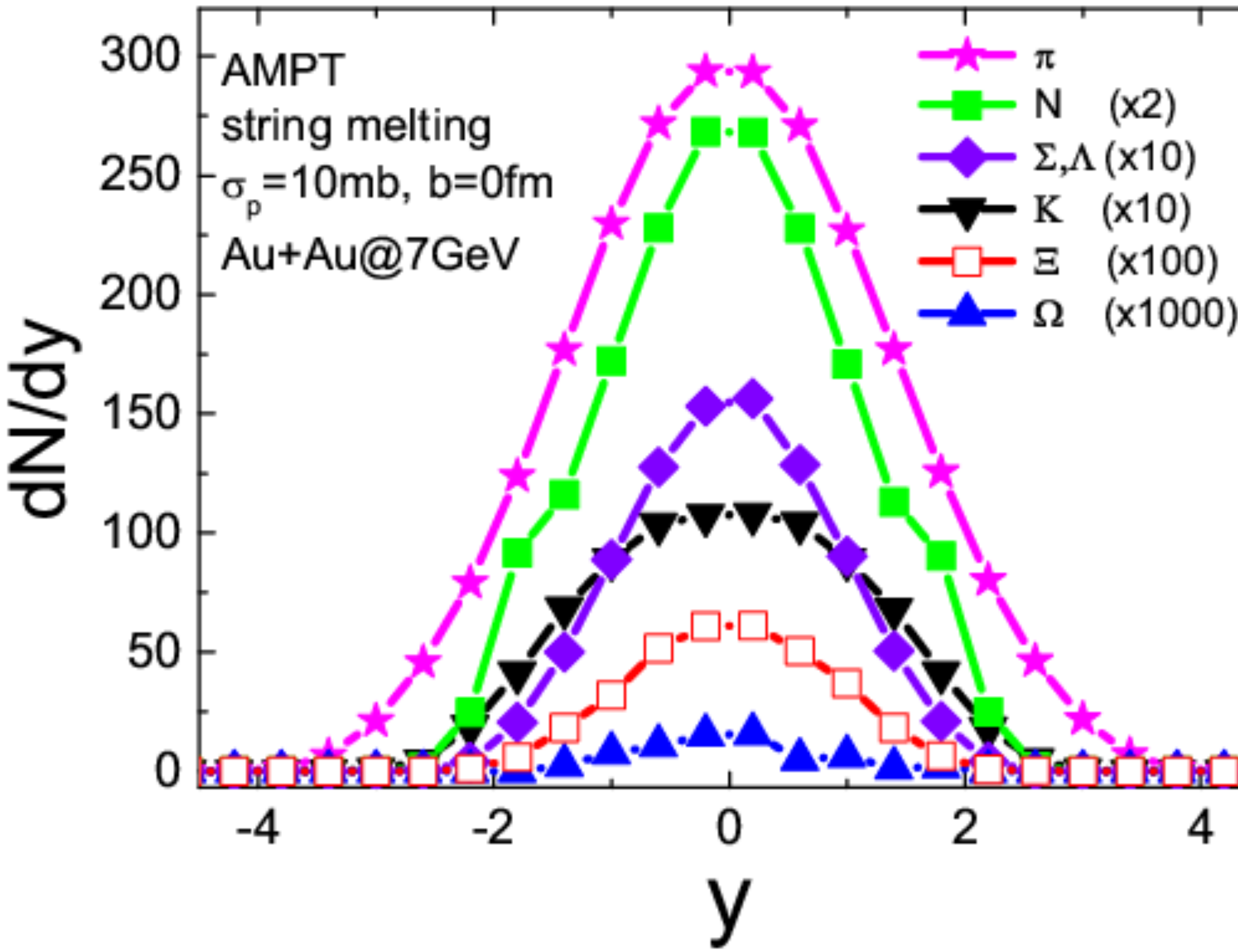

Elliptic flow

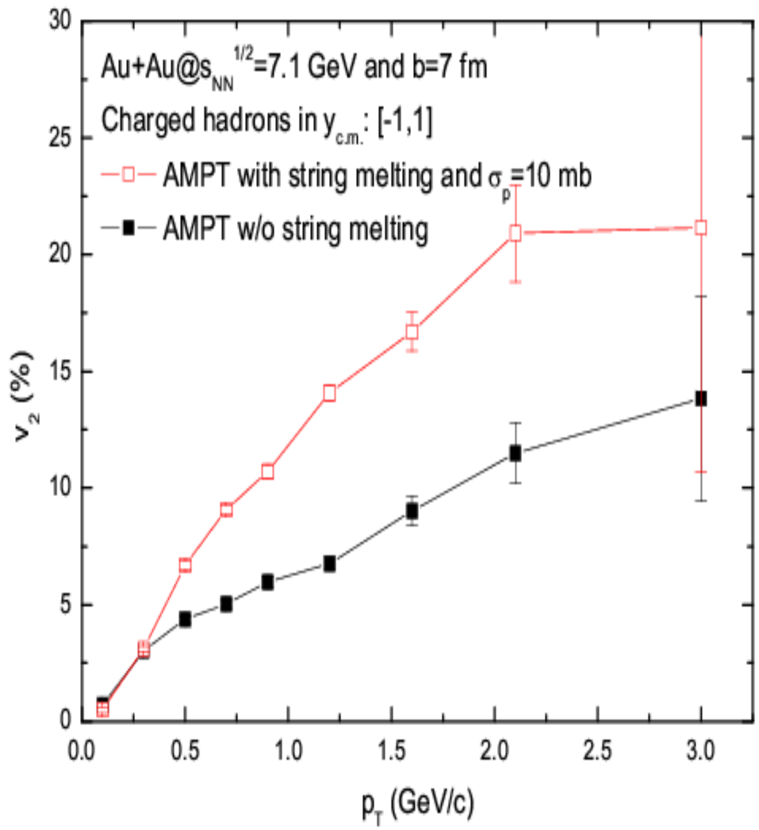

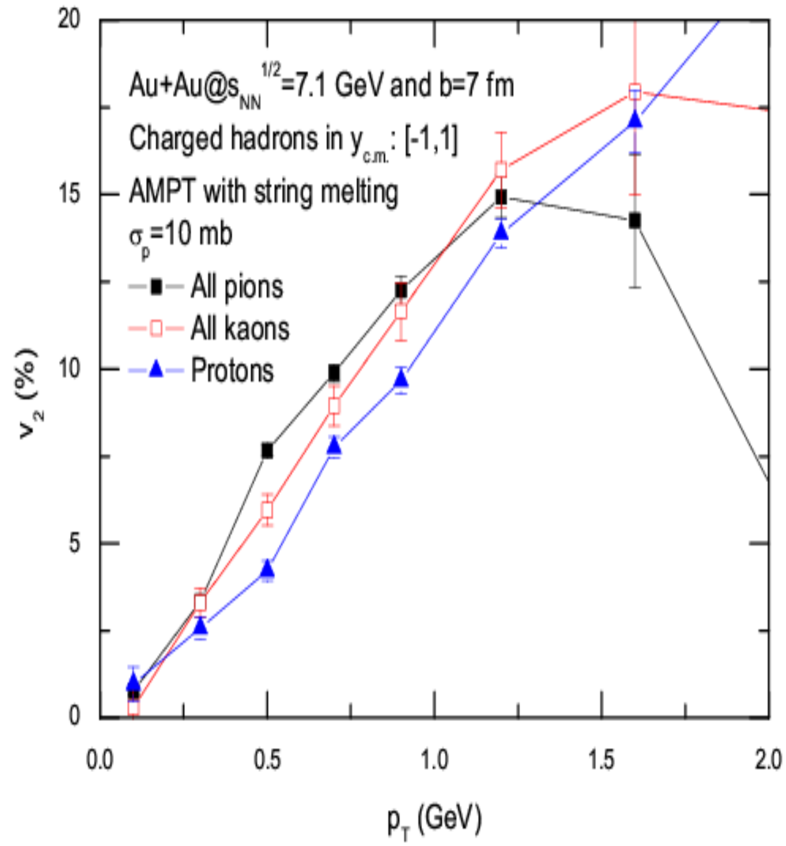

Partonic scattering enhances elliptic flow

Mass ordering of hadron elliptic flows

Comparison of transport model predictions of elliptic flow

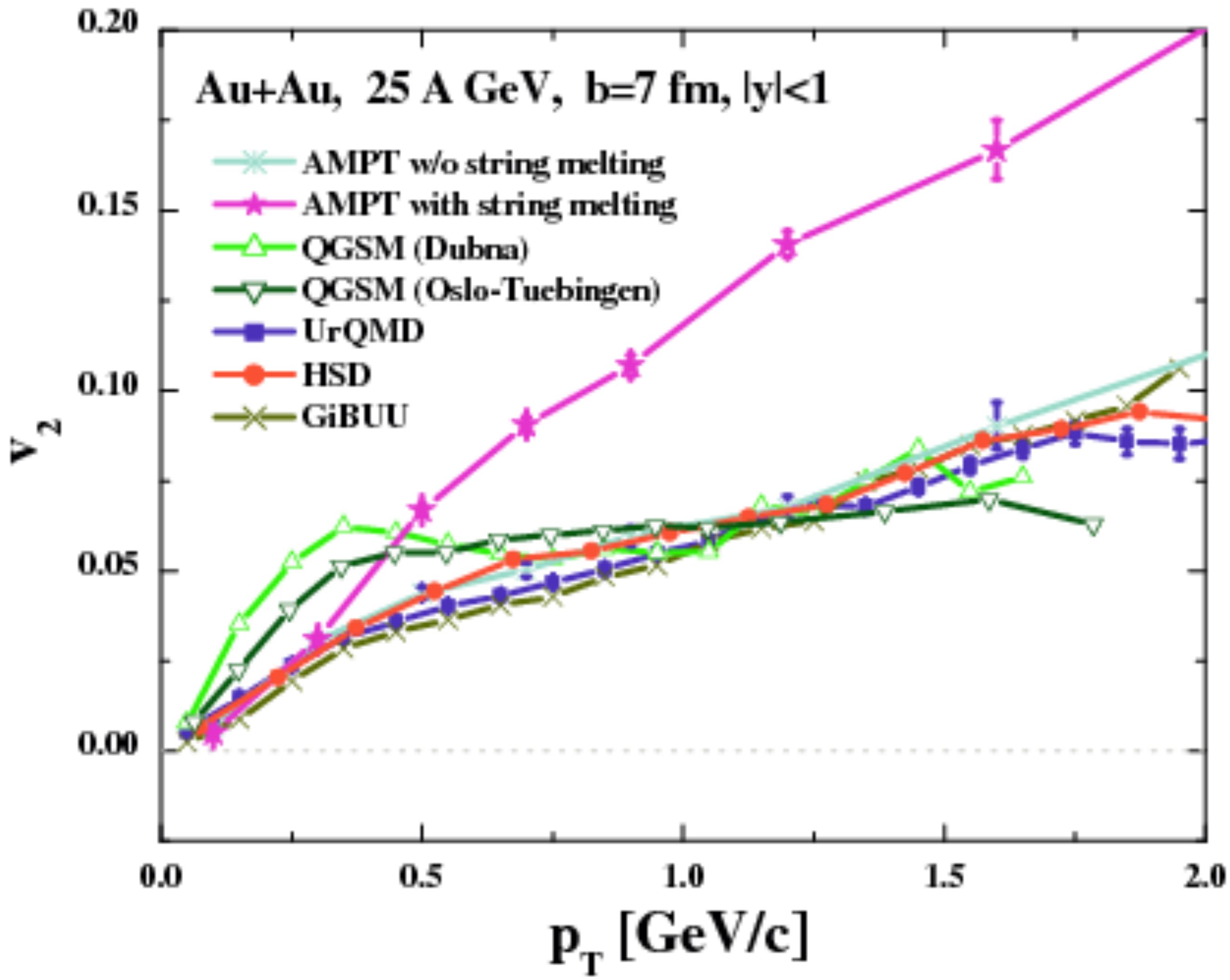

Phase transition and effect of hadronic scattering

Without QGP Crossover First order

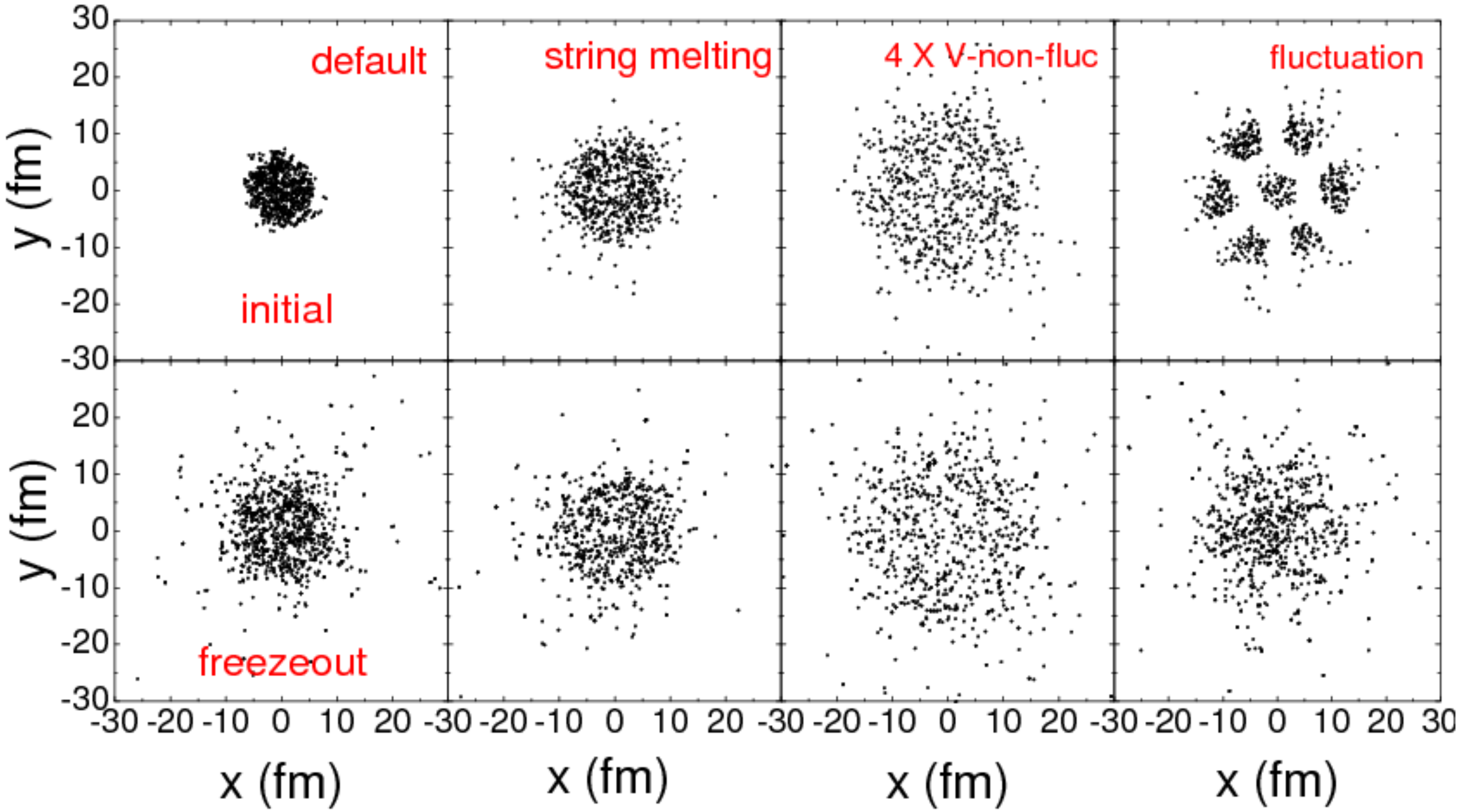

First-order phase transition modeled by increasing initial volume of hadronic matter by 4 and with or without density fluctuation

Mean transverse momentum fluctuation

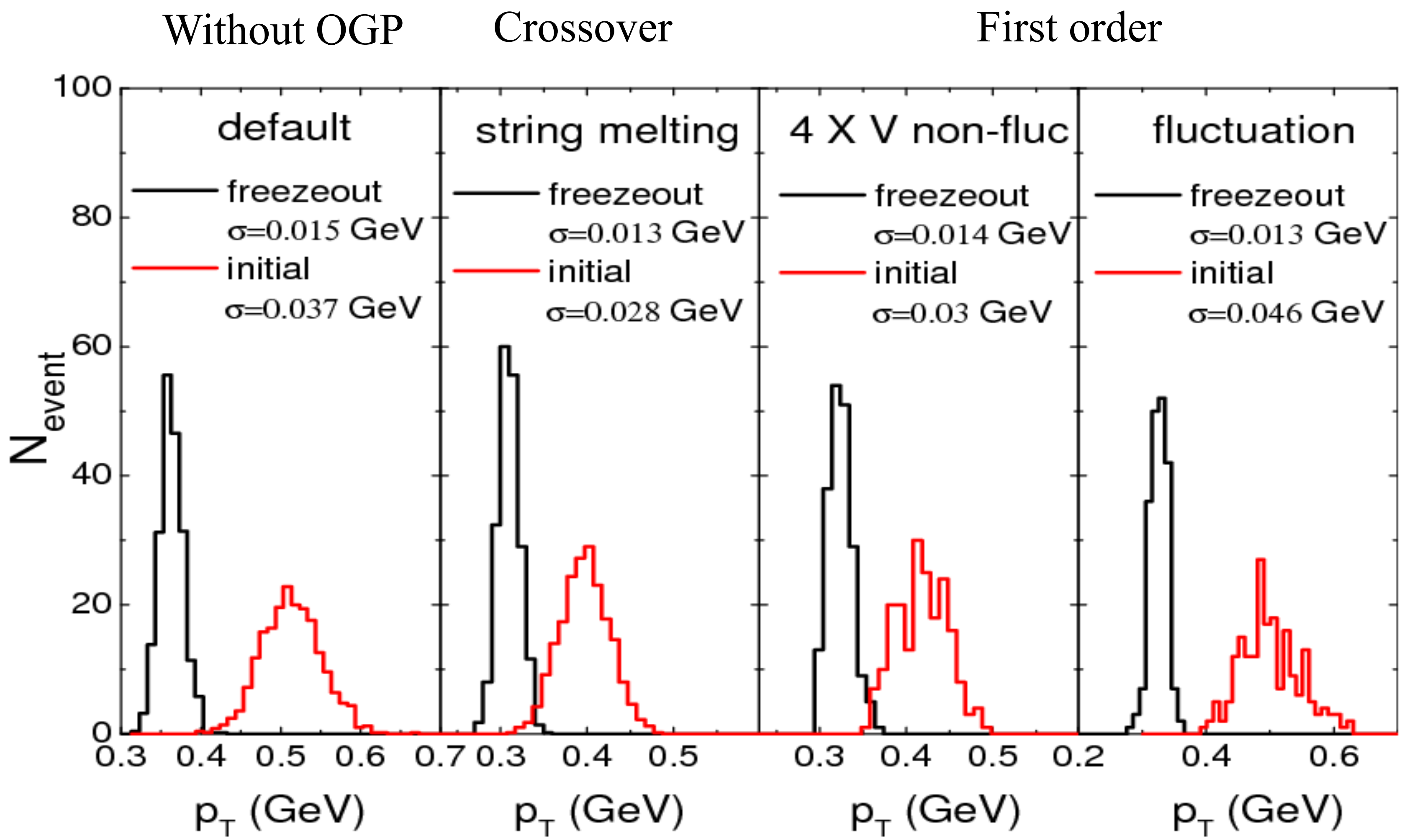

Similar mean transverse momentum fluctuation after hadronic scattering

Deuteron yield

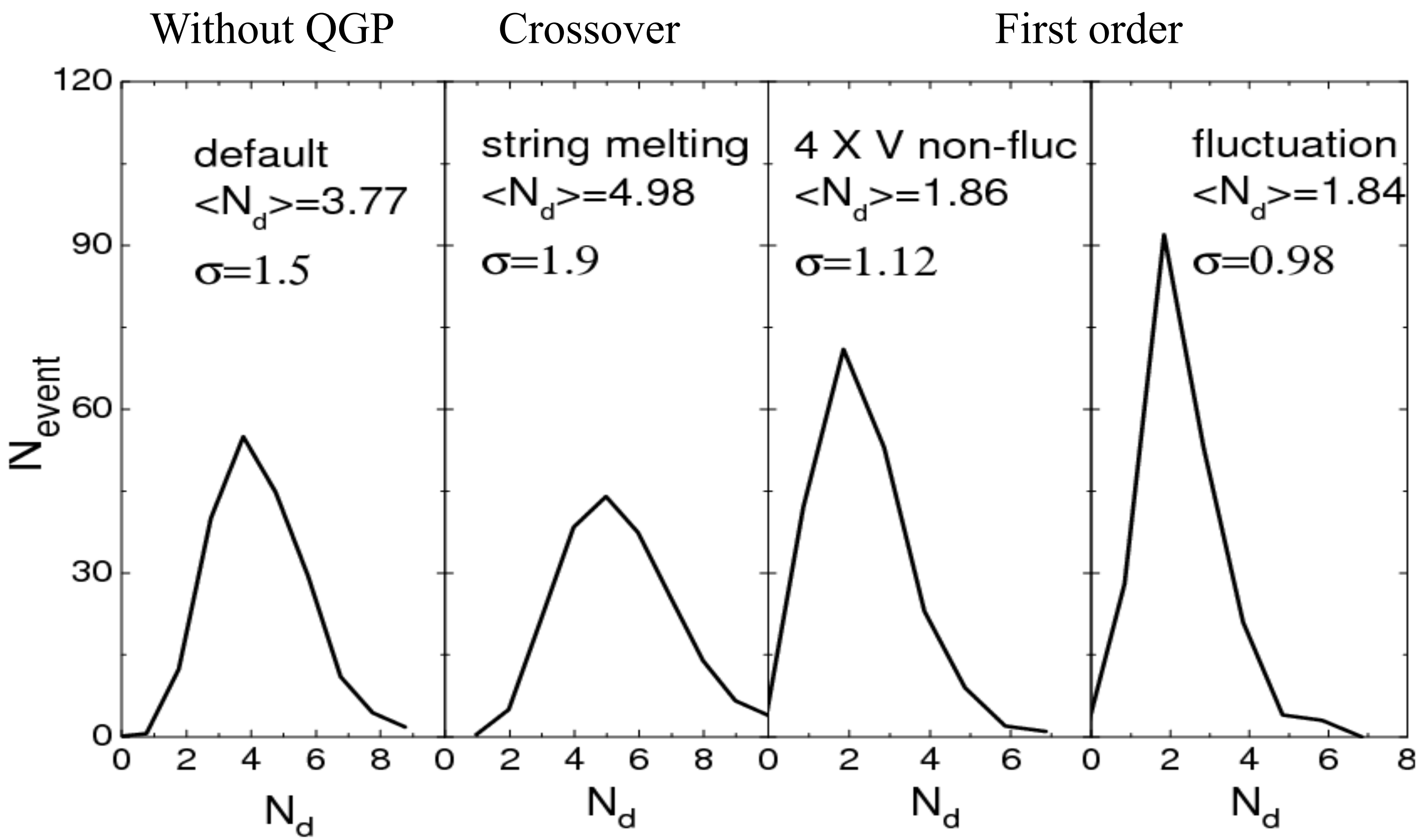

Deuteron yield is reduced if there is a first-order phase transition but is not affected by initial density fluctuation

Two-pion correlation functions

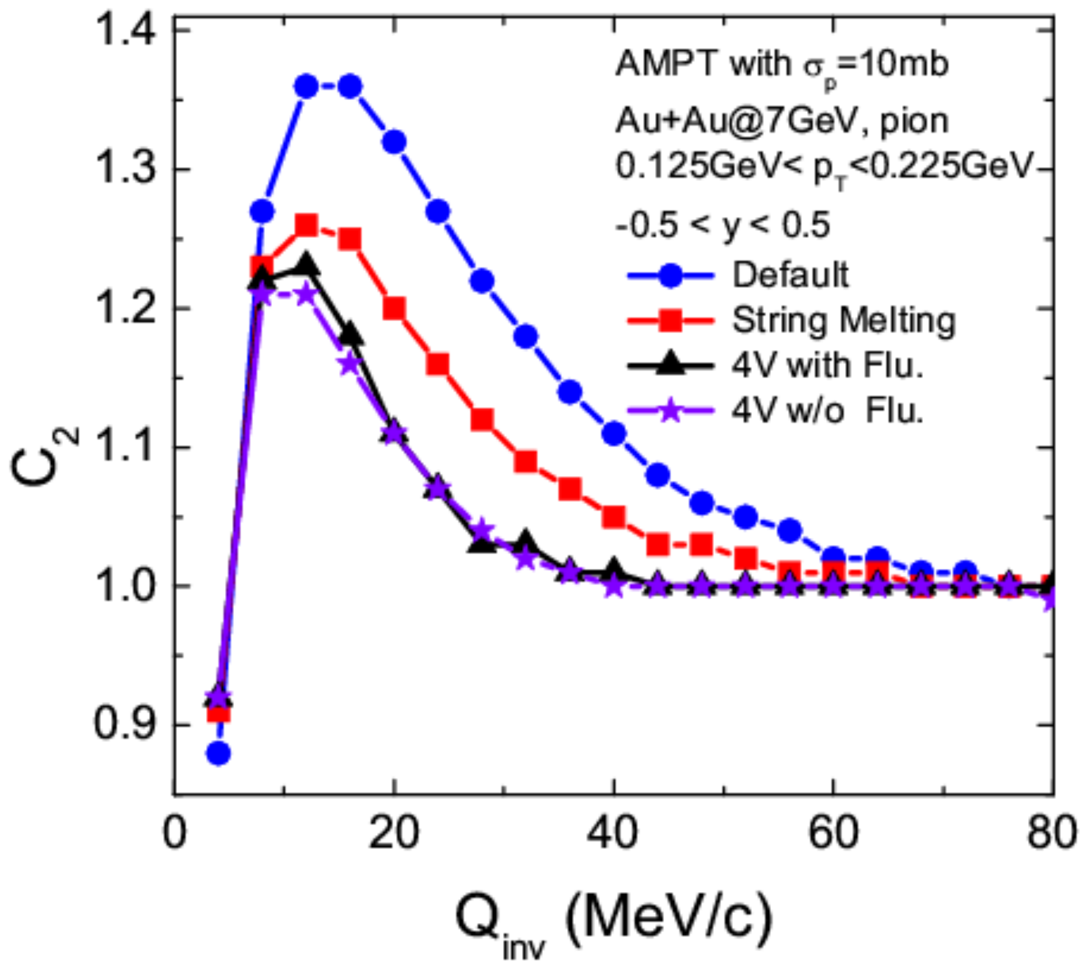

First-order phase transition leads to a narrow correlation function but effect of density fluctuation is not seen

Charm suppression in baryon-rich

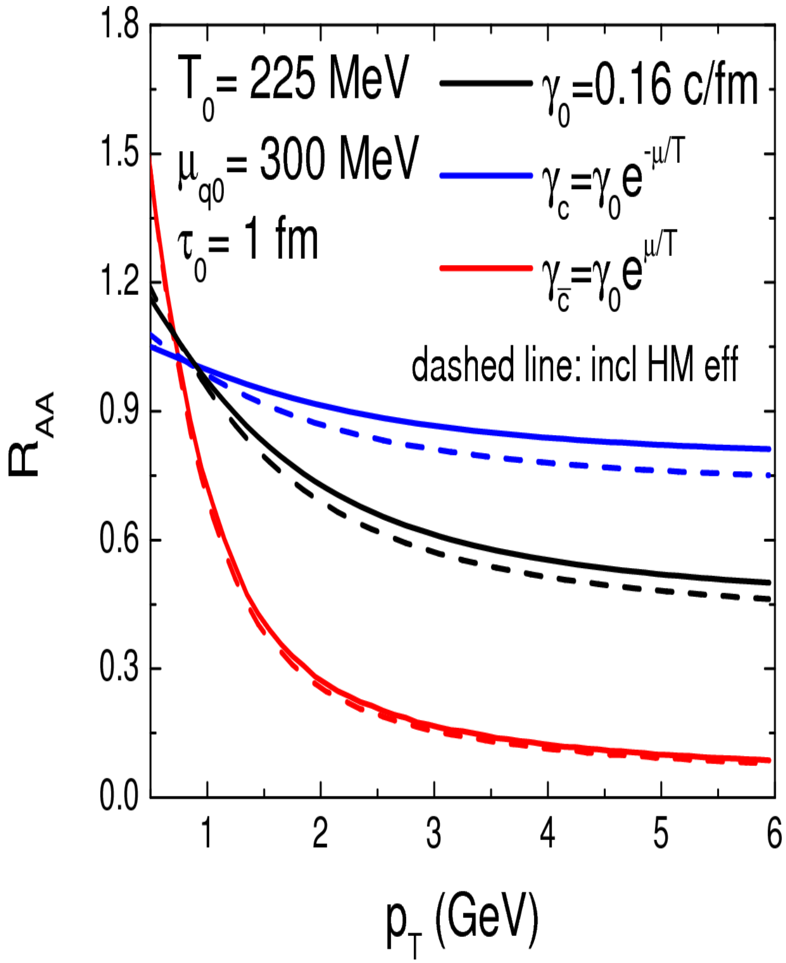

$$R_{AA} = \frac{dN_{Au+Au}}{\langle T_{AA} \rangle d\sigma_{p+p}}$$

- dN_{Au+Au}= differential heavy flavor yield in Au+Au collisions
- $d\sigma_{p+p}$= corresponding differential cross section in p+p collisions
- $\langle T_{AA} \rangle$= nuclear overlap integral

- pQCD gives similar c and cbar cross sections in QGP, irrespective to the baryon chemical potential (solid line).
- Resonance scattering leads to different c and cbar cross sections in QGP with finite baryon chemical potential (solid and dashed lines)

QGP phase transition and Double phi peaks

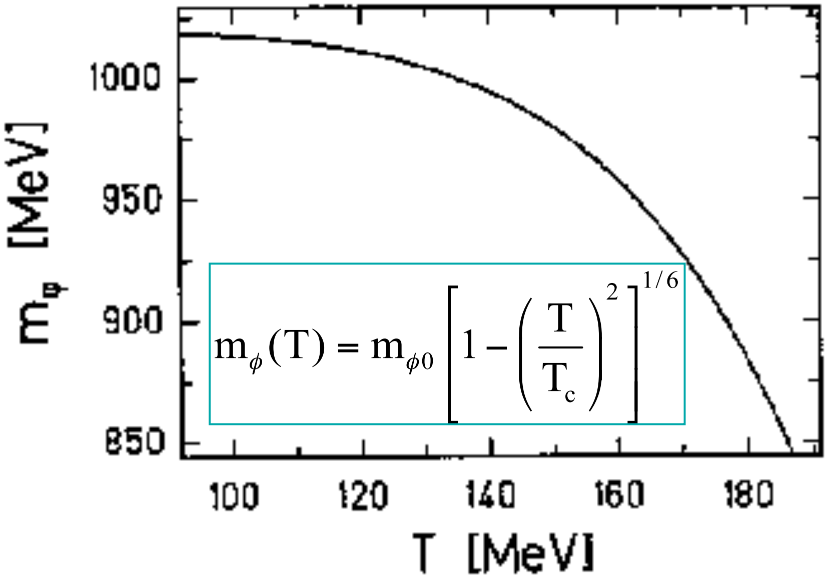

Asakawa & Ko, PLB 322, 33 (1994);
PRC 50, 3046 (1994)

Boost-invariant hydro with transverse flow: T_0=250 MeV; T_c=180 MeV, T_f=120 MeV

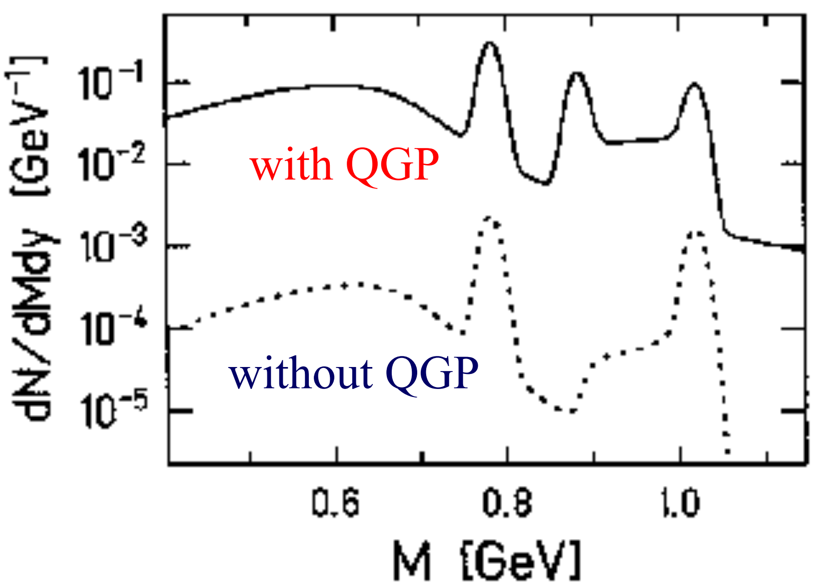

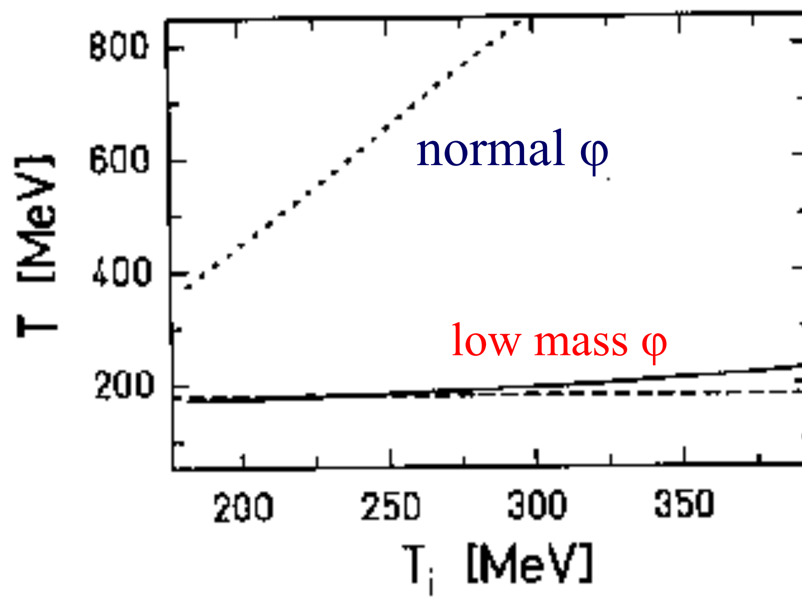

Heavy ion collisions at LHC

$$\boxed{Pb + Pb\ @ \sqrt{s_{NN}} = 5.5\ \text{TeV}}$$

Abrue et al., JPG 35, 05400 (2008)

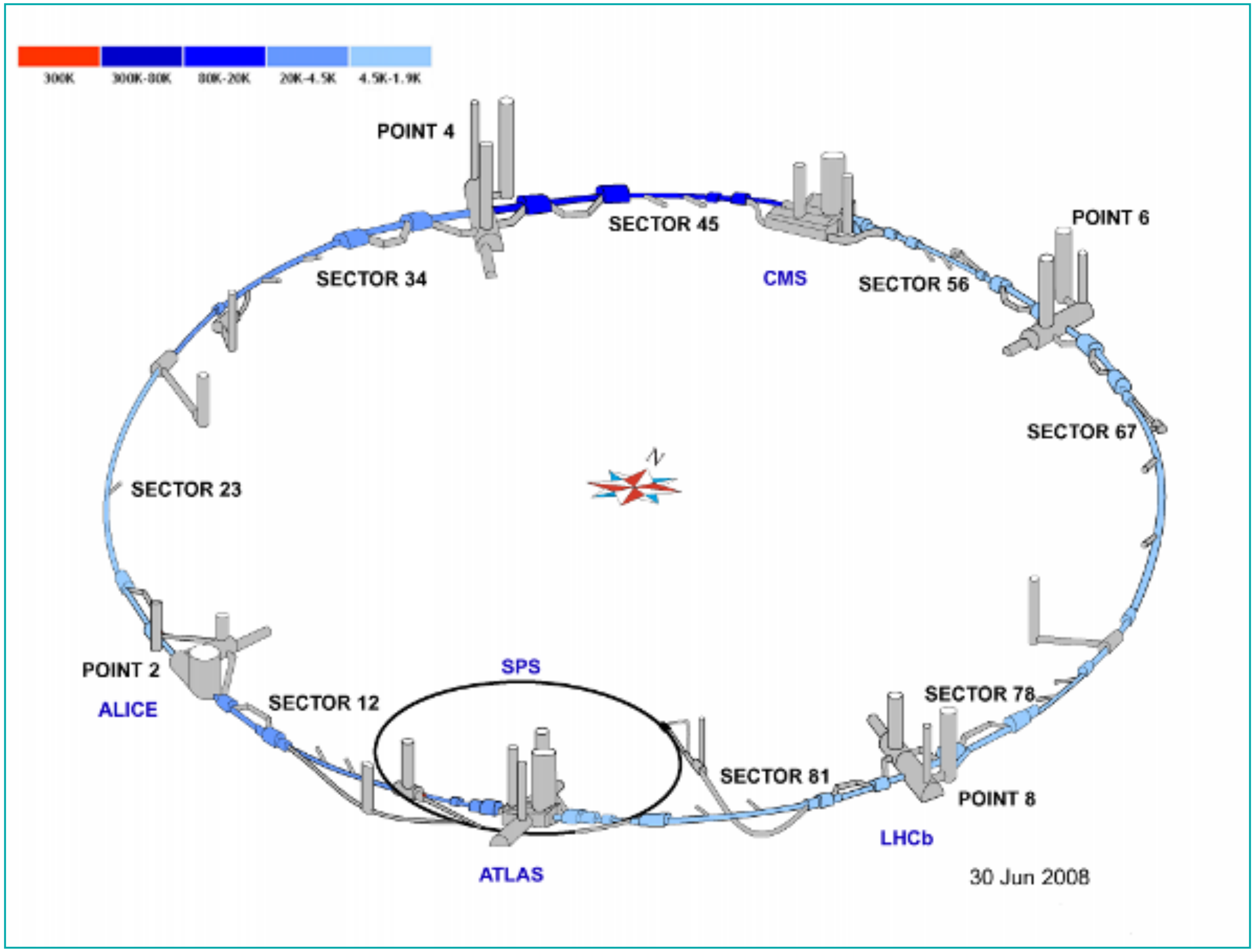

Rapidity distributions at LHC

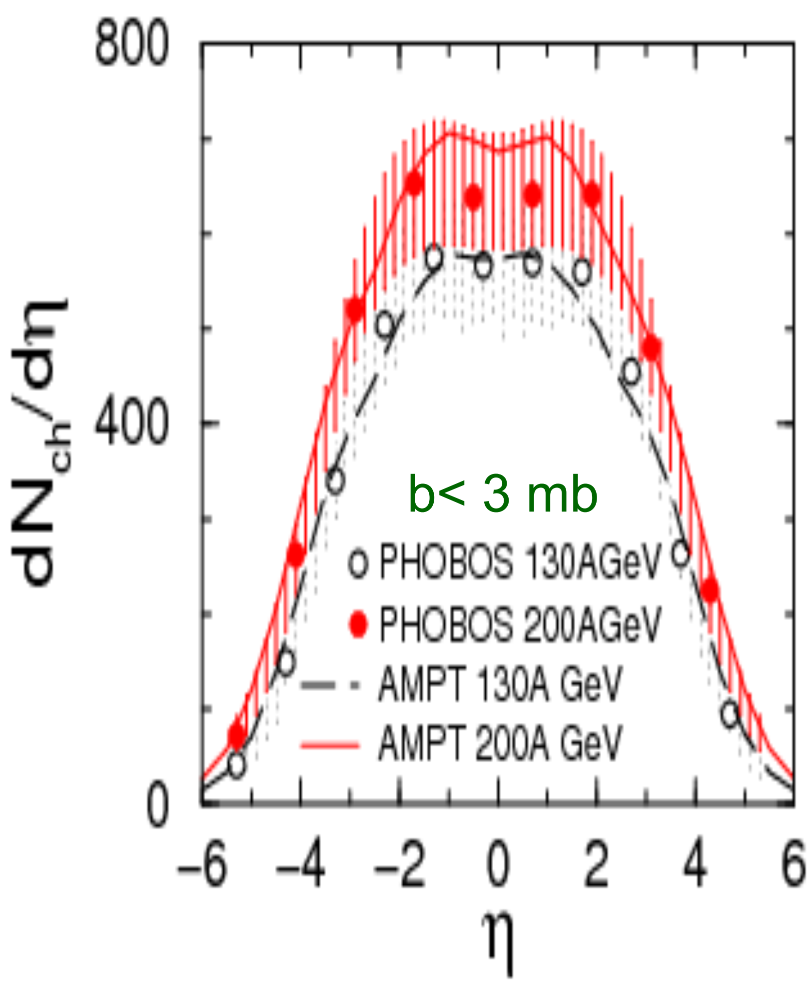

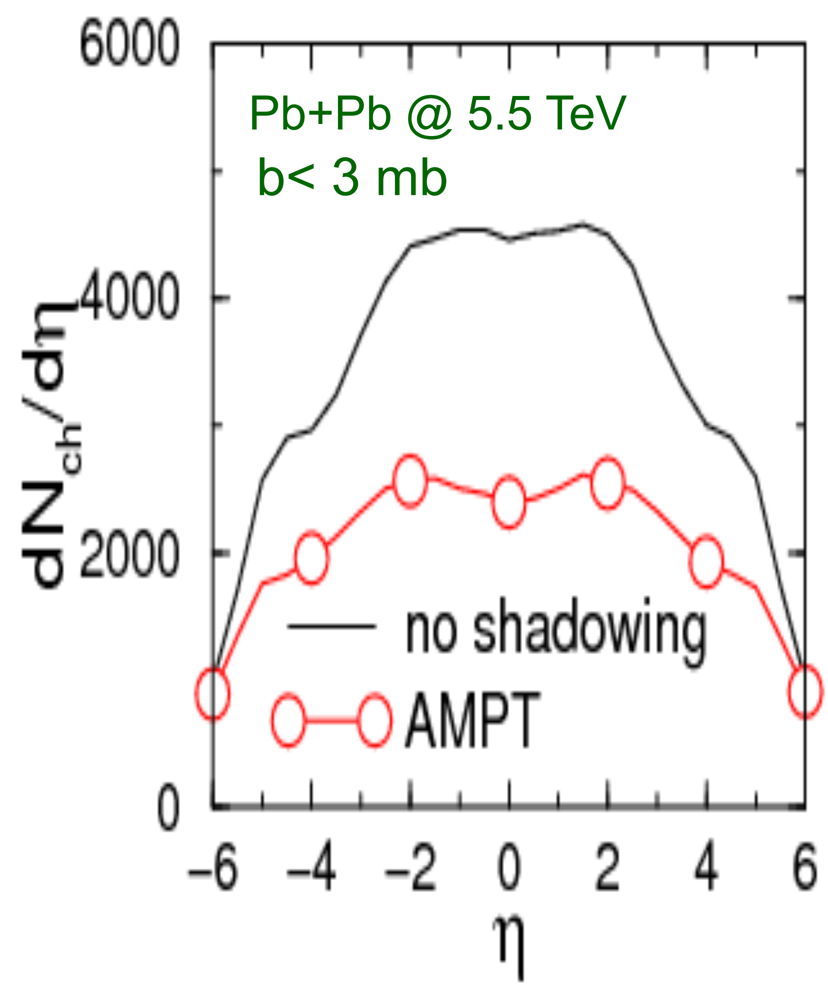

Particle multiplicity at LHC increases by a factor of ~ 4 from that at RHIC

Transverse momentum distributions

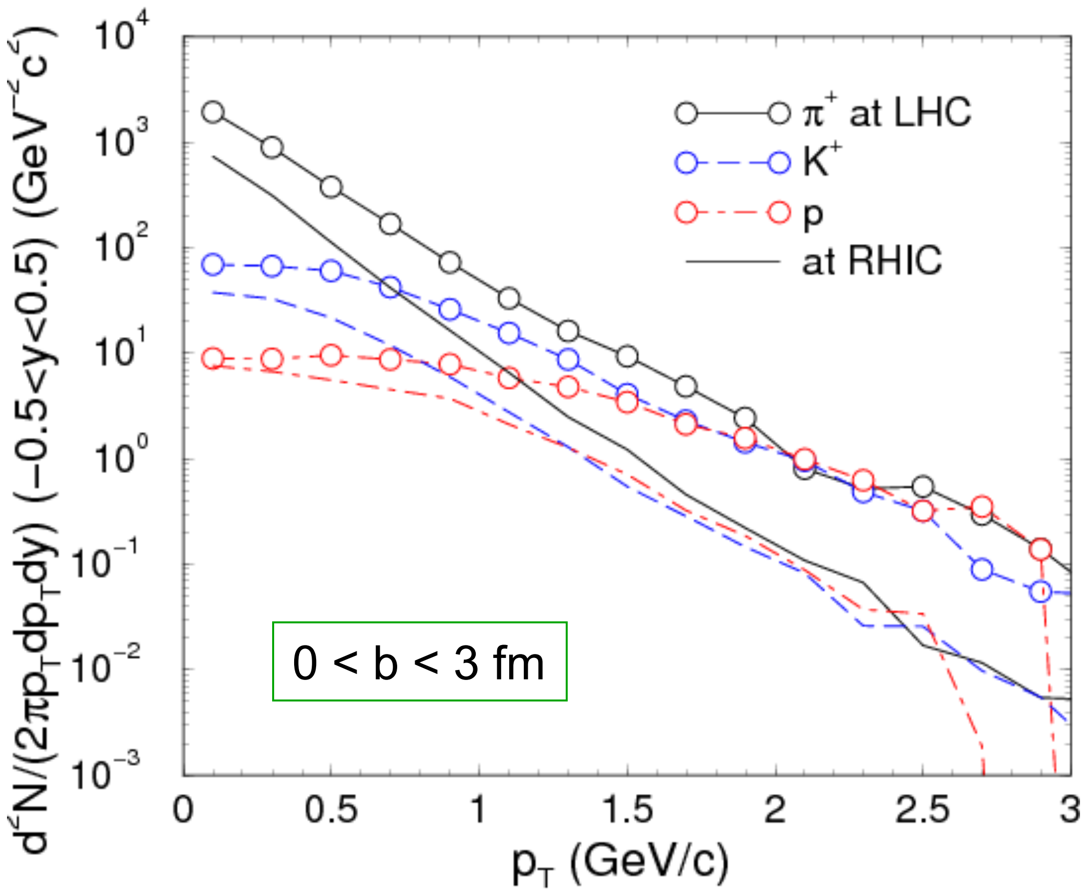

Particle transverse momentum spectra are stiffer at LHC than at RHIC → larger transverse flow

Quark elliptic flows

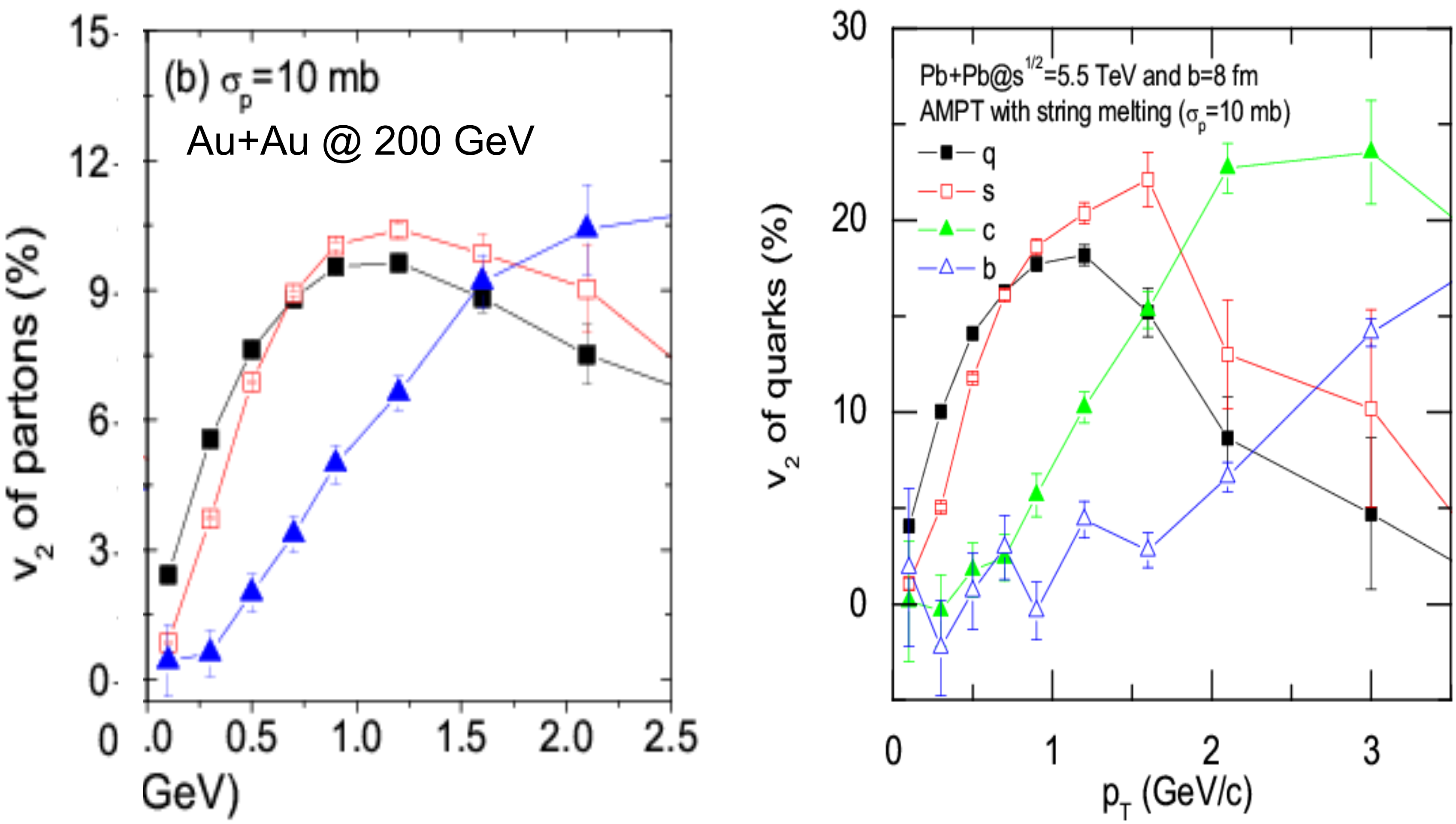

Quark elliptic flows are larger at LHC than at RHIC, reaching ~ 20%

Pion and proton Elliptic flow at LHC

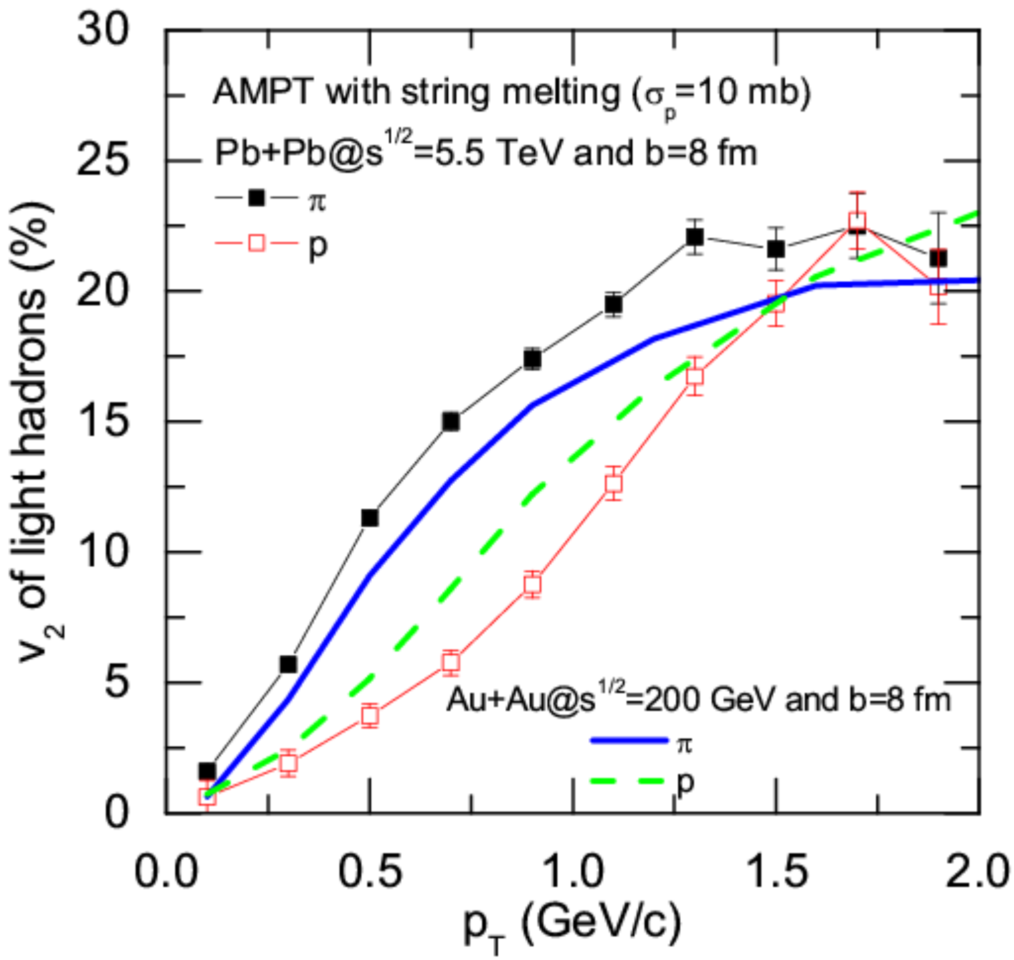

Elliptic flow is larger for pions but smaller for protons at LHC than at RHIC

Heavy meson elliptic flows at LHC

Quark coalescence model

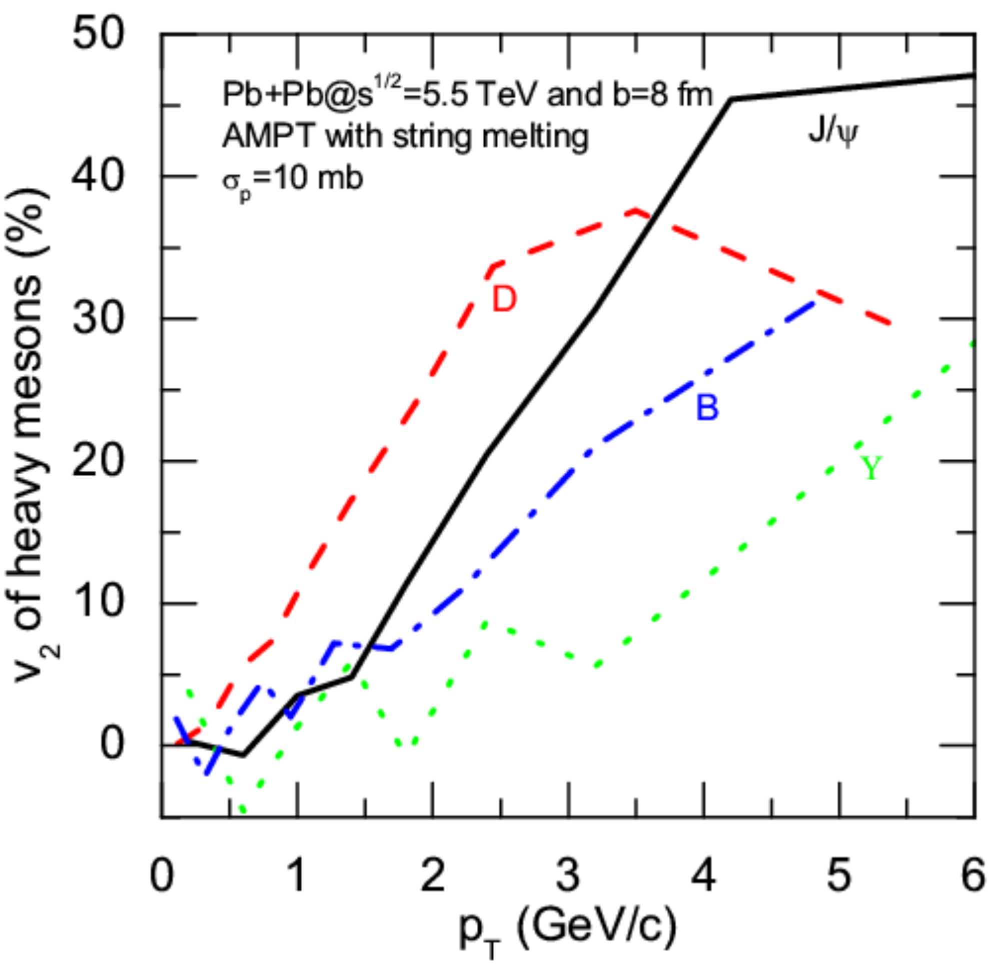

$$v_{2M}(p_T) \cong v_{2,q_1}((m_{q_1}/m_M)p_T) + v_{2,q_2}((m_{q_2}/m_M)p_T)$$

Pion interferometry

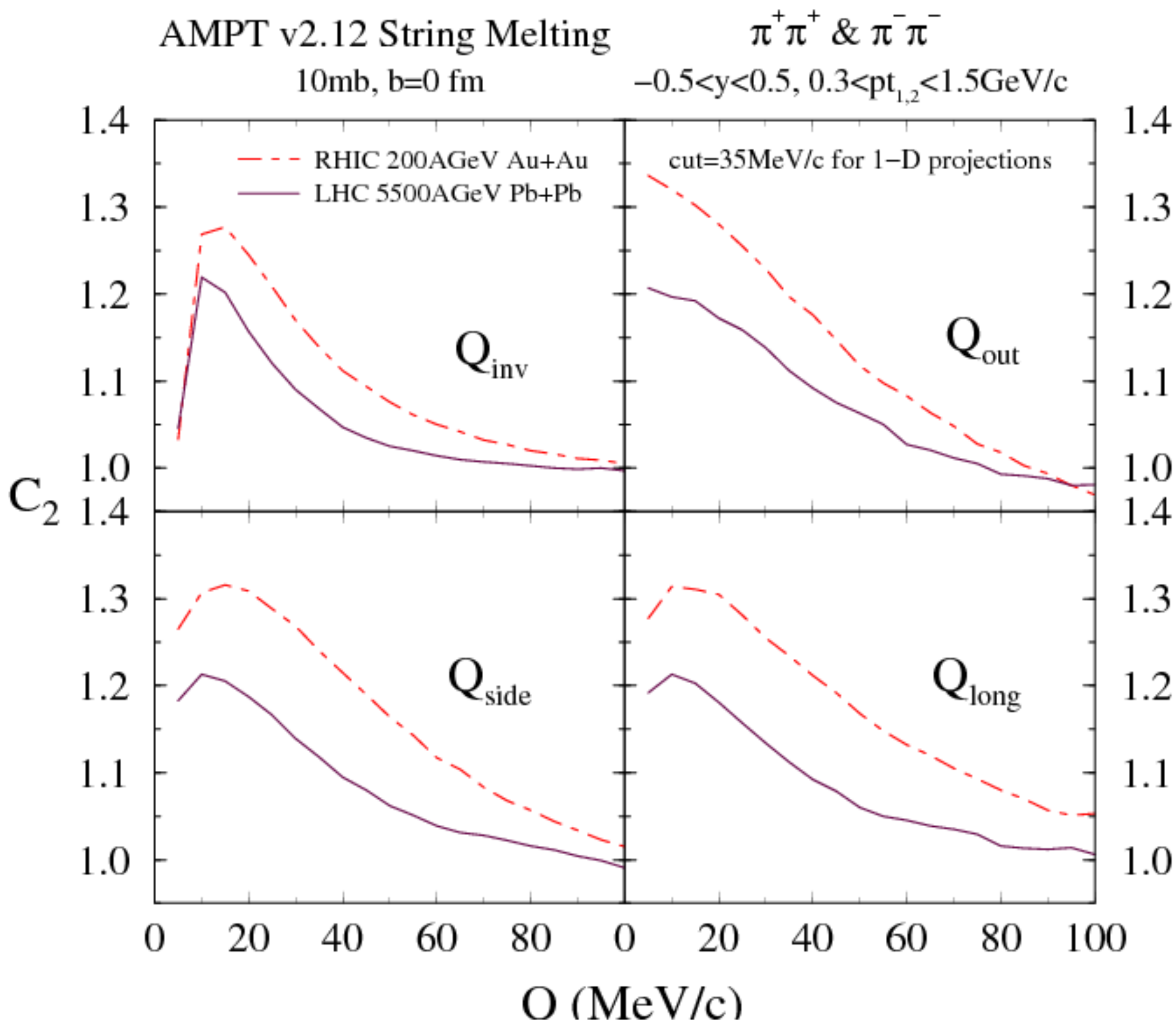

Two-pion correlation functions narrower at LHC than at RHIC

Radii from Gaussian fit to correlation functions

$$C_2(\vec{Q},\vec{K}) = 1 + \lambda \exp\left(-\sum_{i=1}^{3} R_{ii}^2(K) Q_i^2 \right)$$

	R_{out}(fm)	R_{side}(fm)	R_{long}(fm)	λ	$R_{\text{out}}/R_{\text{side}}$
RHIC (π)	3.60	3.52	3.23	0.50	1.02
LHC (π)	4.23	4.70	4.86	0.43	0.90
RHIC (K)	2.95	2.79	2.62	0.94	1.06
LHC (K)	3.56	3.20	3.16	0.89	1.11

Source radii for pions are larger than for kaons and both are larger at LHC than at RHIC

Thermal charm production in QGP

Zhang, Liu & Ko,
PRC 77, 024901 (08)

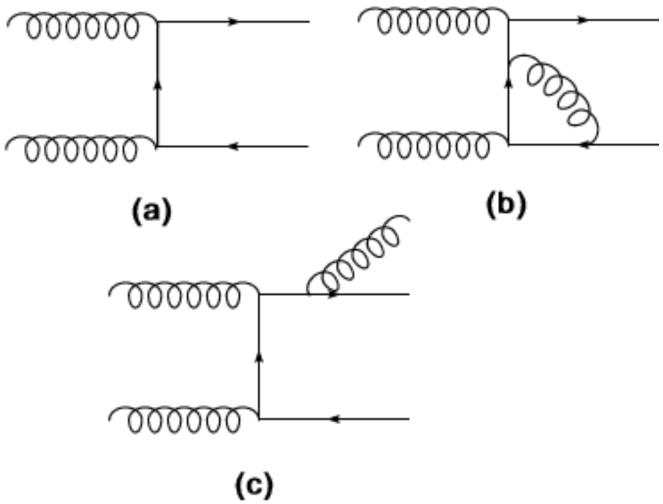

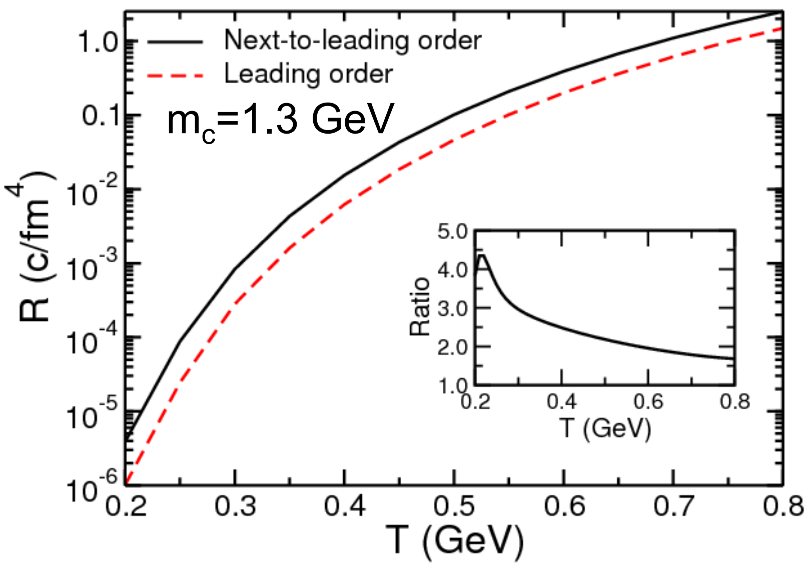

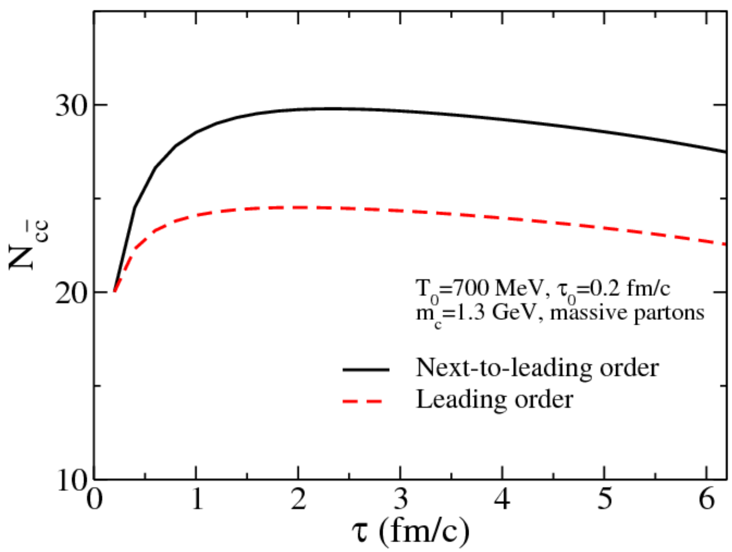

- Thermal production non-negligible
- Next-leading order and leading order contributions are comparable
- Insensitive to gluon masses
- Effect increases by about 2 for initial temperature T_0=750 MeV but decreases by ~ 2 for m_c=1.5 GeV

Charm exotics production in HIC

Lee, Yasui, Liu & Ko
Eur. J. Phys. C 54, 259 (08)

- Charm tetraquark mesons
  - $T_{cc}(ud\bar{c}\bar{c})$ is ~ 80 MeV below D+D* according to quark model
  - Coalescence model predicts a yield of ~5.5X10^{-6} in central Au+Au collisions at RHIC and ~9X10^{-5} in central Pb+Pb collisions at LHC if total charm quark numbers are 3 and 20, respectively
  - Yields increase to 7.5X10^{-4} and 8.6X10^{-3}, respectively, in the statistical model

- Charmed pentaquark baryons
  - $\Theta_{cs}(uds\bar{c})$ is ~ 70 MeV below D+Σ in quark model
  - Yield is ~1.2X10^{-4} at RHIC and ~7.9X10^{-4} at LHC from the coalescence model for total charm quark numbers of 3 and 20, respectively
  - Statistical model predicts much larger yields of ~4.5X10^{-3} at RHIC and ~2.7X10^{-2} at LHC

Summary

- Most proposed QGP signatures have been observed at RHIC.
- Strangeness production is enhanced and is consistent with formation of chemical equilibrated hadronic matter at $T_{c.}$
- Large elliptic flow requires large parton cross sections in transport model or earlier equilibration and small viscosity in hydro model.
- HBT correlation is consistent with formation of strongly interacting partonic matter.
- Jet quenching due to radiation requires initial matter with energy density order of magnitude higher than that of QCD at $T_{c.}$
- Quark number scaling of elliptic flow of identified hadrons is consistent with hadronization via quark coalescence or recombination.
- Electromagnetic probes and heavy flavor hadrons will be studied by upgraded RHIC.
- Experiments from future low energy run at RHIC and FAIR as well as LHC allow for probing QGP at finite baryon chemical potential and even higher temperature, respectively.